EUROPEAN COMMISSION

Community Research

SEVENTH FRAMEWORK PROGRAMME

CARBOWASTE

Treatment and Disposal of Irradiated Graphite and Other Carbonaceous

Characterisation and Chemical Treatment of Irradiated UK Graphite Waste

Deliverable Number: T-4.3.3-b

Author(s): **Lorraine McDermott**
UoM, UK

Date of first issue of this report: 01/12/2011

Start date of project : **01/04/2008** Duration : **60 Months**

Project co-funded by the European Commission under the Seventh Framework Programme (2007 to 2011) of the European Atomic Energy Community (EURATOM) for nuclear research and training activities		
Dissemination Level		
PU	Public	
RE	Restricted to the partners of the CARBOWASTE project	
CO	Confidential, only for specific distribution list defined on this document	**X**

Distribution list

Person and organisation name and/or group	Comments
WP3 & WP4 partners	
Executive Board	
Coordinator	
European Commission	

CARBOWASTE		
Work package: 4 **Task: :** 4.3	**CARBOWASTE document no:** CARBOWASTE-1203-T-4.3.3-b	**Document type:** T=Technical Report
Issued by: UoM **Internal no.:** CW1206-Deliverable-T-4-3-3-b		**Document status:** Final

Document title
Characterisation and Chemical Treatment of Irradiated UK Graphite Waste

Executive summary

The main objectives of the research were:

- Set up an active laboratory for research
- Isotopic determination of ^{3}H and ^{14}C
- Location and migration of ^{3}H and ^{14}C
- Mobility / removal of ^{3}H and ^{14}C
- Mechanism / species and rate determining steps of ^{3}H and ^{14}C release

It has been demonstrated that thermal analysis is an excellent technique for ^{3}H and ^{14}C determination; this has been validated through the Round Robin comparisons with other CARBOWASTE partner's results. Leaching has provided insight into ^{3}H and ^{14}C locations, mobility and removal mechanisms. This data has been used to suggest a possible mechanism behind ^{3}H and ^{14}C release rates and the differences in how ^{3}H and ^{14}C behave.

Revisions

Rev.	Date	Short description	Author	Internal Review	Task Leader	WP Leader
00	Dd/mm/yyyy	Issue	Name, Organisation	Name, Organisation *Signature*	Name, Organisation *Signature*	Name, Organisation *Signature*
01	01/12/2011	First issue	McDermott UoM	Jones UoM	Vulpius FZJ	von Lensa FZJ
02	19/03/2012	Final Issue	McDermott UoM	Jones UoM	Vulpius FZJ	von Lensa FZJ

Table of Contents

Table of Contents 4

List of Tables 9

Table of Figures 12

List of Analytical Equipment 16

Table of Symbols and Abbreviations 17

Abstract 21

Declaration 23

Copyright Statement 23

Acknowledgements 24

1. INTRODUCTION 25

1.1. Decommissioning the UK Graphite Moderated Reactors 25

1.2. Graphite Moderator, Reflector and Other Structural Components 26

1.3. Manufacturing Processes and Implications 28

1.4. UK Sources of Material and the Change in Raw Products 30

1.5. Activation of Graphite Impurities 35

1.6. UK Isotopic Inventory 37

1.7. Inventory Mechanism (Origins and Pathways) 38

1.8. Short and Long Lived Isotopes 42

1.9. Volumes of Waste 43

1.10. Classification of Waste 46

1.11. UK Repository Situation 48

1.12. Graphite in a UK Repository 49

1.12.1. Structural and Volume Changes to I-Graphite 51

1.12.2. Radiation Damage 51

1.12.3. Radiolytic Oxidation 52

1.12.4. Stored Energy 53

1.12.5. UK Disposal Facility - Drigg 53

1.12.6. Radioisotopic Release Pathways 55

1.13. Waste Management Options 56

1.13.1. Future Waste Management Options 57

1.13.2. Geological Repository 57

1.13.3. Thermal Treatment and recycling options 60

1.14. Summary of Introduction 64

2. LITERATURE REVIEW 65

2.1. Decommissioning 65

2.2. Chemical Leaching 66

2.2.1. Leaching Behaviour Determining Factors 71

2.3. Thermal Analysis 74

2.4. CARBOWASTE Current Initiative 78

2.5. Summary of Literature Review 80

2.6. Objectives of this Research 82

3. MATERIALS AND METHODOLOGY 83

3.1. Irradiated Graphite Used in this Study 83

3.1.1. BEPO Reactor History and Material Background 83

3.1.2. Isotopic Inventory and Material Availability 86

3.1.3. Wylfa Magnox Reactor History and Material Background 86

3.1.4. Wylfa Magnox Isotopic Inventory 89

3.1.5. I-Graphite Availability 90

3.2. Methodology 90

3.2.1. Controlled Laboratory Setup 90

3.3. Leaching Methodology 92

3.3.1. Liquid Scintillation Counting 92

3.3.2. Cocktail Analysis and Suitability 95

3.3.3. Leaching Parameters Investigated 97

3.3.4. Leaching Program 100

3.3.5. Leaching Phase One conditions 102

3.3.6. Leaching Phase Two conditions 104

3.4. Thermal Methodology 106

3.4.1. Furnace Setup 106

3.4.2. Trapping Agents 107

3.4.3. Recovery Checks and Validation 108

3.4.4. Validation of Inventory Through Round Robin Analysis 110

3.4.5. Comparisons to Pre and Post Leached Data 111

3.5. Microstructural Characterisation 112

3.5.1. Pore Structure Analysis 112

3.5.2. Tomography 112

3.5.3. Brunauer, Emmett and Teller (BET) Surface Area Analysis 114

3.5.4. Scanning Electron Microscopy (SEM) 116

3.5.5. Confocal Microscopy 117

3.5.6. Isotopic Distribution by Autoradiography 118
3.5.7. Crystal Structure Determination by RAMAN 121
3.5.8. Summary of Materials and Methodology 126

4. RESULTS AND DISCUSSIONS 127

4.1. Chemical Leach Treatment 127

4.2. Chemical Treatment Phase One 129
4.2.1. ^{3}H release under Phase One Conditions 129
4.2.2. ^{14}C release under phase One Conditions 132
4.2.3. Surface Area Effects on ^{3}H release 136
4.2.4. Surface Area Effects on ^{14}C release 138
4.2.5. Leaching Discussion 140

4.3. Chemical Treatment Phase Two 141
4.3.1. BEPO Channel 1 Leaching Results - All Conditions 141
4.3.2. pH 1 and pH13 Conditions 144
4.3.3. Acids Conditions 146
4.3.4. MAGNOX graphite leaching 149
4.3.5. Leach Rate Calculations 152
4.3.6. Leach Rate Results 153
4.3.7. Leach Rate Comparison of BEPO to Wylfa Graphite 159
4.3.8. Discussion of Chemical Leaching Results 162

4.4. Thermal Treatment 164
4.4.1. Round Robin Test (RRT) Validation 164
4.4.2. Determination of ^{3}H and ^{14}C Isotopes in BEPO Graphite 166
4.4.3. Determination of ^{3}H and ^{14}C Isotopes in Magnox Wylfa Graphite 169
4.4.4. Post Leaching Thermal Analysis 171
4.4.5. Summary of thermal treatment 175

4.5. Microstructural characterisation 176

4.5.1. Pore structure determination 176
4.5.2. Change in structure with irradiation – Confocal Microscopy 176
4.5.3. Tomography 179
4.5.4. Isotopic distribution by autoradiography 181
4.5.5. Crystal structure changes with irradiation damage 183
4.5.6. Surface Area Results 186
4.5.7. Overall Summary of Results 188

5. CONCLUSIONS AND FUTURE WORK 189
5.1. Major Findings 190
5.2. Comparison of Chemical Leaching Results 192
5.3. Suggestions for Future Research and Technical Developments 193
5.3.1. Publications 194

6. REFERENCES 196

List of Tables

Table number	Description
Table 1	Comparison of nuclear power reactor moderator materials, with values for the scatter, σs, and absorption, σa, cross-section, advantages and disadvantages
Table 2	Former UKAEA Gas Cooled Reactors (All shut-down)
Table 3	Magnox Reactors
Table 4	Advanced Gas Cooled Reactors
Table 5	Graphite impurity levels
Table 6	Activation reactions for producing ^{14}C
Table 7	Origins of tritium
Table 8	Types of decay and half life information for radioisotopes commonly found in irradiated graphite
Table 9	Former UKAEA Gas Cooled Reactors (All shut-down)
Table 10	Magnox Reactors in the UK
Table 11	Comparison of Magnox reactor core volumes
Table 12	Classification levels of Radioactive waste
Table 13	Shows the volume of waste that will be produced at all nuclear sites and final packaged volumes
Table 14	Parameters affecting leaching experiments and the possible variations
Table 15	Irradiation conditions of Wylfa samples used in this study
Table 16	Isotopic inventory data provided by NNL on the two Wylfa samples supplied for this research.
Table 17	LSC Terminology
Table 18	Prosafe HC analysis results showing the swamping nature of the cocktail used under 2.5M hydrogen peroxide conditions

Table 19 GoldStar analysis results showing the swamping nature of the cocktail used under 2.5M hydrogen peroxide conditions

Table 20 Leaching conditions employed in this research

Table 21 Stage One leaching conditions for BEPO channel 16 and 20 samples

Table 22 Stage Two leaching conditions for BEPO and Magnox Wylfa samples

Table 23 Background measurement performed on Instrument 406183 (5mls leachant added to 10mls Goldstar)

Table 24 Background measurement performed on Instrument 421298 (5mls leachant added to 10mls Goldstar)

Table 25 Background measurement performed on Instrument 406183 (5mls leachant added to 15mls Goldstar)

Table 26 Background measurement performed on Instrument 421298 (5mls leachant added to 15mls Goldstar)

Table 27 Thermal analysis definitions

Table 28 X-TEK HMX CT instrument settings

Table 29 Labeling of Raman Bands for Graphite

Table 30 Leaching Stage One BEPO channel 16 Leach rates

Table 31 Leaching Stage One BEPO channel 20 Leach rates

Table 32 Leaching Stage Two leach rates for BEPO Channel 1 samples

Table 33 Leaching Stage Two leach rates for BEPO Channel 16 samples

Table 34 Leaching Stage Two leach rates for BEPO Channel 20 samples

Table 35 Leaching Stage Two leach rates for Wylfa Magnox samples

Table 36 Comparison of chemical species used in leaching experiment

Table 37 Isotopic inventory data provided by NIREX on the BEPO graphite 7th December 2007

Table 38 Isotopic inventory data provided by NIREX on the BEPO graphite with half life correction to 2nd June 2011

Table 39 Isotopic inventory data determined by thermal analysis

Table 40 Isotopic inventory data provided by NNL on the two Wylfa samples supplied for this research

Table 41 Isotopic inventory for Wylfa samples determined

Table 42 Surface Area Results

Table of Figures

Figure number	Description
Figure 1	SEM image of PGA graphite showing needle-shaped coke particles
Figure 2	Schematic of the graphite manufacturing process
Figure 3	SEM image of SGL Coke used in the manufacturing process
Figure 4	Common radioisotopes found during decommissioning nuclear graphite
Figure 5	Principle particle energies of various radioisotopes relevant to decommissioning nuclear graphite waste
Figure 6	Waste volumes arising from each sector from existing facilities
Figure 7	Nuclear waste by volume
Figure 8	NIREX identification of information requirements related to repository design and construction
Figure 9	NDA Strategy for Magnox Stations: Decommissioning Approach
Figure 10	Comparison of ^{14}C to ^{12}C fractional release rate in solid and power Merlin graphite samples (MM and MP respectively) under various thermal conditions
Figure 11	The incremental dose to a member of the world population as a function of time after the year 2000 which was proposed as a start date for Magnox graphite burning
Figure 12	Schematic breakdown of the Carbowaste consortium
Figure 13	Photograph of the BEPO reactor
Figure 14	Graph of BEPO neutron fluence against channel number
Figure 15	Graph showing total activity of each graphite sample in MBq/g
Figure 16	Highlighted in red are the samples taken in 2007 from the Wylfa reactor 1 and used in this research
Figure 17	Graph showing the isotopic inventory present in the trepanned samples taken from the Wylfa reactor core in April 2007

Figure 18 Schematic representation of combustion furnace used during this project

Figure 19 Schematic and photograph of X-ray tomography scanner; the sample on the turntable would be inside an aluminum can

Figure 20 Calibration graph of thickness of HOPG sample inside a Harwell can versus the attenuation intensity of the transmitted incident photons

Figure 21 Photograph of the Tristar II 3020

Figure 22 Schematic of an SEM

Figure 23 Photograph of the Olympus LEXT OLS4000

Figure 24 ^{14}C Autoradiography calibration showing the correlation between activity and intensity

Figure 25 Raman spectrometer apparatus. The source of emission in Raman spectroscopy is generated using a laser

Figure 26 Vibrational modes of graphite showing Raman active and Infrared active breathing modes of the graphite structure

Figure 27 Two intense modes which are Raman Active for graphite

Figure 28 Photograph of Leaching stage two on test.

Figure 29 BEPO Channel 16 ^{3}H release under water conditions

Figure 30 Powder BEPO Channel 16 ^{3}H release under potassium bromate conditions

Figure 31 Powder BEPO Channel 16 ^{3}H release under hydrogen peroxide conditions

Figure 32 BEPO Channel 16 ^{14}C release under water conditions

Figure 33 Powder BEPO Channel 16 ^{14}C release under potassium bromate conditions

Figure 34 Powder BEPO Channel 16 ^{14}C release under hydrogen peroxide conditions

Figure 35 BEPO Channel 16 ^{3}H release under 0.3M potassium bromate conditions

Figure 36 BEPO Channel 16 ^{14}C release under 0.3M potassium bromate conditions

Figure 37 BEPO Channel 16 ^{3}H release under 1.5M hydrogen peroxide conditions

Figure 38 BEPO Channel 16 ^{14}C release under 1.5M hydrogen peroxide conditions

Figure 39 BEPO Channel 1 graphite ^{3}H release

Figure 40 BEPO Channel 1 graphite ^{14}C release

Figure 41 BEPO graphite ^{3}H release under pH1 and pH13 conditions

Figure 42 BEPO graphite ^{14}C release under pH1 and pH13 conditions

Figure 43 BEPO Channel 16 graphite ^{3}H release under acidic conditions

Figure 44 BEPO Channel 16 graphite ^{14}C release under acidic conditions

Figure 45 Magnox Wylfa ^{3}H release under all leaching conditions

Figure 46 Magnox Wylfa ^{14}C release under all leaching conditions

Figure 47 ^{3}H Leach rate comparison under all leaching conditions

Figure 48 ^{14}C Leach rate comparison under all leaching conditions

Figure 49 ^{3}H results from the RRT analysis for each laboratory

Figure 50 ^{14}C results from the RRT analysis for each laboratory

Figure 51 ^{3}H results for BEPO Channel 1 thermal and leaching data combined

Figure 52 ^{14}C results for BEPO Channel 1 thermal and leaching data combined

Figure 53 ^{3}H results for Wylfa Magnox thermal and leaching data combined

Figure 54 ^{14}C results for Wylfa Magnox thermal and leaching data combined

Figure 55 ^{3}H results for BEPO Channel 20 thermal and leaching data combined

Figure 56 ^{14}C results for BEPO Channel 20 thermal and leaching data combined

Figure 57 A three dimensional depth profile of BEPO Channel 1 sample

Figure 58	Laser images for BEPO Channel 1 and BEPO Channel 16
Figure 59	Laser images for BEPO Channel 1 and BEPO Channel 16
Figure 60	2D tomography Radiographs of BEPO sample 16 graphite contained within a Harwall can
Figure 61	3D volume reconstructions of BEPO Graphite using Amira© software
Figure 62	Graph showing the average intensity for BEPO samples calculated from Autoradiography greyscales
Figure 63	Autoradiograph photograph of increasing greyscale intensities for exposed BEPO samples
Figure 64	Raman Spectra of HOPG, PGA, Gilsocarbon, Magnox Wylfa and all BEPO samples
Figure 65	ID/IG ratios versus the crystallite size for polycrystalline graphite, irradiated PGA Magnox Wylfa and irradiated BEPO graphite
Figure 66	Graph shows full width half maximum of the G peak (FWHM) against ID/IG ratio for virgin and irradiated graphite

List of Analytical Equipment

Equipment	Model	Standard operational parameters
Autoradiography	Typhoon 9410 Amersham	Section 3.5.6.
Carbolite Furnace	Carbon-14 & Tritium Analyser (MTT)	Section 3.4.1.
Confocal microscopy	Olympus LEXT OLS4000	Section 3.5.5.
Liquid Scintillation Counter	Packard Tri-carb 3100TR	Sections 3.3.1. & 3.3.2.
Raman Spectrometer	Renishaw inVia spectrometer	Section 3.5.7.
Scanning Electron Microscope	Jeol JSM6300 Zeiss EVO60 VPSEM	Accelerating voltage 5 - 20kV Section 3.5.4
Tomography	X-TEK HMX CT	See Table 28

Table of Symbols and Abbreviations

Symbol / Abbreviation / Acronym	Definition
α	Alpha
AGL	Anglo Great Lakes Graphite Plant
ANDRA	The National Radioactive Waste Management Agency
Å	Angstroms
ANS	American Nuclear Society Standards
BAEL	British Acheson Electrodes Ltd
BEPO	British Experimental Pile Zero Reactor
β	Beta
CEA	Commissariat à l'énergie atomique et aux énergies alternatives
CNRS-ENS	Centre national de la recherche scientifique - Ecole Normale Supérieure
CoRWM	Committee On Radioactive Waste Management
COSHH	Control of Substances Hazardous to Health
CPM	Counts per minute
DIDO	Di-Deuterium Oxide Reactor
DPA	Displacements per atom
DPM	Disintegrations per minute
ε	Electron capture
EDF	Electricité de France
EDND	Equivalent DIDO Nickel Dose
EMN	The Ecole des Mines de Nantes

ENEA	Italian National Agency for New Technologies, Energy and Sustainable Economic Development
ENRESA	Empresa Nacional de Residuos Radiactivos,S.A
FNAG	Furnaces Nuclear Application Grenoble
FZJ	Forschungszentrum Jülich
γ	Gamma
GLEEP	Graphite Low Energy Experimental Pile
HOPG	Highly ordered pyrolytic graphite
HLW	High Level Waste
IAEA	International Atomic Energy Agency
ICRP	International Commission on Radiological Protection
ILW	Intermediate Level Waste
INR	Institute for Nuclear Research
IPNL	The Institute of Nuclear physics of Lyon
JRC	Joint Research Centre
LEI	Lithuanian Energy Institute
LLW	Low Level Waste
LLWR	Low Level Waste Repository
LSC	Liquid Scintillation Counting
LWR	Light Water Reactor
MW	Megawatt
MW(th)	Megawatt Thermal
n	neutron
NCRP	National Council on Radiation Protection and Measurements
NDA	Nuclear Decommissioning Authority

NECSA	The South African Nuclear Energy Corporation Limited
NII	Nuclear Installations Inspectorate
NITTETSU	Nittetsu Mining Co. Ltd
NNL	National Nuclear Laboratory
NRG	Nuclear Research and consultancy Group
OECD	Organisation for Economic Co-operation and Development
PBMR	Pebble Bed Modular Reactor
p	proton
PGA	Pile Grade A
pH	measure of the acidity or basicity of an aqueous solution
PIE	Post Irradiation Examination
pKa	Dissociation Constant is a measure of the strength of an acid or base
PMT	Photo-multiplier tube
RRT	Round Robin Test
σs	scattering cross-section
σa	absorption cross-section
SCK•CEN	Studiecentrum voor Kernenergie - Centre d'Etude de l'énergie Nucléaire
SIS	Spectral Index of sample
tSIE	Transformed spectral index of the external standard
UCAR	Union Carbide Industrial Gases Inc
UKAEA	United Kingdom Atomic Energy Authority
VLLW	Very Low Level Waste
WAGR	Windscale's Advanced Gas-cooled Reactor

Abstract

Once current nuclear reactor operation ceases in the U.K. there will be an estimated 99,000 tonnes of irradiated nuclear graphite waste which may account for up to 30% of any future UK geological ILW disposal facility [1]. In order to make informed decisions of how best to dispose of such large volumes of irradiated graphite (I-graphite) within the UK nuclear programme, it is necessary to understand the nature and migration of isotopes present within the graphite structure. I-graphite has a combination of short and long term isotopes such as ^{14}C, ^{3}H and ^{36}Cl, how these behave prior to and during disposal is of great concern to scientific and regulatory bodies when evaluating present decommissioning options.

Various proposed decontamination and immobilisation treatments within the EU Euroatom FP7 CARBOWASTE program have been explored [2, 3]. Experiments have been carried out on UK irradiated British Experimental Pile Zero and Magnox Wylfa graphite in order to remove isotopic content prior to long term storage and to assess the long term leachability of isotopes. Several leaching conditions have been developed to remove ^{3}H and ^{14}C from the irradiated graphite using oxidising and various acidic environments and show mobility of ^{3}H and ^{14}C. Leaching analysis obtained from this research and differences observed under varying leaching conditions will be discussed. Thermal analysis of the samples pre and post leaching has been performed to quantify and validate the ^{14}C and ^{3}H inventory.

Finally the research objectives address differences in leachability in the graphite to that of structural and operational variation of the material. Techniques including X-ray Tomography, Scanning Electron Microscopy, Autoradiography and Raman spectroscopy have been examined and show a significant differences in microstructure, isotope distribution and location depending of irradiation history, temperature and graphite source. Ultimately the suitability of the developed chemical treatments will be discussed as whether chemical treatment is a viable option prior to irradiated graphite long term disposal.

Declaration

That no portion of the work referred to in the thesis has been submitted in support of an application for another degree or qualification of this or any other university or other institute of learning;

Copyright Statement

i. The author of this thesis (including any appendices and/or schedules to this thesis) owns certain copyright or related rights in it (the "Copyright") and s/he has given The University of Manchester certain rights to use such Copyright, including for administrative purposes.

ii. ii. Copies of this thesis, either in full or in extracts and whether in hard or electronic copy, may be made only in accordance with the Copyright, Designs and Patents Act 1988 (as amended) and regulations issued under it or, where appropriate, in accordance with licensing agreements which the University has from time to time. This page must form part of any such copies made.

iii. iii. The ownership of certain Copyright, patents, designs, trade marks and other intellectual property (the "Intellectual Property") and any reproductions of copyright works in the thesis, for example graphs and tables ("Reproductions"), which may be described in this thesis, may not be owned by the author and may be owned by third parties. Such Intellectual Property and Reproductions cannot and must not be made available for use without the prior written permission of the owner(s) of the relevant Intellectual Property and/or Reproductions.

iv. iv. Further information on the conditions under which disclosure, publication and commercialisation of this thesis, the Copyright and any Intellectual Property and/or Reproductions described in it may take place is available in the University IP Policy (see http://documents.manchester.ac.uk/DocuInfo.aspx?DocID=487), in any relevant Thesis restriction declarations deposited in the University Library, The University Library's regulations (see http://www.manchester.ac.uk/library/aboutus/regulations) and in The University's policy on Presentation of Theses

Acknowledgements

I would like extend my thanks to Professor Barry Marsden who has been my supervisor throughout my studies and has continually supported my research and provided graphite expertise and valuable insight into graphite moderated reactors. I would also like to extend my thanks to the team at the Nuclear Graphite Research Group at the University of Manchester for continued support and would like to give special thanks to the following people who have contributed in some way to the direction of my research; Professor James Marrow, Professor Anthony Wickham and Dr Abbie Jones.

Additionally I would like to extend my gratitude to the following people from external institutes who have provided me with interesting feedback and many fruitful discussion; Professor Gareth Neighbour (Oxford Brooks University), Dr Werner Von Lensa (FZJ), Dr Johannes Fachinger (FNAG) and Dr Gabriel Piña (CIEMAT).

I am indebted to EPRSC, NDA and The CARBOWASTE Program for financial support throughout my research.

1. Introduction

This chapter provides an introduction to UK graphite moderated reactors and the graphite waste generated at the end of life. This research focuses on the origins of the graphite and various manufacturers which results in different characteristics and impurities present in the virgin material. Subsequently this chapter will outline the links between these virgin characteristics and impurities and how these parameters may contribute to nature the irradiated material and isotopic inventory. A review of waste management and UK repository options are discussed for irradiated graphite disposal. Outstanding factors from this information have driven forward this project and the need for further understanding of the irradiated material prior to disposal is highlighted here.

1.1. Decommissioning the UK Graphite Moderated Reactors

Graphite has been used as a moderator and neutron reflector in more than 100 nuclear power plants worldwide and in many research and plutonium-production reactors [4]. There are approximately 42 nuclear power stations in the United Kingdom (18 still operational), which when closed will produce somewhere in the region of 99’000 tonnes of irradiated graphite waste [5]. In a reactor nuclear graphite does not take part in the nuclear reaction, but in acting as a moderator it is subjected irradiation damage to the graphite crystal structure and in a carbon dioxide cooled reactors such as a Magnox or AGR radiolytic oxidation significantly reduces its weight. In considering the final graphite irradiated waste there are many variables to account for as each reactor design employed a different type of graphite and each reactor has a different operational lifetime history due to different coolant compositions, fast neutron dose and temperature history. Some of the initial impurities in the graphite will be transmuted into gamma and alpha emitting isotopes and radioactive impurities maybe entrained into the graphite microstructural porosity. As well as moderator graphite which may amount to approximately 2000 tonnes per reactor there is also a considerable amount of graphite operational waste mostly associated with the fuel [1,

6, 7]. All of this irradiated graphite waste will exhibit a range of isotopic contamination, weight loss and radiolytic oxidation that needs to be characterised and understood before an informed decisions can be made as how best to safely dispose of this considerable volume of waste.

Dismantling of reactor cores and empting wet and dry silos containing radioactive graphite waste followed by the management of radioactive graphite waste is becoming progressively an important issue in the UK and other countries, such as France, Germany, Spain, Italy, Russia, Ukraine, Lithuania, Japan, China and the USA [8-13]. Particular concerns associated with disposal of this material include the presence of several radioactive isotopes namely ^{3}H, ^{14}C, ^{36}Cl, ^{41}Ca, ^{55}Fe, ^{60}Co, ^{63}Ni, ^{90}Sr, ^{133}Ba, ^{137}Cs, ^{152}Eu, ^{154}Eu and some transuranics arising from trace uranium and fission products from failed fuel. One isotope of major importance is Carbon-14. ^{14}C it has a long half life of 5730 years and the environmental concerns related to this isotope are partly due to the possible release of radioactive methane gas or other harmful organics whilst decommissioning. It is a particular problem as the separation of ^{14}C from the majority of ^{12}C graphite waste is at present not practical. Tritium, ^{3}H, is also a significant issue whilst decommissioning as it is released easily from materials when they are drilled or moved. Cobalt 60, ^{60}Co, and Caesium 137, ^{137}Cs, are well documented on the radiation poisoning and harmful effects these two isotopes have on the environment and human population when released [14]. Chlorine 36 is also of major importance due to its incredibly long half life of 301,000 ± 4,000 years and its hydrophilic nature [15, 16]. Chlorine is readily dissolved by water meaning that Chlorine has a direct pathway into groundwater systems; this is of concern to several producers of i-graphite waste that contains ^{36}Cl however ^{36}Cl isn't covered in this research as the i-graphite used has no recorded amount of ^{36}Cl present.

1.2. Graphite Moderator, Reflector and Other Structural Components

Graphite was chosen as the material of choice for a nuclear moderator due to its ability to slow down the neutrons produced by the nuclear fission reaction, as a result of its high scattering cross-section and low cross-section for neutron capture. In order

to achieve the best performance from the graphite it requires the highest possible density and the greatest degree of purity. Other properties such as good mechanical strength [17], machine ability, high thermal conductivity and low thermal expansion are also important [18-20].

Table 1 Comparison of nuclear power reactor moderator materials, with values for the scatter, σs, and absorption, σa, cross-section, advantages and disadvantages [21].

Material	Density (gcm^{-3})	σs (barns)	σa (barns)	Advantages	Disadvantages
H_2O	1.0	49.2	0.66	Inexpensive	High absorption cross-section
D_2O	1.1	10.6	0.001	Good moderator	Expensive
Graphite	1.6	4.7	0.0045	Possible to construct entire reactor from it	High mass number therefore low slowing down power

Table 1 show how graphite may be used to slows down the fission products (neutrons) via the high scattering cross section in order to increase their probability of a future collision hence controlling the reaction rate. This material property of graphite is related the carbons low atomic number, just as the hydrogen molecules in water also acts a moderator within Pressurised Water Reactors the trade off is that water has a high absorption cross-section compared to graphite.

As well as acting as a neutron reflector or neutron moderator, graphite is also used for other features of reactor cores such as shield-wall graphite. It is also used for fuel channel liners (Chapelcross) fuel sleeves (AGRs and Hunterston A), fuel support struts (Berkley), Windscale boats and dowels. The core volumes range from 1100 tonnes in

early Magnox stations to over 3400 tonnes of graphite material in the largest reactors (e.g. the Wylfa Magnox reactors).

The speed of the neutrons that result from the fission reaction is travelling at 10,000,000 metres per second upon passing through the graphite moderator brick their speed slows to 2,000 metres per second [22]. If a neutron hits a carbon nucleus directly it consequently travel at a speed of 1,000,000 metre per second resulting in vacancies, interstitial atoms and cascades of movement within the carbon structure. The moderator within a commercial power generation reactor will change shape everyday of power generation with each carbon atom displaced approximately 20 times within the lifetime of a reactor.

1.3. Manufacturing Processes and Implications

It is well documented that nuclear graphite is manufactured from petroleum or natural pitch cokes [23]. Non-irradiated (virgin) nuclear graphite is a polygranular crystalline material that has an initial density in the range 1.6 - 1.8 g cm^{-3}. This can be compared with a theoretical graphite crystal density of 2.265 g cm^{-3}, the difference being due to internal porosity in the manufactured structure [4, 20]. The type and size of coke used and the manufacturing route largely determines the virgin graphite material physical properties. PGA was the graphite used in the Magnox reactors, and was produced from a Petroleum coke, which is a by-product of oil refining industry. The PGA coke has needle-shaped coke particles as seen in Figure 1. The PGA blocks were produced by an extrusion process, which tended to align the needle coke particles thus the crystallographic basal or layer planes tend to lie parallel to extrusion axis, giving rise to the anisotropic properties of PGA graphite.

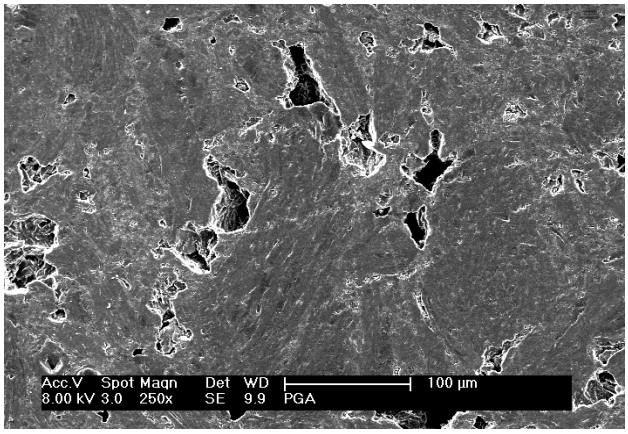

Figure 1 SEM image of PGA graphite showing needle-shaped coke particles.

In comparison to PGA, Gilsocarbon is a “more robust” graphite, especially developed for the AGRs. The final polycrystalline microstructure of Gilsocarbon is determined by the structure of the coke, the binder and also by the manufacture process. The naturally occurring asphalt pitch-coke was mined from Gilsonite veins, found between Colorado and Utah, USA [24]. The coke particles have an “onion skin” structure and the blocks were produced by a moulding process, which aimed to give a random coke orientation. This leads to the generally near-isotropic Gilsocarbon graphite properties. Gilsocarbon graphite has a higher density and strength compared to PGA and a lower porosity, which gives a lower radiolytic oxidation rate.

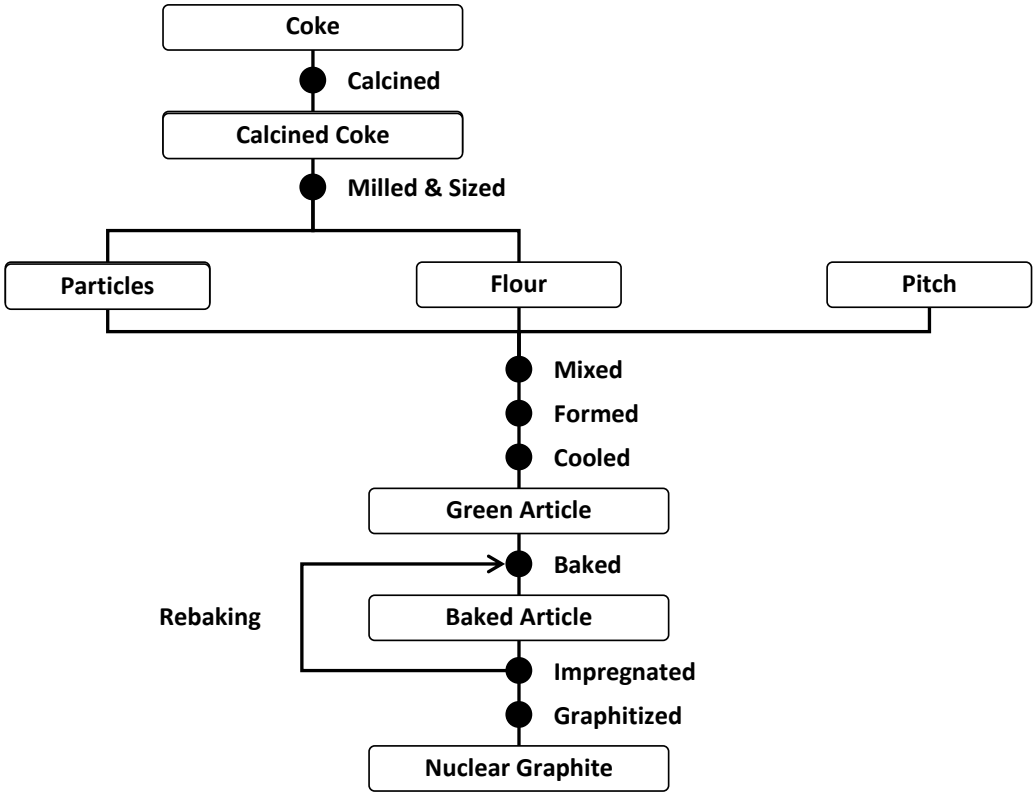

Figure 2 Schematic of the graphite manufacturing process

Figure 3 shows an SEM image of SGL Coke used in the manufacturing process which is explained by the schematic in Figure 2.

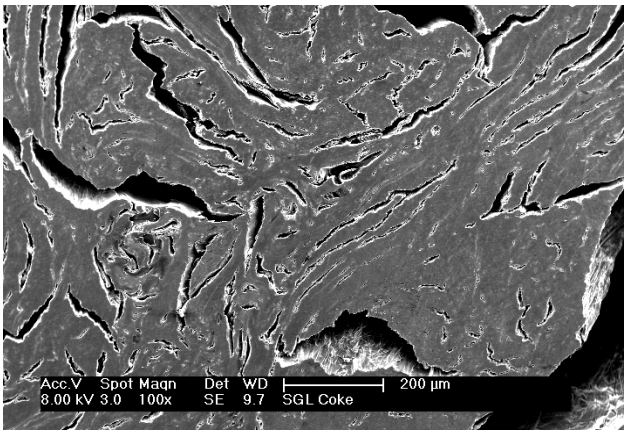

Figure 3 SEM image of SGL Coke used in the manufacturing process

1.4. UK Sources of Material and the Change in Raw Products

The UKAEA was responsible for the graphite supply to all the Magnox reactors, under the direction of Mr. (later Lord) Christopher Hinton. All Magnox Pile Grade A is

understood to have been produced from the same coke supply in Pernis, Holland. However various binder and impregnation pitches are likely to have been used in the graphite manufacture. Pile Grade B was used for the Magnox reflectors. In the first eight duel power plutonium and power production Calder Hall and Chapel Cross reactors this was the same grade as used in the Windscale Pile cores, however shortages in graphite supplies for the new range of “Civil” power producing reactors lead to the reflector graphite being manufactured from various sources depending on what was available at the time [25, 26].

Table 2 gives the details of the type of graphite used and manufacturer for the UKAEA reactors. The Graphite Factory was based at Anglo Great Lakes, Welland, Canada and the coke was sourced from Oil Refining Lockport, Illinois.

Table 2 Graphite source for former UKAEA Gas Cooled Reactors

Reactor	Graphite Manufacturer	Type	Pitch and Coke source	REF
GLEEP	Electro-metallurgical company	AGXP	Welland, Canada Lockport, Illinois	[27]
BEPO	Electro-metallurgical company	AGXP	Welland, Canada Lockport, Illinois	[28, 29]
Windscale Pile 1	Electro-metallurgical company, British Acheson Electrodes, British aluminum company	Sorted into Grade A Grade B Grade C	Welland, Canada Lockport, Illinois	[30]
Windscale Pile 2	Electro-metallurgical company British Acheson Electrodes British aluminum company	Sorted into Grade A Grade C	Welland, Canada Lockport, Illinois	[30]
WAGR	Electro-metallurgical company	PGA same as Magnox		[31]
DRAGON	Electro-metallurgical company	Various experimental graphites		[32]

Tables 2 and 3 breakdown the grade of graphite used in both the UKAEA gas cooled reactors and the Magnox reactors. With Lockport, Illinois and Sarnia, Venezuelan being the oil suppliers for the graphite manufacturing process and Welland, Canada the refinery. For all Magnox reactors the PGA Coke was sourced from Shell Oil refinery, Pernis, Holland and manufactured by AGL and BAEL. The PGB grade graphiote was initially AGXP then due to shortage of supply any “pure” graphite they could get hold of was used as PGB.

Table 3 Graphite source for UK Magnox Reactors

Station	Graphite Manufacturer	Type	Pitch and Coke source	REF
Calder Hall	British aluminum company	PGA PGB	Shell Oil refinery, Pernis, Holland Manufactured by AGL and BAEL	[33]
Chapelcross	British aluminum company	PGA PGB	Shell Oil refinery, Pernis, Holland Manufactured by AGL and BAEL	[33]
Berkley	British aluminum company	PGA PGB	Shell Oil refinery, Pernis, Holland Manufactured by AGL and BAEL	[33]
Bradwell	British aluminum company	PGA PGB	Shell Oil refinery, Pernis, Holland Manufactured by AGL and BAEL	[33]
Hunterston A	British aluminum company	PGA PGB	Shell Oil refinery, Pernis, Holland Manufactured by AGL and BAEL	[33]
Trawsfynydd	British aluminum company	PGA PGB	Shell Oil refinery, Pernis, Holland Manufactured by AGL and BAEL	[33]
Hinkley Point A	British aluminum company	PGA PGB	Shell Oil refinery, Pernis, Holland Manufactured by AGL and BAEL	[33]
Dungeness A	British aluminum company	PGA PGB	Shell Oil refinery, Pernis, Holland Manufactured by AGL and BAEL	[33]
Sizewell A	British aluminum company	PGA PGB	Shell Oil refinery, Pernis, Holland Manufactured by AGL and BAEL	[33]
Oldbury on Severn	British aluminum company	PGA PGB	Shell Oil refinery, Pernis, Holland Manufactured by AGL and SGL	[33]
Wylfa	British aluminum company	PGA PGB	Shell Oil refinery, Pernis, Holland	[33]

			Manufactured by AGL and SGL	

1.5. Activation of Graphite Impurities

The activation of isotopes in graphite may arise from several sources, these include elemental concentrations from impurities present within the graphite, transportation through the reactor system during operation via coolant, introduction through secondary processes such as fuel channel contamination or from core structural materials in contact with the moderator. In order to calculate the activity level of isotopes in irradiated graphite data from the elemental composition of nuclear graphite should be considered. Reference impurities concentrations have been taken from chemical analysis of graphite during early 1980's and is documented by White, Smith and Saunders [12]. Table 5 shows the typical impurity composition in parts per million (ppm) for PGA graphite used in Magnox reactors.

Table 5 Graphite impurity levels in PGA [12]

Element	Magnox (ppm)	Element	Magnox (ppm)	Element	Magnox (ppm)
Li	0.05	Mn	0.4	Gd	0.005
Be	0.02	Fe	10	Dy	0.008
B	0.1	Co	0.02	W	0.12
N	10	Ni	1.0	Pb	0.15
Na	1.0	Zn	0.13	Bi	0.08
Mg	0.1	Sr	0.4		
Al	1.0	Mo	0.1		
Si	35	Ag	0.001		
S	50	Cd	0.04		
Cl	2.0	In	0.05		
Ca	35	Sn	0.05		
Ti	3.0	Ba	1.5		
V	12	Sm	0.04		
Cr	0.35	Eu	0.005		

1.6. UK Isotopic Inventory

Particular concerns associated with disposal of this graphite include the presence of several radioactive isotopes namely:

^{3}H, ^{14},C ^{36}Cl, ^{41}Ca, ^{55}Fe, ^{63}Ni, ^{60}Co, ^{152}Eu, ^{90}Sr, ^{133}Ba and ^{137}Cs and some transuranics.

The isotopes of significance depend on quantity, half life, and free neutron kinetic energy. Figures 4 and 5 show the varying half lives and free neutron kinetic energy of the commonly found radioisotopes in nuclear graphite. The majority of activity present in nuclear graphite is associated with ^{14}C and ^{3}H.

Although graphite does not react with the nuclear reaction itself it is subjected to the activation products produced as a result of the nuclear fusion reaction and the high temperatures within a nuclear reactor. These activation products are radionuclides induced by the absorption of radiation, usually neutrons. Cobalt 60 is a significant activation product when decommissioning a reactor core as it has a half life of 5.3 years and it gives off both beta and gamma radiation. Tritium has a half life of 12.3 years and although it's a beta emitter the energy released by this radionuclide is very low making the main issue with tritium one of time. Tritium is derived from water, especially deuterium in heavy water and lithium in concrete. Large amounts of tritium are known to be removed easily during removal and transportation of nuclear graphite which gives rise to contamination of unwanted area's and increases the possibility of contaminating ground water systems.

1.7. Inventory Mechanism (Origins and Pathways)

The source of the radionuclides in graphite is likely to be a combination of the activation of an original impurity in the graphite (some of which may be gas trapped in the closed pores) together with general reactor operations including;

- Contamination introduced by the coolant during reactor operations
- Fuel types / changes in fuel cladding
- Fluence
- Location within reactor
- Contamination during PIE

Majority of activity present in i-graphite under analysis during this study is contributed by ^{14}C and ^{3}H. Table 6 shows some of the main activation reactions for producing ^{14}C and Table 7 shows some of the main activation reactions for producing tritium.

Table 6 Activation reactions for producing ^{14}C [22, 34, 35]

Reaction	Cross section (barns)		
	2200 m/s neutrons	**LWR neutron spectrum**	**Fast reactor neutron spectrum**
$^{13}C(n,\gamma) \rightarrow {}^{14}C$	0.9×10^{-3}	1×10^{-3}	0.5×10^{-6}
$^{14}N(n,p) \rightarrow {}^{14}C$	1.81	1.48	12.6×10^{-3}
$^{15}N(n,d) \rightarrow {}^{14}C$	0	0	1×10^{-3}
$^{16}O(n,{}^{3}He) \rightarrow {}^{14}C$	0	0	0.03×10^{-6}
$^{17}O(n,\alpha) \rightarrow {}^{14}C$	0.235	0.183	0.12×10^{-3}

Table 7 Origins of tritium

Pathway	Origin
$^{6}Li(n) \rightarrow {}^{3}H + {}^{4}He$ $^{238}U(n) \rightarrow$ tertiary fission products + ^{3}H	Contamination from association with tritiated material Direct material activation Contamination from the fission process

^{14}C is a long-lived beta emitter with a half life of 5730 years, it is produced by three nuclear reactions between ^{14}N (n, p) ^{14}C and ^{13}C (n, γ) ^{14}C that are contained in the graphite moderator and ^{17}O. ^{3}H has a half life of 12.3 years and is mainly produced from the neutron activation reaction ^{6}Li (n, α) ^{3}. Very small amounts of ^{3}H probably occur also from ^{3}He (n, p) ^{3}H and ^{2}H (n, γ). ^{3}H is a low energy beta emitter, leading to issues with tritium of detection and contamination. The environmental problems related to these isotopes are due to the possible release of radioactive methane gas or other harmful organics whilst decommissioning [36-38].

Table 8 Types of decay and half life information for radioisotopes commonly found in irradiated graphite

Radioisotope	Type of Radioactive decay				Half life (years)
	α	β	γ	ε	
^{3}H		✓			12.3
^{14}C		✓			5730
^{36}Cl		✓			300000
^{41}Ca				✓	130000
^{60}Co		✓	✓		5.3
^{85}Kr		✓			10.8
^{94}Nb		✓	✓		20000
^{95}Nb		✓	✓		0.096
^{133}Ba			✓	✓	10.5
^{134}Cs		✓	✓		2.06
^{137}Cs		✓	✓		30.2
^{152}Eu			✓	✓	13.3
^{154}Eu		✓	✓	✓	8.5
^{155}Eu		✓	✓		4.96
^{238}Pu	✓				87.75
^{239}Pu	✓				24390
^{240}Pu	✓				6537
^{241}Am	✓		✓		433
^{241}Pu	✓	✓			14.89

Other active contributory isotopes include ^{60}Co and ^{36}Cl [15]. ^{60}Co is a significant activation product when decommissioning a reactor core as it has a short half life of 5.3 years, emitting both beta and gamma radiation. ^{36}Cl has a half-life of ~ 300,000 years and is produced as a daughter product from krypton (produced the fission of U and Pu [39] and from trace amounts in the atmosphere) and from neutron activation of ^{35}Cl (n, γ), which remains from the purification of graphite in the manufacturing process. The long half-life of ^{36}Cl (with its subsequent low-specific activity) combined with the relatively low energy of its beta particle and small amount of gamma radiation limit the hazards associated with this radionuclide. Figure 4 shows a comparison of the half lives of commonly found isotopes present in i-graphite and Figure 5 shows the principle particle energies of these isotopes.

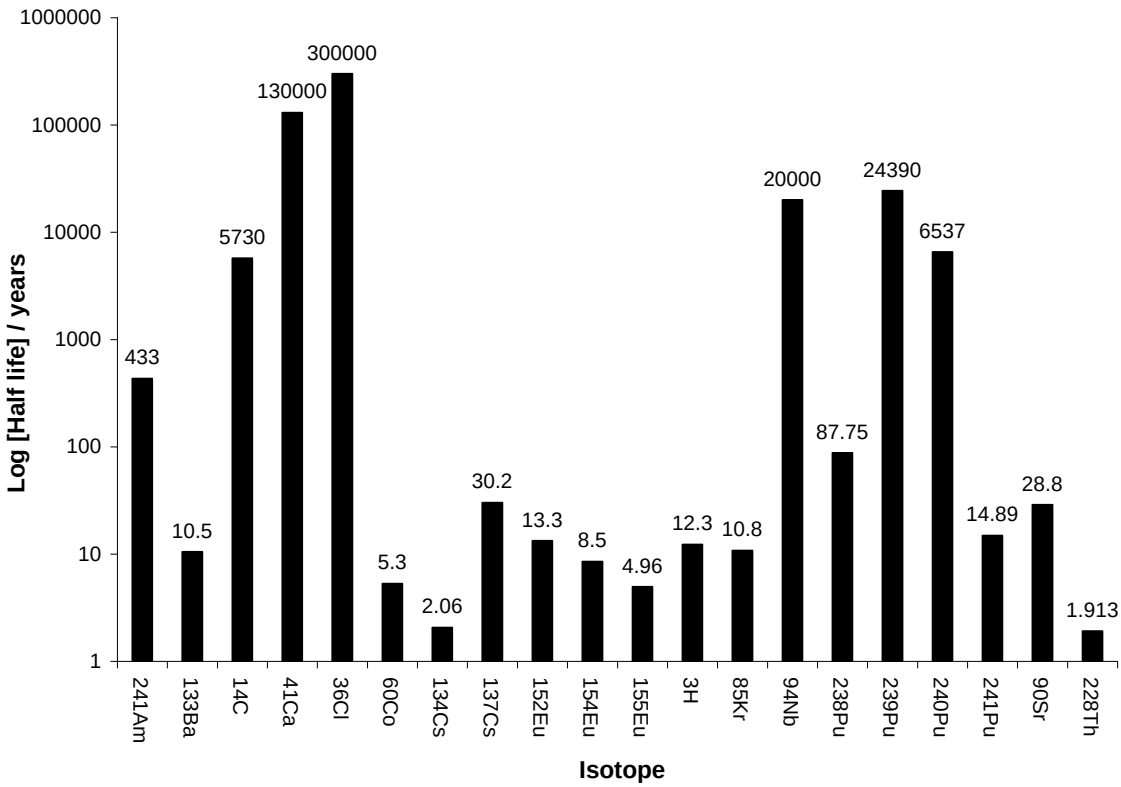

Figure 4 Common radioisotopes found during decommissioning nuclear graphite

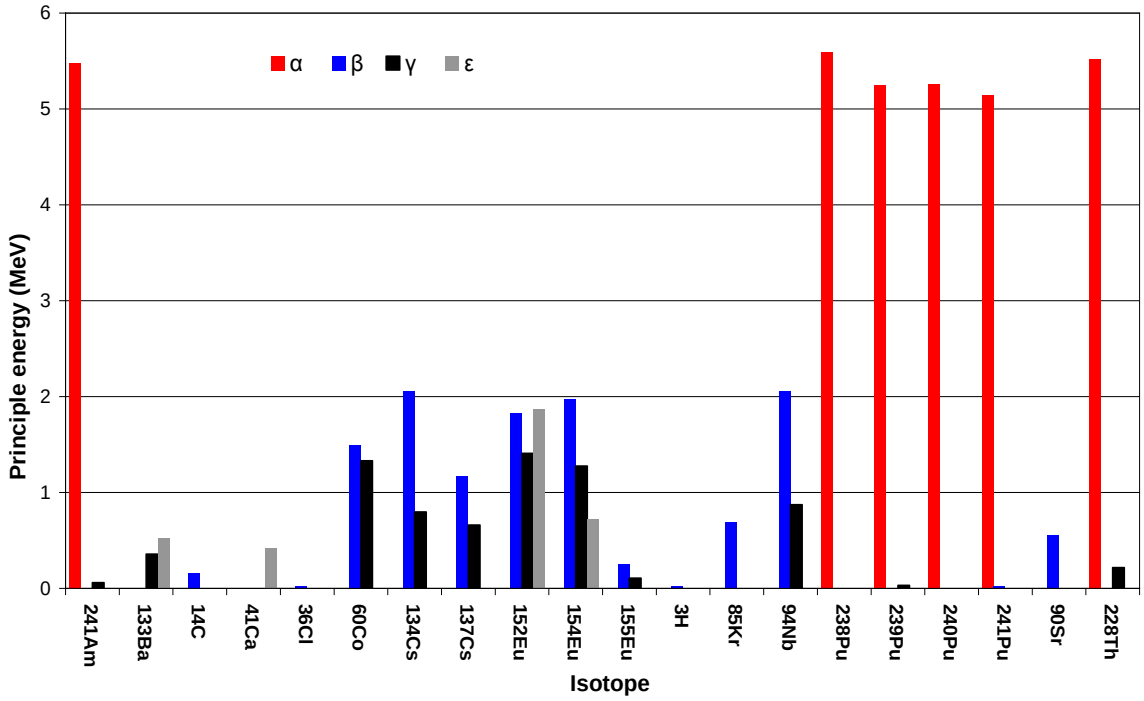

Figure 5 Principle particle energies of various radioisotopes relevant to decommissioning nuclear graphite waste

1.8. Short and Long Lived Isotopes

The radionuclide inventory of graphite can be divided into two categories:

Short lived isotopes: These isotopes have short half-lives <30 years and decay to insignificant levels after a few tens of years. They may pose issues for handling graphite immediately after reactor shutdown, but are less relevant to the consideration of reactor graphite disposability due to NDA's current Safe Store policy which delays Magnox reactor decommissioning for 80 to 100 years. Short lived radionuclides typically include, ^{60}Co (half-life of 5.3 years) and ^{3}H (half-life of 12.3 years).

Long- lived isotopes: These are key radionuclides for extraction during graphite treatment processing because they may pose radiological health issues through their release to the biosphere over the long term >30years. These typically include, ^{36}Cl (half-life 301,000 years), but principally ^{14}C (half-life 5,730 years).

1.9. Volumes of Waste

The main sources of UK Graphite Waste are from the ex-UKAEA reactors and the commercial fleet of reactors used for power generation. The ex-UKAEA, detailed in Table 9 Windscale Piles, British Experimental Pile Zero (BEPO) and Graphite Low-Energy Experimental Pile (GLEEP, now dismantled) plus a large quantity of operational waste from the Windscale Piles. There is also the High Temperature OECD Dragon Reactor at ex-UKAEA Winfrith [32]. This graphite included grades such as AGXPT, AGXP, Welland etc. see Tables 2 and 9 for the origin of the graphite used and the details of the reactor power and size. The Magnox Reactor as detailed in Tables 3 and 10 used Pile Grade A (PGA) graphite as a moderator and Pile Grade B (PGB) used in the reflectors (PGB consists of several grades of graphite). Significant numbers of fuel sleeves were manufactured from either PGA (early Magnox sleeves) or PGB graphite.

Table 9 Former UKAEA Gas Cooled Reactors (All shut-down) [40]

Reactor	Site	Type	Power MW(th)	Volume of graphite (te)
GLEEP	Harwell	Graphite moderated air cooled	0.05	505
BEPO	Harwell	Graphite moderated air cooled	6	766
PILE 1 & 2	Windscale	Graphite moderated air cooled	180	1966 (per pile)
WAGR	Windscale	Graphite moderated CO_2 cooled	105	210
DRAGON	Winfrith	Graphite moderated He cooled	20	27

Table 10 details all the magnox reactors built in the UK. This table gives information on commissioned date, total electrical power and shutdown date.

Table 10 Magnox Reactors in the UK

Station	Reactors	Commission date	Total electrical power(MW per reactor)	Shutdown date	Expected closure
Calder Hall	4	1956-1959	200	2003	
Chapelcross	4	1959-1960	200	2004	
Berkley	2	1962	276	1988-1989	
Bradwell	2	1962	246	2002	
Hunterston A	2	1964	300	1990	
Trawsfynydd	2	1965	390	1993	
Hinkley Point A	2	1965	470	2000	
Dungeness A	2	1965	440	2006	
Sizewell A	2	1966	420	2006	
Oldbury	2	1968	434	Reactor 2 2011	Reactor 1 2012
Wylfa	2	1971	950		2012

Table 11 shows the dimensions of several Magnox rectors in the UK today. This gives a clear image of the volume of material requiring decommissioning arising from each reactor core.

Table 11 Comparison of Magnox reactor core volumes

Station	Height (meters)	Diameter (meters)	Weight (tonnes)	
Windscale Piles	7.4	15.3	1966	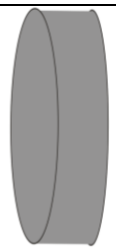
Calder Hall	6.4	9.45	1164	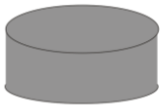
Chapelcross	6.4	9.45	1164	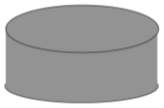
Hunterston A	7	13.5	1780	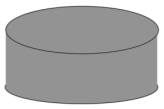
Hinkley Point A	8.8	16.2	2210	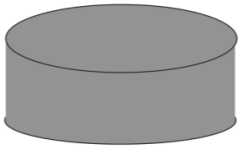
Oldbury	9.8	14.2	2090	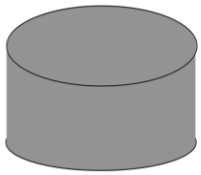
Wylfa	9.14	17.4	3470	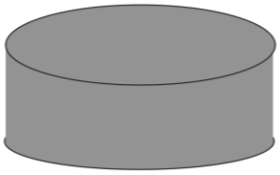

1.10. Classification of Waste

Material that is of not further use and has an activity above 0.001 GBq/te α or 0.04 GBq/te or β/γ is considered radioactive waste and requires consideration when disposal. Radioactive waste is divided into three main categories, high level waste (HLW), intermediate level waste (ILW) and low level waste (LLW). Very low level waste (VLLW) is typical used to allow institutions with very small quantities of radioactive waste to dispose of it via ordinary refuse or incineration. The classification of radioactive waste depends on the activity present and whether any heat is emitted. Table 12 breaks down the various classifications of radioactive waste based on its activity and heat emission.

Table 12 Classification levels of Radioactive waste [41].

Activity	Category	Description
>4 GBq/te α >12 GBq/te â/ã Increase in Temp.	HLW	Wastes which the temperature may significantly rise as a result of their radioactivity – must be factored into any disposal facility containing HLW.
>4 GBq/te α >12 GBq/te â/ã	ILW	Wastes which exceed the limits for low level waste but which do not require heat emission to be taken into account in the design and storage or disposal facilities.
<4 GBq/te α <12 GBq/te β/γ	LLW	Waste containing radioactive materials other than those acceptable for disposal with ordinary refuse, but not exceeding 4 GBq/te α or 12 GBq/te β/γ activity.
0.004 GBq/m^3	VLLW	Wastes which can be disposed of within ordinary refuse (dustbin), each 0.1 m^3 of material containing less then 400 kBq β/γ activity or single items containing less than 40 kBq β/γ activity. (Note no α allowance.)
<0.0004 GBq/te	Exempt	Materials which are exempt from regulations.

1.11. UK Repository Situation

A comparison of radioactive waste production in the UK compared to normal domestic waste claimed that 50,000 m3/year radioactive wastes are produced with an estimated 90% of this waste classified as low level waste. Normal domestic waste produces 40,000,000 m3/year of which 3,000,000 m3/year is poisonous solid waste which does not necessarily decay in toxicity over time [41, 42]. Focusing on the volume of activity was produced in the UK to date is 4.7 million cubic meters and Figure 6 shows the contribution from each industry within the nuclear sector [7, 43].

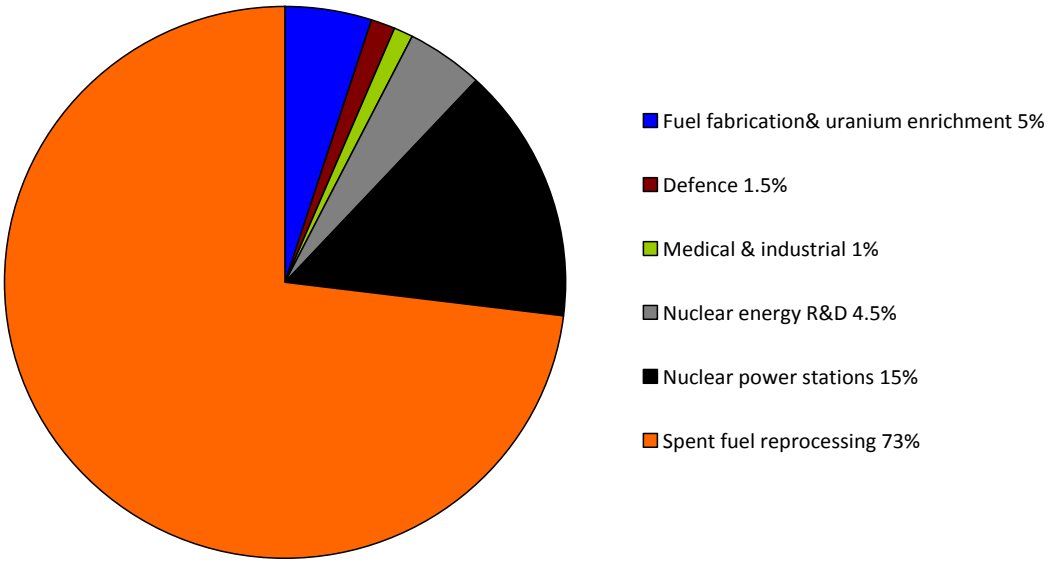

Total volume 4.7 million cubic metres

Figure 6 Waste volumes arising from each sector from existing facilities [7].

Approximately 94% of all this waste falls under LLW classification with the majority having risen from dismantling and demolition of nuclear facilities and removing contaminated land. The remaining 6 % is ILW and 0.1% is HLW, Table 13 gives these values in cubic meters [44]. Although the volume of HLW is small compared to the other waste types it will contain 95% of all radioactivity present across all waste categories [7].

Table 13 Shows the volume of waste that will be produced at all nuclear sites and final packaged volumes [44].

	Volume (cubic meter)	
Waste Type	**Raw, partly treated and conditioned wastes**	**Lifetime total once all wastes are packaged**
HLW	1020	1330
ILW	287000	488000
LLW	4430000	4550000

1.12. Graphite in a UK Repository

Graphite in a UK repository will make up 30% of the total proposed available volume [7]. Figure 7 shows a pie chart comparing nuclear waste by volume, highlighting what other nuclear wastes will make up the rest of the repository allowance.

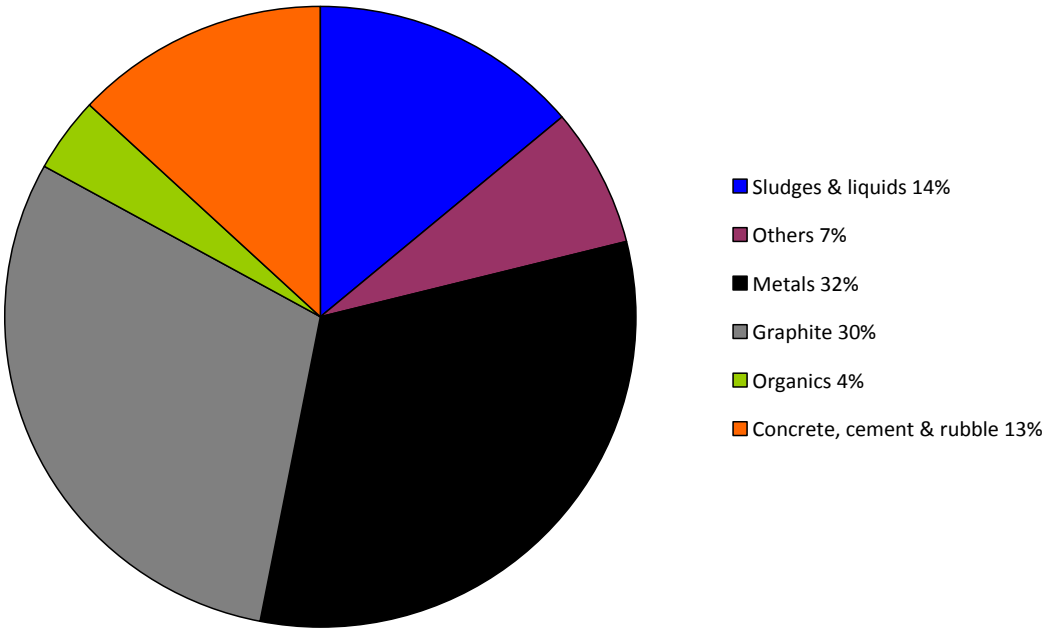

Figure 7 Nuclear waste by volume [45].

1.12.1. Structural and Volume Changes to I-Graphite

Irradiation damage to graphite induces significant changes to the properties including the strength of nuclear graphite. With increased irradiation the modulus increases until at very high doses the graphite structure starts to degenerate and the modulus falls significantly. The initial increase in modulus is accompanied by an increase in strength, which with continued irradiation follows a similar pattern to the modulus until the graphite degenerates at very high doses. Thermal and radiolytic oxidation also reduces the modulus and strength [46].

Bradford and Steer [47] note that it has been common practice in the nuclear industry to equate the change in graphite strength with its irradiation history. The bulk modulus of a graphite specimen may be influenced by the underlying crystal moduli, the degree of structural interconnectivity and the degree of porosity. Some care is required when relying only on the irradiation history as thermal annealing has been shown to reverse damage caused by the displacement of atoms from the graphite lattice. Nightingale [48] studied the thermal annealing kinetics of interlayer space damage in irradiated graphite at 100-750°C observed a reduction in the distance between graphite layers (indicating the removal of lattice defects).

1.12.2. Radiation Damage

Nuclear graphite is polycrystalline in nature and physical irradiation property changes are dominated by irradiation induced changes to the graphite crystallites [49]. The effect of irradiation on the crystallites is to expand in one direction and shrink, to a lesser extent, in the other direction. The consequence of this crystal dimensional change on the polycrystalline graphite component is critically dependent on the manufacturing route and the irradiation temperature. The changes in bulk volume lead to corresponding changes in density [46].

The irradiation damage produced in graphite by energetic neutrons has been extensively studied [50-52] because of the use of graphite as a moderator in thermal nuclear reactors. The effects of irradiation on the structure of graphite have also been

reviewed by Bradford and Steer [47]. In the early stages of irradiation, crystal dimensional change rates may be slow and there will be little, if any, closure of porosity and increase in structural connectivity. As irradiation proceeds, the rate of graphite material growth in the c-axis will increase and the original thermal stress cracks produced during manufacture will be closed. The rate at which this occurs is initially slow but increases as irradiation proceeds. This crystal shape change in the graphite matrix drives closure of porosity and an increase in the structural connectivity, causing the modulus to increase slowly.

Under continued irradiation, expansion along the c-axis will begin to strain the graphite structural network. Where this strain cannot be relieved by the breaking and reforming of connecting bonds, new porosity will be generated by microcracking. It was highlighted that due to the distribution of the pore and crystallite sizes, pore generation will not occur simultaneously and uniformly in all regions of the material. Consequently some regions of the bulk material will still be undergoing pore closure whilst others undergo pore growth.

1.12.3. Radiolytic Oxidation

Radiolytic oxidation occurs when carbon dioxide reacts with ionising radiation to produce an oxidizing species [53-57]. These reactive oxidising species absorb on a graphite surface, and lead to graphite oxidation. The rate of radiolytic oxidation of the graphite depends on the gamma energy absorbed by the carbon dioxide within the pores of the graphite. Graphite exhibits various degrees of radiolytic oxidation, which may be up to ~40% weight loss from the virgin state. This will have lead to degradation of the graphite properties, including hardness, strength and thermal conductivity. In the Dragon high temperature helium cooled reactor, at UKAEA Winfrith, where the graphite operated in an inert atmosphere radiolytic oxidation is not an issue.

For the Windscale Piles and in BEPO (Harwell), the irradiated graphite waste contains significant levels of stored (Wigner) energy. The rate of release of stored energy on heating has been known to exceed the specific heat of graphite, thus the release of

stored energy can be self propagating under certain circumstances. In Magnox reactor graphite the rate of release of stored energy does not exceed the specific heat of graphite due to the higher operating temperature. Hence even though there is a significant amount of stored energy in some of the Magnox graphite, the release of this energy has been shown not to be self propagating [50, 58, 59]. Stored energy is not an issue in the AGR graphite wastes, as these operate at higher temperatures.

1.12.4. Stored Energy

Irradiated graphite waste may contain stored Wigner energy [46], which may have consequential affects both in terms of dismantling and future repository environment. Wigner energy is energy stored within the graphite matrix in the form of displaced atoms. The quantity of accumulated stored energy is a function of fast neutron flux, irradiation time and temperature. The higher the irradiation temperature, the lower is the amount of stored Wigner energy. Wigner energy may be released if the graphite is heated to above its irradiation temperature, although a temperature in excess of 2000 °C is required to purge all Wigner energy [46].

It has been stated that in Magnox-type reactors, graphite temperatures lie in the range 180 - 360°C and accumulation of Wigner energy is limited to the cooler regions and even here the total stored energy saturates at levels which ensure that release rates upon heating are comfortably below the specific heat capacity[60].

The potential risk of triggering an inadvertent release of Wigner energy during graphite decommissioning, packaging, disposal and treatment is recognised as being small for the UK commercial reactor fleet. However, a management strategy for graphite may require the safe release of any stored Wigner energy to be taken into account.

1.12.5. UK Disposal Facility - Drigg

Drigg is a low level waste repository (LLWR) situated on the west cumbrian coast it has been operating since 1959, Drigg accepts waste from nuclear companies, defence sites, the healthcare sector, research establishments, hospitals, universities,

medical companies and the oil industry. The six radionuclide's considered in the Drigg database are ^{3}H, ^{14}C, ^{137}Cs, ^{226}Ra, ^{234}U and ^{239}Pu.

1.12.6. Radioisotopic Release Pathways

The location and bonding of radionuclides within graphite are important factors to understand in order to optimise treatment technologies that target the removal of radionuclides without significantly affecting the bulk graphite.

The location of radionuclides is a difficult to measure and may be spatially variable, thereby complicating the ease with which representative samples may be obtained. For activation products, the one way to improve our knowledge is to understand how radionuclides are generated and, if mobile, how they may migrate throughout the system. An understanding of graphite composition, initial impurity content, distribution of impurities and presence of open versus closed pores should allow an initial assessment to be made. For example, activation products may exist in lattice positions, in the spaces between graphite layers, in closed pores or on external surfaces and open pores.

An understanding of the operational history of the graphite, and potential impurities in reactor gases, will also give an insight into the potential for contamination which may be located on the external surfaces of the graphite.

There is scope for initial experiments to examine which radionuclides can be removed as a guide to location. These experiments could range from neutral solutions (water, most benign system) to increasingly more acidic solutions (aggressive systems). The species removed under different treatment conditions (e.g. concentration of acid) may give an insight into the distribution of nuclides, especially if the physical properties of the samples are also measured (e. g. surface area and porosity). The type and quantities of contamination and activation products in solution coupled with differing graphite sample behaviours may be used to draw some tentative conclusions about radionuclide location and ease of removal.

Investigation of the location, speciation and bonding of radionuclides in graphite is complicated by the low concentration of radionuclides relative to carbon, and the difficulty in determining the location of radionuclides in the graphite structure. It has been considered that leaching or desorption of radionuclides out of graphite matrices

(either by thermal or chemical treatments) is dependent on location and bonding mechanism [61].

Fission product transport through graphite matrices in unclad matrix type fuels has been reviewed [62]. Mobile elements identified were Xe, Kr, I, Br, Cs, Rb, Te and their daughter products of interest (Sr, La, Ba, Ca, Nb, Y, Te) were also studied. Gaseous products diffused easily throughout the graphite as would be expected. Non-volatile species were also able to disperse through the structure by diffusing across the surface of the graphite. The rate of migration was found to be dependant on temperature with significant increases in migration rates between 800 and 1500°C for precursors. Some species (Y and Zr) were found to form stable carbides and showed little diffusion and Barium contents were found to be reduced by 95% after heating for 16 hours at 1500°C. This shows certain nuclides may be more mobile than anticipated however it may be more of an issue for thermal processing techniques where these temperatures are regularly attained.

^{14}C produced from ^{13}C has been shown to concentrate at external surfaces in test graphite samples [63]. Neutron capture by ^{13}C resulted in the formed ^{14}C being ejected from the lattice. Dissipation of the resulting stored Wigner energy resulted in the annealing of these formed defects by re-forming the lattice structure.

1.13. Waste Management Options

Three general principles are employed in the management of radioactive waste.

- concentrate and contain
- dilute and disperse
- delay and decay

Concentrate and contain and dilute and disperse are also used for disposal of other types of waste not just radioactive waste. Concentration and isolation of waste is often used for highly toxic materials where other waste options are not available. Dilute and disperse focuses on reducing the volume of waste by dilution to an acceptable level prior to release to the environment. The third principle delay and decay is only applied

to radioactive waste and utilizes the possibility of temporary storage whilst the material decays prior to any other treatment of permanent disposal option.

Initially nuclear waste generated was dealt with in-house by the nuclear industry at each site. Waste being dumped at sea was the method utilized until this practice was suspended in 1983 and an international treaty prohibiting it in 1993.

Today any material that can not be treated and reprocessed or diluted and dispersed safely and within site allowances is either stored on site or transported to Sellafield or Dounraey for storage [64].

1.13.1. Future Waste Management Options

Listing all the possible waste management options for nuclear waste has already been carried out by the Committee on Radioactive Waste Management (CoRWM) [65]. CoRWM made recommendations for the long-term management of the UK's higher activity wastes that was designed to protect the public and the environment in 2006 [65]. The CoRWM committee came up with a very long list of possible waste management options which it then presented it’s final report with 15 recommendations. The CoRWM committee recommended that geological repository as the best form of long term management for the UK’s legacy nuclear waste. Further sections will go on to detail the present position of the UK’s Geological Repository and other treatment and recycling options that have been evaluated further aboard.

1.13.2. UK Geological Repository

In 2002 Nirex produced a report focusing on waste management and repository strategic decisions [66]. This report detailed the required assessment of six main aspects relating to repository design and construction as see in Figure 8. It also detailed the assessment of suitable sites for a repository as well as the monitoring procedure of a geological disposal facility for radioactive waste. This was based on the IAEA definition of repository monitoring which focuses on the engineering, environmental and radiological parameters ensuring that the repository is continuously in good working order and its operational impact on the environment.

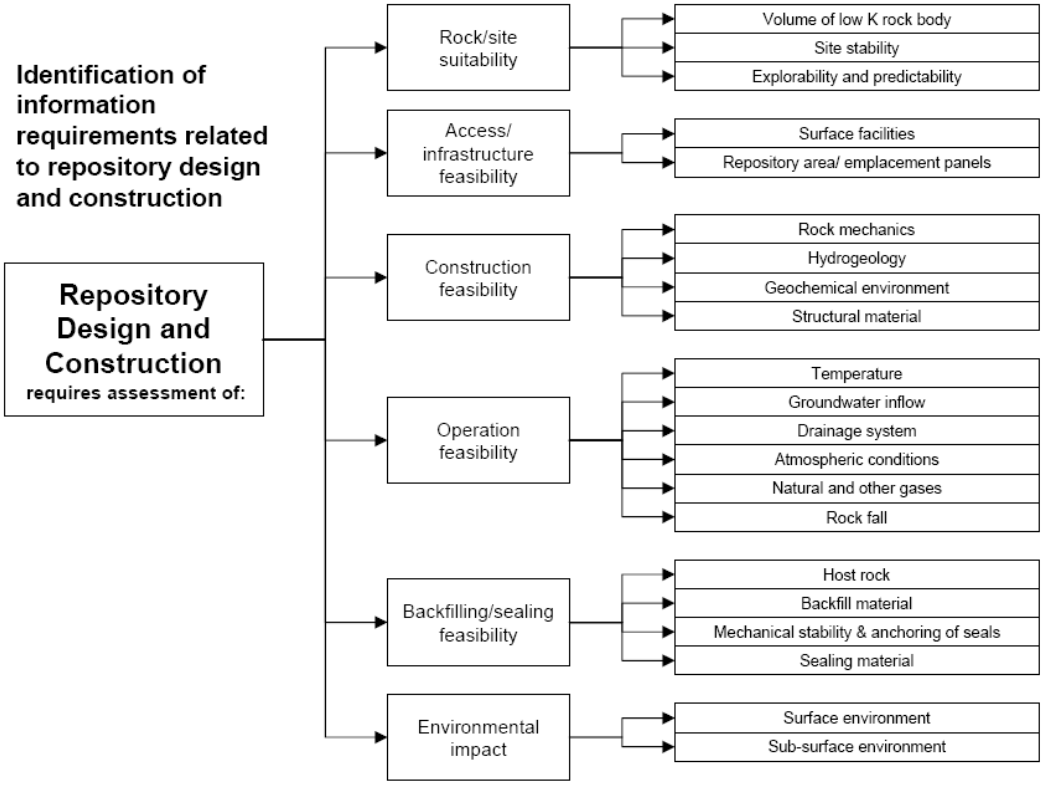

Figure 8 Nirex identification of information requirements related to repository design and construction [66].

The NDA's strategy was set out in 2006 in a very detailed document that explained the NDA's approach to decommissioning and long term storage of all the nuclear waste in the UK at that time [67]. The NDA policy on decommissioning and waste management was detailed in this document making reference to the CoRWM report [65]. This document details the plans for each nuclear site in the UK, detailing the type of waste produced, classification of this waste and how/when it will be decommissioned and stored. Figure 9 shows the schematic for the Magnox reactor decommissioning approach.

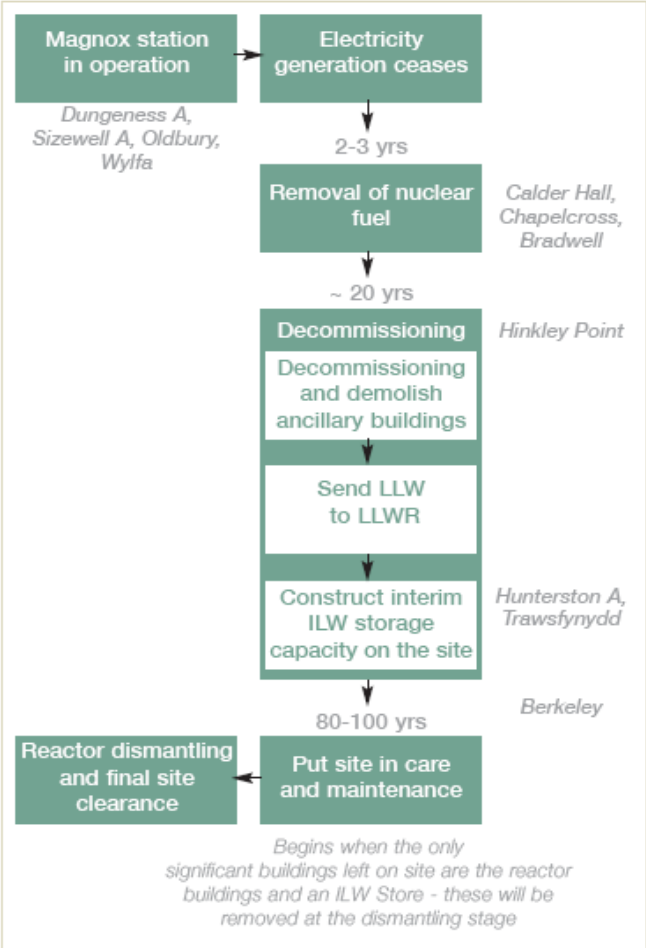

Figure 9 NDA Strategy for Magnox Stations: Decommissioning Approach [67].

In 2008 the NDA released a report on the consultation of the strategic environmental assessment (SEA) of the revised NDA Strategy and the UK Nuclear Industry Low Level Waste(LLW) Strategy [68]. This document detailed the amended geographical scope of the NDA's policies and included input from several government departments, council / heritage departments, the environment agency, NII, LLW Repository Ltd to name but a few. This list represents what factors are taken into considerable by the NDA, however some are specific to certain geological areas and as well as varying in importance on a local, national and international scale [68].

- Air Quality
- Global Climate Change and Energy
- Biodiversity, Flora and Fauna

- Landscape and Visual
- Cultural Heritage
- Geology, Ground and Groundwater Quality
- Surface Water Resources and Quality
- Waste
- Economy, Society and Skills
- Traffic and Transport
- Land Use, Natural and Material Assets
- Noise and Vibration
- Health and Safety
- Hazard Reduction
- Value for Money and Affordability

1.13.3. Thermal Treatment and recycling options

An example of thermal treatment and disposal of nuclear graphite is the Graphite Low Energy Experimental Pile (GLEEP) [69]. No radiological characterisation parameters are documented in this report, however GLEEP graphite is reported as LLW. The successful disposal of graphite from the GLEEP reactor using this methodology indicates graphite decommissioning using thermal treatment is a viable option [27, 70]. GLEEP graphite blocks were thermal treated in an industrial incinerator at 1423K for approximately 3 hours under a forced air supply. It is noted there is also the presence of other miscellaneous waste within the incinerator. Typically, 87% of tritium and 63% ^{14}C activity were removed from each block and a very crude net weight loss assessment of 6% calculated post-treatment.

To date there is little published work reported in the open literature which investigates the impact of thermal treatment, characterisation parameters and resulting isotopic release on irradiated graphite from commercial large scale graphite moderated reactors.

Recent studies conducted by FJZ (Germany) [71] have examined the corrosion behaviour of graphite under final repository conditions. Characterisation parameters included structural assessment of density, thermal conductivity, Young's Modulus, Thermal Expansion co-efficient and electrical resistivity. Radiochemical experiments were performed to assess the isotopic inventory using Gas-Chromatography mass spectroscopy, Optical and electron microscopy, surface area (BET), Gamma spectroscopy and X-ray diffraction. Thermal treatment showed that the highest concentration of ^{14}C is bonded to the surface and therefore is loosely bound in chemical terms. Chemical treatment have proved this ^{14}C may be removed from the ^{12}C through thermal treatment with Ar / O_2 [2]. These initial studies concluded that up to 60% of the ^{14}C and 80% of the tritium may be removed with a mass loss to the ^{12}C of only 5%. Although these studies are in their infancy, there is scope within FZJ to scale this up to a pilot treatment plant and the group are confident to achieve up to 95% ^{14}C loss in future experiments [72].

The recent international collaborative program: CARBOWASTE examines pyrolysis and thermal treatment further within the Treatment and Purification work package. Reactive gases such as Chlorine and Oxygen have been identified and are undergoing considerable investigation. The thermal radionuclide release could be increased by steam or other reactive gases (oxygen, halogens, hydrogen). However, this could lead to an increase of the graphite oxidation therefore; the influence of these components will be studied with respect to the radionuclide release rates and optimised with respect to a minimised graphite oxidation.

Steam Reformation has been proposed by Studsvik, and Bradbury [69] where the company quotes:

"graphite fragments are transformed by high temperature interaction with steam into two combustible gases (hydrogen and carbon monoxide). The gas treatment at the outlet of the reformer consists of a quencher, a scrubber, and a water condenser. After

oxidation and transformation into CO_2 and H_2O, the gas is released to the atmosphere through a HEPA filter."[46]

This published work claims "approximately 1200 tonnes of graphite" could be transformed into 10000 tonnes of calcium carbonate or 20000 tonnes of barium carbonate, which is very insoluble and prevents the release of radionuclide's into the environment [8] however initial volume reduction and radiological assessment is required.

Studsvik Inc. have a demonstration Steam Pyrolysis plant at Erwin, Tennessee with which Bradtec is a collaborator [73]. Studsvik have performed extensive work on processing low level radioactive waste via a patented Thermal Organic Reduction (THOR) process. THOR is a combined pyrolysis / steam reforming, fluidised bed treatment system [69]. THOR can process liquid, solid or slurry low level active waste. Studsvik claim THOR can offer consistent, reliable, robust operating characteristics with a volume reduction up to 80:1 and weight reductions up to 100:1 when processing is complete. Typical radionuclide partitions are used to separate ^{14}C, ^{3} A safety aspect advantage of THOR includes the plant housed in tightly controlled containment and therefore any loss of hazardous gases or materials are reduced significantly. Other advantages of this system include removal of Wigner energy, retention of gasified carbon for further processing if necessary, and separation of graphite (carbon) from radioactive contaminants and possible in-situ treatment of graphite from reactor core.

There is one final characteristic of decontamination by heating [8]. If the carbon in graphite is completely gasified (e.g. by steam reformation or air oxidation) the remaining non-volatile isotopes will be left behind as a residue, while semi-volatile isotopes (such as ^{137}Cs) may be collected with the non-volatile ones, or in adjacent low temperature zones. This behaviour has been confirmed in the Jülich study [71]. Total gasification provides the means to collect these isotopes in a concentrated form for waste management. This is a significant outcome, since the non- and semi-volatile isotopes include all the principal gamma-emitting ones. This allows all further

downstream operations with the carbon to be performed “hands on”. The separation of volatile non-carbon isotopes such as tritium and ^{14}C can be readily accomplished during gas phase processing: for example tritium can be converted to water and separated from the off gas, carbon dioxide; this off gas could incorporate with future carbon sequestration programs.

1.14. Summary of Introduction

This introduction section provides background information on the generation of irradiated graphite waste produced in the UK and the isotopes of concern. To summarise 99,000 tonnes of irradiated graphite is expected to be produced from the UK nuclear program which will take up approximately 30% of the proposed NDA repository [7]. A brief history of the reasoning behind why the UK has decided to focus on a repository approach to long term nuclear waste disposal [65, 67]. Given these decisions a need for irradiated graphite characterisation is urgent with both structural properties and radionuclide inventory essential to support engineering, environmental and radiological parameters of any proposed repository. Understanding the location and migration of the isotopes present in the UK graphite waste will play a large role in setting the repository parameters. Treatment options employed in this research focus on the leachability of ^{3}H and ^{14}C prior to long term storage in a repository. Removal of mobile isotopes and the reduction in i-graphite inventory will have significant affects on all aspects of long term storage and provide better understanding of just how mobile ^{3}H and ^{14}C are from i-graphite.

2. Literature Review

2.1. Decommissioning

The main issue associated with the disposal of irradiated graphite is the large volume of relatively low active waste to be dealt with [9, 11]. Current data released by the Nuclear Decommissioning Authority (NDA) [42] reports that 56,000 tonnes of Magnox, 25,000 tonnes of AGR plus graphite[74] from other sources including Windscale Piles and test reactors will lead to 99,000 tonnes of nuclear waste graphite in the UK. It should be noted that this weight estimate does not include the effects of oxidation weight loss, which will affect the majority of this graphite. The NDA current available option for 99,000 tonnes of irradiated nuclear graphite waste is deep geological disposal [6]. The NDA have calculated that the NDA-owned graphite would be in excess of 50,000 m^3, with packaged volumes in excess of 100,000 m^3 dependent on packaging factor volume taking into account that the graphite components are mainly large blocks with holes running through them which will significantly increase the packing volume. This volume would take up two thirds of a proposed UK deep repository. Various management/treatment options exist that may enable alternative re-use routes, the reduction of activity in the waste to levels that may enable disposal to LLWR and hypothetical alternative near surface facilities, or reduction in volumes that would allow a reduction in any proposed geological footprint.

In order to make informed decisions of how best to dispose of large volumes of irradiated graphite waste from the nuclear programme, it is necessary to fully understand the waste character and the consequent effectiveness of the various proposed decontamination and immobilisation treatments. These include various methods of encapsulation, and alternative preparative treatments for radiological reduction to LLW including disposal [75], reprocessing [76] and decontamination [46].This requires knowledge of the radionuclide inventory of the graphite and the behaviour of the graphite. Several studies in the UK, Europe and USA have attempted to understands the behaviour of radionuclides through chemical leaching [35, 46].

There has also been work carried out to thermally treat graphite waste in order to remove the long lived isotopes and significantly reduce the inventory, this chapter will detail the major findings of this research and outline the proposed methods which will be taken forward to drive the main aims and objectives of this thesis.

2.2. Chemical Leaching

The previous studies have focused on the decommissioning of nuclear graphite including both leaching and the thermal treatment of radioactive graphite. The first work published in the public domain on radioisotope analysis of Grade A graphite was carried out at the Argonne National Laboratories by Libby in 1946 [77], examining the radiocarbon chemical methods analysis to determine ^{14}C concentration and diffusion in the environment. Leaching studies on radioactive material by Hespe et al [78] in 1971 focused on standardising graphite leaching methods. Hespe concluded through measuring the changes in pH, gross alpha activity and gross beta / gamma activity, the most likely method mechanism for removal for radioisotopes in graphite would be transported by water in environmental conditions. In addition Hespe found radioisotopes of significant interest including the first reports on ^{14}C. Little reported work was carried out during the 1970's, however the interest in radioisotopes release was stepped up during the 1980's where many governmental groups concentrating their efforts on radioisotope release and mechanisms.

In 1982, Bush, Smith and White [22], discussed in detail the origins, production pathways of ^{14}C in reactor graphite and ^{14}C waste arising for each reactor type in production this was based on calculations of 10ppm of N_2 [1.8] Bush details analytical methods for the determination of ^{14}C and predicts both the gaseous and solid waste arising from ^{14}C from several reactor systems including Magnox and AGR. Little detail was published in the report by Bush, Smith and White[22] on leaching methodology, however the report documents conditioning of graphite waste through reduction, gaseous trapping and solid immobilisation which leads to a overview of final options of ^{14}C contain waste and radiological impact.

The oxidation of graphite in liquid water for radioactive waste storage applications was reported by Gray [79] in 1982, and provides useful background knowledge into the leaching behaviour of graphite in water. Gray found that graphite reacts with dissolved oxygen with water acting as a catalyst. In addition Gray carried out experiments on graphite irradiated by in a ^{60}Co radiation field. Gray carried out numerous experiments to confirm and correct gaseous leakage issues during his leaching experiments and demonstrated that through using a fused quartz vessel instead of Pyrex corrected this issue. Gray also compares graphite leach rates in water with various other materials such as concrete to find that graphite is at least three orders of magnitude more durable with a reaction rate 100 times lower than concrete. Gray's results obtained from the leaching experiments under ^{60}Co radiation show H_2 and CO_2 were the only gases released and hence the graphite was degassed after irradiation and prior to analysis, in order to determine whether a direct correlation between the graphite and oxygen concentration could be found. This was not the case and it was concluded that whilst irradiation had a substantial effect on the release of H_2, it had no measurable effect on the behaviour of any of the other gases.

In 1984, White, Smith and Saunders studied the assessment of graphite management options in terms of reactor decommissioning [12]. A full radiological assessment including methodology and models for common disposal routes with costing is well documented. Characterisation parameters of graphite included elemental analysis, decay routes, neutron flux profile, reactor inventory, activation inventory and reported knowledge of the operational and irradiation history of each reactor. The group detected ^{3}H, ^{14}C, ^{133}Ba, ^{60}Co and ^{134}Cs in the leachant from Magnox graphite which had been irradiated for approximately 13 years to ~ 1600 MWd/t, the samples had been removed from the reactor three years prior to the leaching analysis. Leaching rates were in the order of 10^{-5} cm / day White et al [12] reported that leach rates decreased by factors of 50-100 after 100 days and obtained steady state release rate for ^{14}C. Data specifying graphite weight loss post-treatment and surface area measurements are also published. Other radioisotopes may have been present in the graphite however; these were below the limits of detection. White, Smith et al.[12] also concluded that

any ^{134}Cs originated from the activation of ^{133}Cs, present as a trace impurity in the graphite.

Gray and Morgan [80] studied the leaching rates of ^{14}C and ^{36}Cl in Hanford reactor graphite. Leaching was conducted using solid graphite samples in deionised water and Hanford ground water for 52 days at 25°C. ^{14}C and ^{36}Cl leaching mass loss rates are reported in the order of 10^{-6} g m^2 / day with results and a cumulative leach fraction quoted in the range of 1.6 $x10^{-6}$ averaged for five samples. Characterisation parameters published include radiological analysis of the graphite; the activity of ^{14}C leached out and the specific surface (BET) area. The recommendations of this paper suggest further testing to be carried out more in-depth concentration profiles of individual isotopes, which is a reflection on the uncertainties of the results produced.

The leaching of ^{14}C and ^{36}Cl of irradiated French graphite was studies by Gray and Morgan in 1989 [81]. This report is based on comparative work between France and the US in 1988 [80]. Leaching both French and Hanford graphite for conducted for 90 days at 20°C using deionising water, where the entire volume of leachant was changed at the given sample intervals. The leach rates of solid submerged samples are compared in both studies and contrasted with that of White et al in 1984 [12]. The leach rate of Hanford graphite is in the order of 10^{-5} and 10^{-3} from that of the French. The data obtained from the French graphite support the hypothesis that ^{14}C leach rate exceeds that of ^{12}C.

In Japan, Takeshiat [82] and Takahash [61] have investigated the morphology and impurity of nuclear grade graphite. Leaching mechanism of ^{14}C concluded to a disposal safety assessment in terms of public safety for decommissioning a reactor in Japan with a graphite moderator known to have large amounts of ^{14}C. Leaching tests were carried out on the irradiated graphite for 720 days. Prior to any experimental work, the graphite surface was removed to minimise any contamination, which is a common trend among leaching experiments. Contamination of i-graphite can arise from:

- The coolant gas

- Experiments carried out during the reactor lifetime
- Accidents
- Changes to operational parameters
- Sample extraction, transportation and PIE
- Interim storage such as a contaminated / heavily used glove box or cave

In Takeshiat [82] and Takahash [61] experiments three different size particle powders were produced, it is unclear as to whether whole graphite pieces were analysed, however a full radiological characterisation programme was performed prior to leaching using Inductively Coupled Plasma Mass Spectroscopy (ICPMS) and leaching ratios for $^{14}CO/^{12}CO$ where published. These leaching experiments were carried out under alkaline (oxygen) conditions $H_2SO_4/KMnO_4$ solution, however no precise concentrations of volumes are detailed in the paper regarding the leaching solutions. $H_2SO_4/KMnO_4$ was reported to be used to accelerate the leaching of ^{14}C, however over 90% of the ^{14}C activity, remained in the graphite with a leach rate ratio of 10^{-5} reported.

AMEC [83] have published limited data from leaching tests performed on a PGA WAGR graphite spigot ring, which were used to locate the WAGR moderator blocks together in the vertical direction as well as to centre the fuel element. This ring was removed some ~23 years after WAGR was shut down. Specific radiological activity of the ring was characterised using ICPMS before leaching, however the operational history of the spigot ring and the fluence was not reported, and it is known that WAGR operated with a variety of coolant compositions including a high methane concentration. Despite very low detection limits of 0.002 Bq / ml for ^{14}C and 0.007 Bq / ml ^{3}H; the measured activity in the blank samples was the same as in the experiments, demonstrating inconclusive results. 33 samples in total were crushed, which may contribute to the low detection of Tritium and large error observed in leaching rates, also the deviation in graphite surface area may have been a contributing factor in the experiment procedure.

AMEC [31] published a further report in April 2009 on the experimental study of WAGR and BEPO graphite. The objective of this work was to measure the release of ^{14}C and ^{3}H under alkaline aqueous conditions against time. The experimental apparatus included two separate catalysts and a pre-bubbler which was designed to capture ^{14}C and ^{3}H release in different chemical forms. Calcium hydroxide solution was used with 20 grams of solid irradiated graphite sample being placed into 250mls of solution. During this experiment it was recorded that the catalyst was contaminated with ^{3}H which gave rise to high blank readings and possible cross contamination between samples. A flushing process was introduced which was deemed effective but significantly increased analysis time; this was implemented from week 12 onwards. Both graphite samples released very small $<10^{-5}$ quantity of active carbon monoxide gas. The BEPO graphite was calculated to have fractionally released 0.08% ^{14}C and 0.31% ^{3}H inventory into the alkaline solution over the course of this experiment. It is unclear whether this leaching procedure was semi-dynamic or dynamic in its approach as the report does not detail whether after 5mls of the solution had been analysed if fresh solution was then replaced.

SERCO released a report on longer term release of carbon-14 from irradiated graphite in July 2009 [84]. The aims of this report focused on speciation and rate of release of ^{14}C gas from BEPO graphite in an alkaline solution (NaOH) over 431 days. Isotopic inventory wasn't performed on the sample prior to analysis this is most reflected on the 368% of tritium released in the aqueous phase. ^{14}C released in the aqueous phase was reported at 0.02% with very low release rates reported for both ^{3}H and ^{14}C in the gaseous phase. It was reported that isotopic release was following a 1st order kinetics and that release rate dropped to 3 Bq day^{-1} per kg towards the end of the 14 month experiment.

A recent summary of the published studies on the leaching of radionuclides from graphite has been comprehensively presented in the IAEA Tecdoc [46]. It was reported that the leaching mechanism for carbon species is a water catalysed oxidation by dissolved oxygen to form carbon dioxide. This report documents evidence that

supports ^{14}C oxidisation rate and release of oxidised species and leached at a greater rate than stable ^{12}C in the early stages.

Known leaching methods for nuclear graphite have not significantly advanced since 1940's. Leaching mechanisms have been predicted however to date have not been widely validated. There has been immense amounts of attention is placed on figure of leaching rates in the order of 10^{-5} however realistically predicting the migration and long term possible unwanted chemical reactions in deep repository conditions is no small task when a standardised universal leaching technique is not well established. Generally, leach rate experiments on irradiated graphite are initially rather erratic tend to stabilise within the experimental timescales which have been on the order of 70–140 days [12, 46, 81]. An interesting observation is that the results quoted on leaching studies illustrate the differences between sample history, geometry, porosity, leaching methodology, sampling frequency and quoted leach rate. This drives a further the need for comparable data on material specific to the reactor of interest prior to decommissioning.

2.2.1. Leaching Behaviour Determining Factors

The reviewed papers detail how techniques and methodology vary from different sources, influencing the interpretation of published leach rate and in affect reduces the comparability of data. It is often difficult to compare leaching data for graphite due to the experiment been designed for a particular application or situation which is not directly transferable. A typical example of this is seen in the usual sample geometry and sample surface area to leachant ratio found in the latest SERCO report for the NDA [85]. Table 14 highlights some of the influencing parameters which have been applied in previous leach tests and how these parameters have been varied. Validation of the parameters can be justified through many sources including application of international Standards[86]. These Standards have been published by the IAEA [87], ISO [88] and ANS-16.1 [89]; adapted for graphite encapsulation leaching. These all highlight important techniques and best practices to apply when considering carrying

out a leaching experiment for the application of an inter-comparison test in addition to the environmental method.

Table 14 Parameters affecting leaching experiments and the possible variations

Influencing Parameter	Variation	Methodology
Type of test	Dynamic Semi-dynamic Static	IAEA[87]
Temperature	Room temperature or elevated	Experimental monitoring through test
Providence and sample history	Graphite source and manufacturer Coolant Fluence Weight loss Post closure history Post closure time Removal method and storage Avoidance of contamination during PIE Location within reactor	Known sample history essential IAEA[87]/ANS 16.1[89]
Inventory	^{14}C and ^{3}H variations and distribution γ isotopes and influences	Pre leaching characterisation γ analysis
Location of isotopes	Homogeneous distribution Inhomogeneous distribution	Structural and Radiochemical
Leaching duration	Short (<90 days) or long term (>90 days)	IAEA[87]
Testing frequency	Daily Weekly Monthly Yearly Combination	IAEA [87]/ ANS 16.1[89]
Results interpretation	Cumulative release rates Fractional release rate Leach ratio Leach rate	Comparison to existing data
Sample type	Solid Powder	Geometry and mass recorded
Porosity	Ratio of open to closed pores	Structural analysis

Influencing Parameter	Variation	Methodology
	Accessibility of internal microstructure	
Sample size	Geometry and mass variations	Geometry and mass recorded
Surface area and volume ratio	Isotopic / chemical solubility Leach rate pH	IAEA[87] / ANS 16.1[89]
Leachant	Acids Alkaline Oxidising environments Water Brine Ground water	IAEA[87] Buffered solutions to provide standardisation
pH	Changes	Buffers
Chemical form	Liquid or gaseous Organic or inorganic	Pre and post isotopic determination ICPGCMS
External environment	Room temperature changes Reduced conditions or in air	Monitoring and recording of all changes

2.3. Thermal Analysis

Thermal analysis of graphite is primarily used quantify the total ^{14}C and ^{3}H content in irradiated graphite waste. In researching the various reviews for thermal analysis, papers which have investigated the use of thermal treatment are comparable in technique. The objectives thermal treatment focuses on reducing a large volume of irradiated waste essentially to a small volume of concentrated high activity waste and a residual LLW or ILW. When evaluating suitable methods to quantify the chemical leaching behaviour of graphite, these treatment methods may be applied to determine the total ^{14}C and ^{3}H content of the pre and post leached graphite The following review will focus on however is not limited to graphite incineration and how this is applied at laboratory scale.

An example of thermal treatment and disposal of nuclear graphite was applied to the UK Graphite Low Energy Experimental Pile (GLEEP) reactor. As the irradiation fluence to GLEEP graphite was very low, the resulting radiological fingerprint associated with the graphite core of GLEEP allowed it to be free released for incineration, which was carried out at 1423K for 3 hours in a forced air furnace. It was reported that 87% of the ^{3}H and 63% ^{14}C was removed with only a approximately 6% graphite weight loss due to thermal oxidation [8, 69]. This was an important observation as it implied that the removed (Oxidised) ^{14}C was located on the surface perhaps in the form of a sooty deposits generated in this low energy low temperature air cooled reactor. The observed reduction in the activity of the graphite from the GLEEP reactor using this methodology pointed to the possibility that graphite decommissioning using thermal treatment maybe a viable option [70, 90]. The experience gained in the decommissioning of GLEEP highlighted both the potential effectiveness of ^{14}C and ^{3}H removal through incineration and the application of thermal treatment on a large industrial scale.

X.Hou [36] carried out the rapid analysis of ^{14}C and ^{3}H in both graphite and concrete samples using both acid digestion and thermal oxidation. The determination of the limit of detection is a well planned approach to calculating the accuracy of the oxidiser

used, even though there are multiple dilutions of the ^{14}C and ^{3}H before liquid scintillation counting. No significant difference was observed between the measured concentrations of ^{14}C and ^{3}H this indicates that using the sample oxidizer method and the acid digestion method for determination of ^{14}C and ^{3}H in graphite and concrete was relatively effective and accurate. A further interesting observation is the varying relative standard deviation (RSD) for the concrete showing that the distribution of ^{14}C and ^{3}H was unevenly distributed in the concrete samples compared to graphite. The oxidiser regularly achieved 95% efficiency when analysing both concrete and graphite. This value was calculated by using a spiked representative sample of known ^{14}C and ^{3}H concentrations and comparing the measured Becquerel's with the known value. Finally this work discussed the possible interference of other isotopes such as ^{129}I, ^{36}Cl and ^{99}Tc and the effect this would have on the efficiency of the LSC.

The most influential recent study was undertaken in Germany (2004) by Fachinger and Podruzhina [71]. This work compared graphite taken from German Merlin research reactor's thermal column and graphite removed from the AVR prototype pebble bed HTR reflector and investigates the fractional release of ^{14}C and ^{3}H as a function of time and temperature (up to 1060°C). Diffusion co-efficient for isotopes contained within the graphite samples were calculated as was the normalised release of ^{14}C and ^{3}H in inert atmospheres. Under all experimental conditions ^{14}C and ^{3}H where found to release faster than the graphite could be oxidised. Under inert atmospheres the release rate of ^{14}C and ^{3}H was 20% and 43% respectively over 15 hours at 1055°C with a reported 0.16 – 1.36% bulk weight loss. Under steam conditions, the release rate of ^{14}C and ^{3}H was 100%, this was over 14 hours at 1055°C with a reported 42% bulk weight loss. This work also concluded that ^{3}H was highly mobile under thermal conditions and significant quantities released regardless of type of thermal treatment employed. A significant finding however was that diffusion of ^{3}H within the graphite matrix was dependent on the graphite's providence and operational conditions as AVR graphite required a longer time to full remove all of the ^{3}H. In addition it was found that ^{14}C was not uniformly distributed through the graphite; it was proposed that this was the result of the uneven distribution of nitrogen gas within the virgin material.

Figure 10 is taken from the Podruzhina report which compares the fractional release rate of ^{14}C to ^{12}C [71] under argon and steam thermal conditions and different temperatures. This graph clearly demonstrates the preferential oxidation and removal of ^{14}C using thermal treatment on a lab scale is an excellent tool for determining the quantities of ^{14}C and ^{3}H in irradiated graphite.

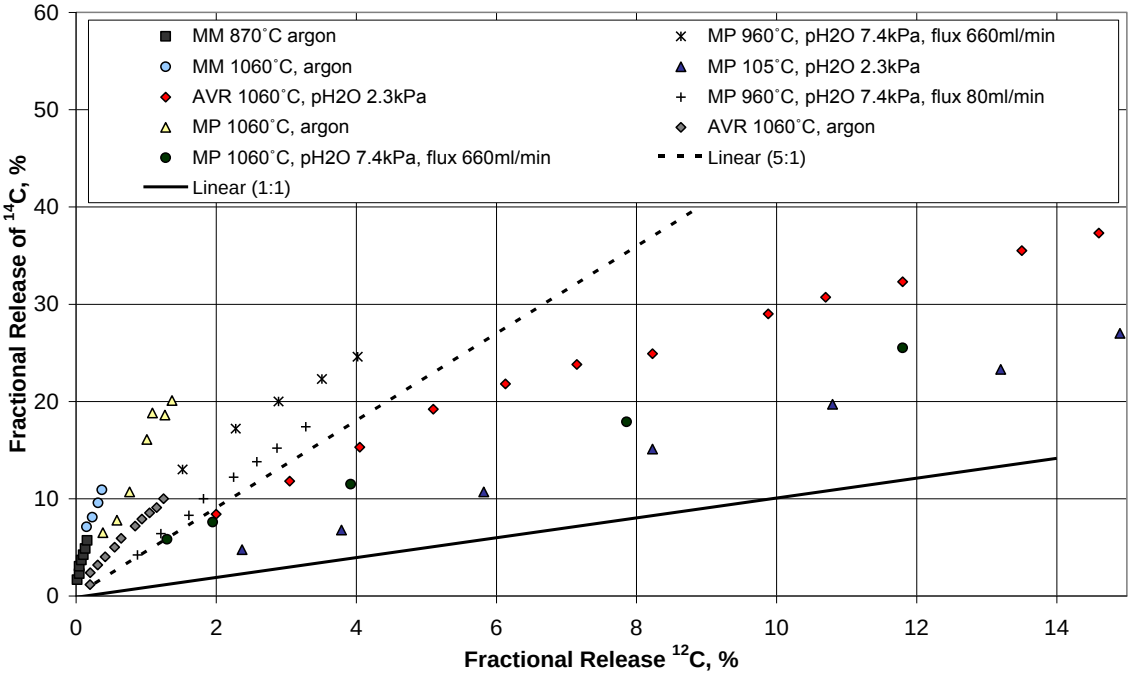

Figure 10 Comparison of ^{14}C to ^{12}C fractional release rate in solid and power Merlin graphite samples (MM and MP respectively) under various thermal conditions [71].

Other approaches to thermal work have examined the recycling aspects, through extraction and separation. The socio-economic implications of total graphite incineration are discussed below.

Nair [91] produced a model for global dispersion of ^{14}C release to the atmospheres as CO_2 in 1983 from theoretical incineration of a Magnox reactor. Nair's research developed models which were validated by comparison to experimental data, the focus was on Global dose rate. The importance of this work highlights the possibility of using thermal treatment on a large scale. The paper proposes the thermal treatment

of one Magnox reactor per year every 20 years and discusses the effect this will have on the environment and global population in the long term. The results show that the incremental dose does not exceed a value three orders of magnitude smaller than the cosmic-ray induced ^{14}C background and six orders of magnitude smaller than the average background dose from all UK sources; Nair's results can be seen in Figure 11.

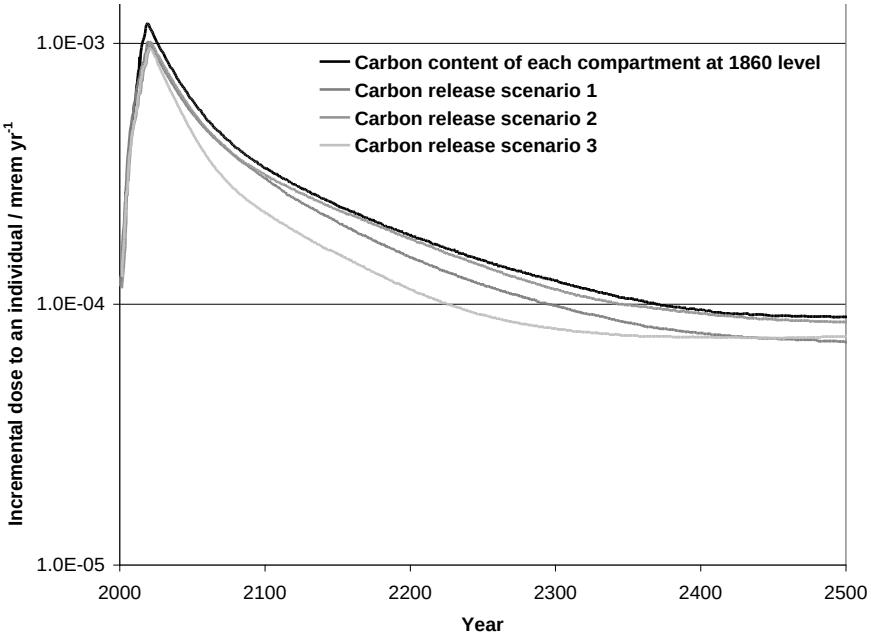

Figure 11 The incremental dose to a member of the world population as a function of time after the year 2000 which was proposed as a start date for Magnox graphite burning [91].

White, Smith and Sauders [12] evaluated the possible of graphite incineration in 1984, and concluded although ^{14}C and ^{3}H content would be discharges into the atmosphere; incineration would constitute an additional cost in decommissioning. In 1984, these costs where estimated to be in the region of £15,000 per tonne of graphite [12].

In 2002 Takeshita et al [82] studied the recovery of ^{14}C from a Graphite moderator of a Gas-Cooled Reactor (GCR) This work focuses on ^{14}C extraction via chemical exchange, with the aim of producing a more recyclable approach to managing irradiated graphite. The work takes a different approach to thermal treatment and focuses on the

application of the re-absorption of ^{14}C and recycling. It was concluded that such high volumes of intermediate irradiated graphite waste would require a more practical ^{14}C enrichment process than ^{14}C extraction via chemical exchange.

Thermal treatment of graphite is an alternative method for graphite decontamination that maybe quite complex due to the emissions of gaseous ^{14}C species and other organics which may have an environmental impact, therefore a detailed understanding of this would be required for any viable scaled up thermal treatment options. On a laboratory scale thermal analysis has a proven track recorded as a suitable tool for ^{14}C and ^{3}H determination in i-graphite. The thermal methodology Section 3.4 details experimental parameters, calibrations, recovery checks and overall accuracy achieved by this technique when used for i-graphite analysis.

2.4. CARBOWASTE Current Initiative

Recent studies have identified that it is possible to decontaminate large amounts of graphite waste through the use of chemical treatments [8]. The objective of the decontamination is usually to remove the surface layer of the graphite (including pore walls) which may contain the majority of the bulk activity (^{14}C) by dissolution. A European Project entitled; Treatment and Disposal of Graphite and other Carboneous Waste (CARBOWASTE) was launched in April 2008 under the 7th EURATOM Framework Programme (FP7-211333), the objectives of the program were to address irradiated graphite examine treatment methodologies and provide a full overview for graphite from disposal to decommissioning [92]. CARBOWASTE is managed under six work packages (WP) which focus on: (WP1) Integrated Waste management approach, (WP2) Retrieval and segregation, (WP3) Characterisation and Modelling, (WP4) Treatment and Purification, (WP5) Recycling and New Products and finally, (WP6) Disposal behaviour of graphite and carbonaceous waste. The CARBOWASTE program aims to achieve experimental work which will underpin modelling and further develop best practice methodologies and databases with a multi-national approach, to order to provide long term assessment and progress towards irradiated graphite disposal.

The CARBOWASTE consortium is comprised of 30 partners from 10 European countries plus the Joint Research Centre (JRC) and South Africa. Figure 2 [93] shows a breakdown of the various members within CARBOWASTE within there sector and includes:

- Nuclear industries (AMEC NNC, AREVA NP, Doosan Babcock, PBMR)
- Waste management companies (Bradtec, Studsvik)
- Utilities (EDF)
- Graphite manufacturers (GrafTech, SGL-Carbon)
- Waste management authorities (ANDRA, NDA, ENRESA)
- Research Facilites (CEA, CIEMAT, ENEA, FI, FZJ, INR, JRC, LEI, NNL, NRG, SCK•CEN, NECSA)
- Universities (EMN, CNRS-ENS, IPNL, The University of Manchester)

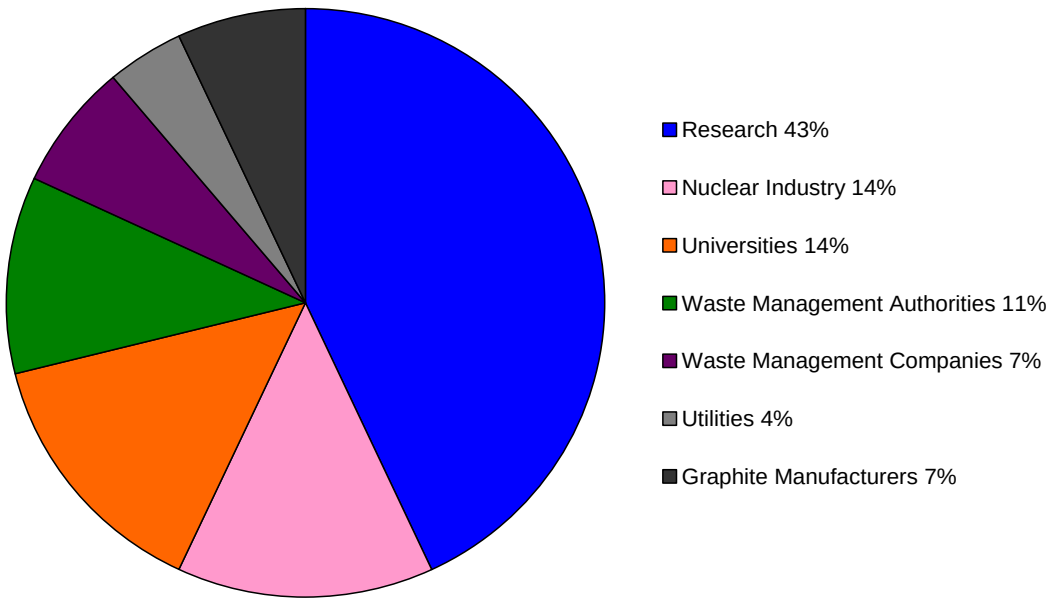

Figure 12 Schematic breakdown of the CARBOWASTE consortium [2]

CARBOWASTE has identified several options for chemical decontamination including, acid treatment, liquid decontamination agents and aggressive leaching. The graphite used in this research consists of Magnox graphite, materials test reactor graphite

(MTR) and EDF (Pechiney) [2]. Full characterisation and modelling program is underway in order to determine the stability of the nuclides in nuclear graphite before and after treatment and to identify the mechanisms by which impurities / radioisotopes may be removed from the nuclear graphite waste. In addition a 'Round Robin cross-comparison exercise has been performed to determine the quantity of isotopes ^{14}C, ^{3}A database of these findings, with possible mechanistic pathways for isotopic removal is a projected outcome from this project which will be available to CARBOWASTE partners and will enable a cross comparison of the findings of this research for validation.

2.5. Summary of Literature Review

This chapter reviews the existing available knowledge on graphite decommissioning and treatment. Leaching studies have highlighted the difficulty in standardisation of leach tests and the ability to compare cumulative fractional release rates against work carried out at different institutions. Often experimental methodologies differ greatly resulting in inconsistent leaching rates, differences in test duration, temperature, sample size, sampling frequency and leachant used. The general trend is to have conducted leach tests under deionised water or Brine (salt water), with the focus principally driven toward long term behaviour in a theoretical repository environment. Comparison of cumulative fraction leach data for such situations ranges significantly from 10^{-2}-10^{-6} at 20 - 25°C. This review highlights in inhomogeneity of irradiated graphite and the need for good characterisation in terms of providence, radiological distribution and inventory.

Little published research exists into the effects of chemical treatment on irradiated graphite in order to leach mobile radioisotopes such as ^{137}Cs and ^{3}H prior to disposal. Methods such as aggressive leaching with acids and oxidising agents have not been extensive investigated. The aim of the studies has mainly been to successfully remove or reduced the graphite waste isotopic content significantly, primarily focusing on ^{14}C as a long lived isotope present in significant quantities within all irradiated graphite. Further characterisation work is now essential in order to understand the mobility, distribution and chemical form of the isotopes. It is evident from this literature review

that there is not sufficient pre and post leaching characterisation analysis at present detailed in the publications. Further characterisation would highlight any irradiated graphite structural or isotopic inhomogenity which may result in discrepancies between tests.

2.6. Objectives of this Research

- To determine the type and location of impurities and radioactive isotopes in virgin and irradiated graphite
- To determine the stability of radioisotopes before and after treatment
- To demonstrate and validate the removal of radionuclide's from graphite waste by chemical treatment
- To understand the structural changes to irradiated graphite before and after treatments and how these changes may influence leach release rates
- To provide treatment options offering the potential to decontaminate, reduce radionuclide inventory and limit uncontrolled release of radioisotopes to the environment with the potential to reclassify irradiated graphite to LLW

3. Materials and Methodology

This chapter gives a detailed history and background of the material used in this project. Material availability and suitability are also discussed as well as any underlining issues arising from the material used. The focus of this chapter then aims to give insight into the equipment used and methodologies employed throughout this research.

3.1. Irradiated Graphite Used in this Study

Two types of irradiated graphite material were used in this project. Irradiated graphite samples where collected from the British Experimental Pile Zero (BEPO) Energy Reactor and made available for research by the University of Manchester. The second irradiated graphite material was sourced from the Wylfa Magnox Reactor 1.

3.1.1. BEPO Reactor History and Material Background

The British Experimental Pile Zero (BEPO) Energy Reactor was commissioned in 1948 and closed in 1968. BEPO was graphite moderated, air cooled and initially fuelled with natural uranium metal in aluminum cans. Two grades of enriched uranium fuel were used at a later date within the reactor. BEPO was initially used for the production of plutonium, but later this function was transferred to the Windscale piles with BEPO becoming a research reactor [94]. BEPO's role as a research reactor included isotope production, studying the irradiation behaviour of graphite and it was also used in studies for coolant compositions for the Magnox and AGR reactors. Figure 13 shows a photograph taken of the BEPO reactor.

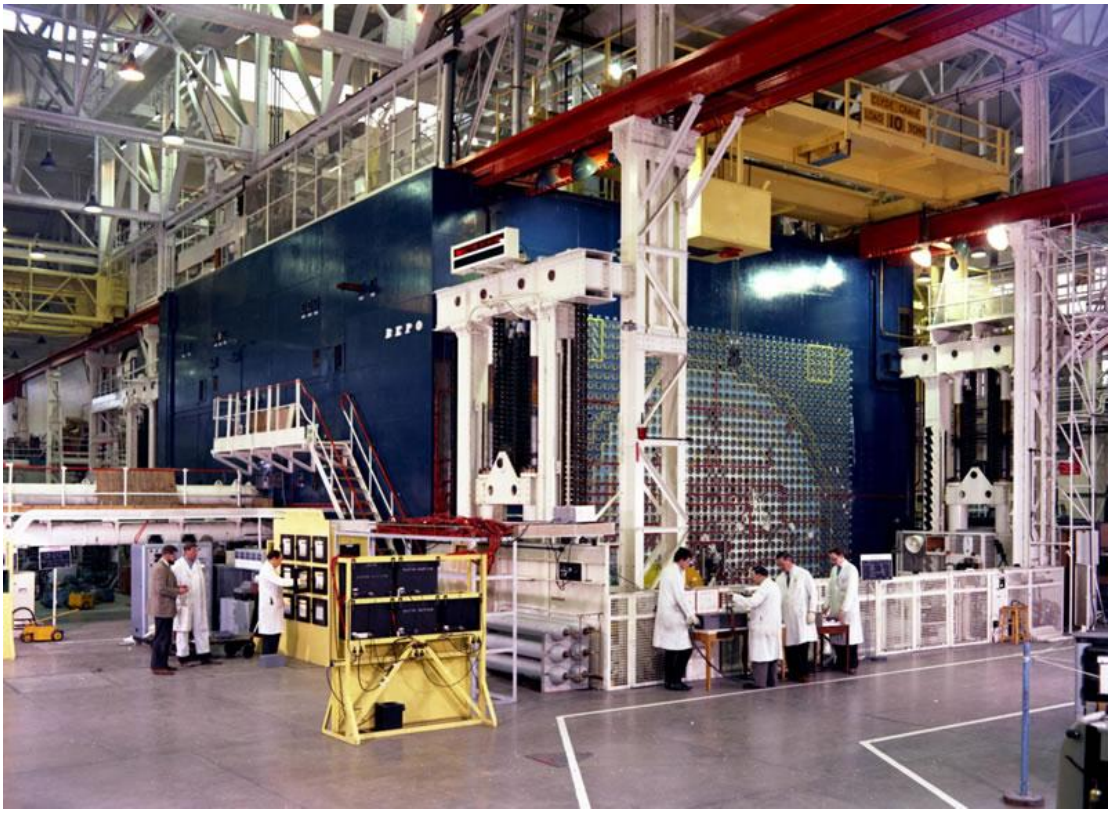

Figure 13 Photograph of the BEPO reactor.

In 1975 a four inch cylindrical sample was trepanned from the BEPO core, through the control face of the pile, steel shielding, concrete bioshield and the 20 columns of graphite blocks [95]. From this core the samples used for analysis at The University of Manchester were taken. Sampling was initially carried out in 1975 to provide radioisotope data on the graphite, steel and concrete, and to evaluate the Wigner energy. It was retrieved using a diamond-tipped hole cutter using no coolant or lubricant. After retrieval the core was re-sealed and the reactor remains this way at Harwell to date [95]. Figure 14 shows the fluence of neutrons experienced by each channel [95].

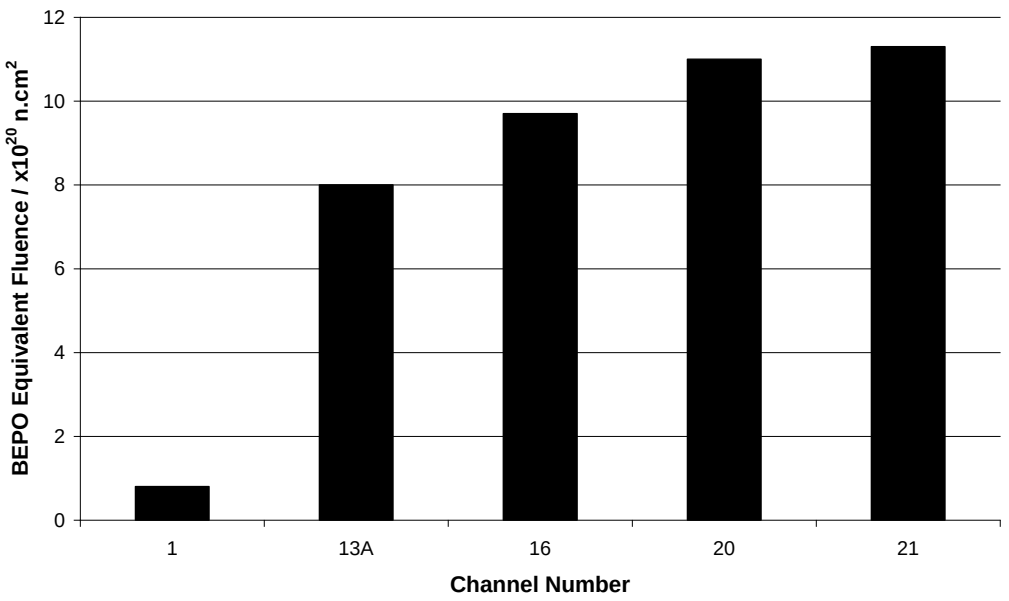

Figure 14 Graph of BEPO neutron Fluence against channel number [85, 96].

The sample number indicates the channel from which the graphite sample was taken, therefore sample 1 (channel 1) was furthest away from the centre of the core and sample 21 (channel 21) was at the centre of the BEPO reactor core. Figure 15 shows graphically the total activity measured for each sample data provided by Nirex [85, 96].

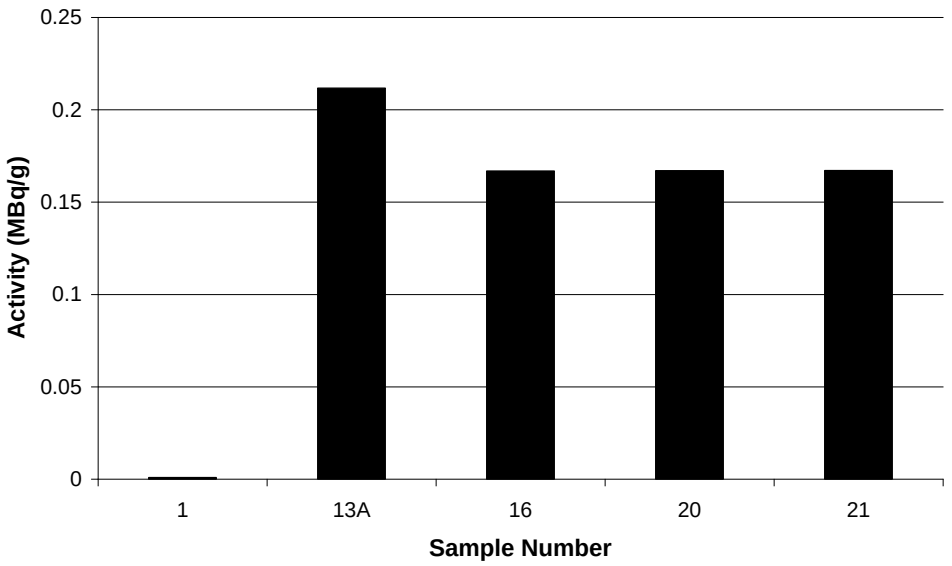

Figure 15 Graph showing total activity of each graphite sample in MBq/g [85, 96].

These two sets of measurements allow an overall view to be formed of how active each BEPO sample is 40 years after reactor shutdown. A clear observation would be to note the very low activity associated with BEPO 1 samples compared to the other channels which are further into the centre of the reactor core. Whenever possible a sample from channel 1 has been used as a virgin comparison to compare the other more irradiated samples to.

3.1.2. Isotopic Inventory and Material Availability

BEPO reactor shut down in 1968 resulting in 43 years of decay to date. Upon receiving this material into the university significant quantities of activity have already decayed leaving behind the long lived isotopes commonly found in all i-graphite. This helps with risk and COSHH assessment and carrying out many of the experiments on this material as a significant quantity of the material present is beta decay which is stopped by 6mm thick Perspex shielding which can be placed in front of most equipment protecting the user. The availability of this material was also a high priority and its reduced isotopic inventory made it can ideal choice for use prior to receiving the significantly more active Magnox material.

3.1.3. Wylfa Magnox Reactor History and Material Background

Wylfa Magnox reactors were commission in 1971 and consist of two reactors with a combined capacity of 980 MW. Wylfa reactors were the largest and last of the magnox reactors to be built in the UK see Table 11 in the introduction section. Each Wylfa core has 6,156 vertical fuel channels and contains over 49,248 natural uranium magnox-clad fuel elements; these large graphite moderated reactors typically supply 23 GW h of electricity per day. The primary coolant used in carbon dioxide.

The samples issues to UoM for this research where trepanned from the fuel channel wall of reactor 1 channels 1413/02 and 1319/12 in April 2007. Figure 16 shows the location of these two sampling points. There are twelve bricks per column in reactor 1

and they are numbered from the bottom of the core. Sample 1413/02 9U comes from an upper position in brick nine and sample 1319/12 8U comes from an upper position in brick eight. Table 15 details the irradiation history of these two samples. Sample 1413/02 was used for leaching experiments and sample 1319/12 was used for Raman analysis.

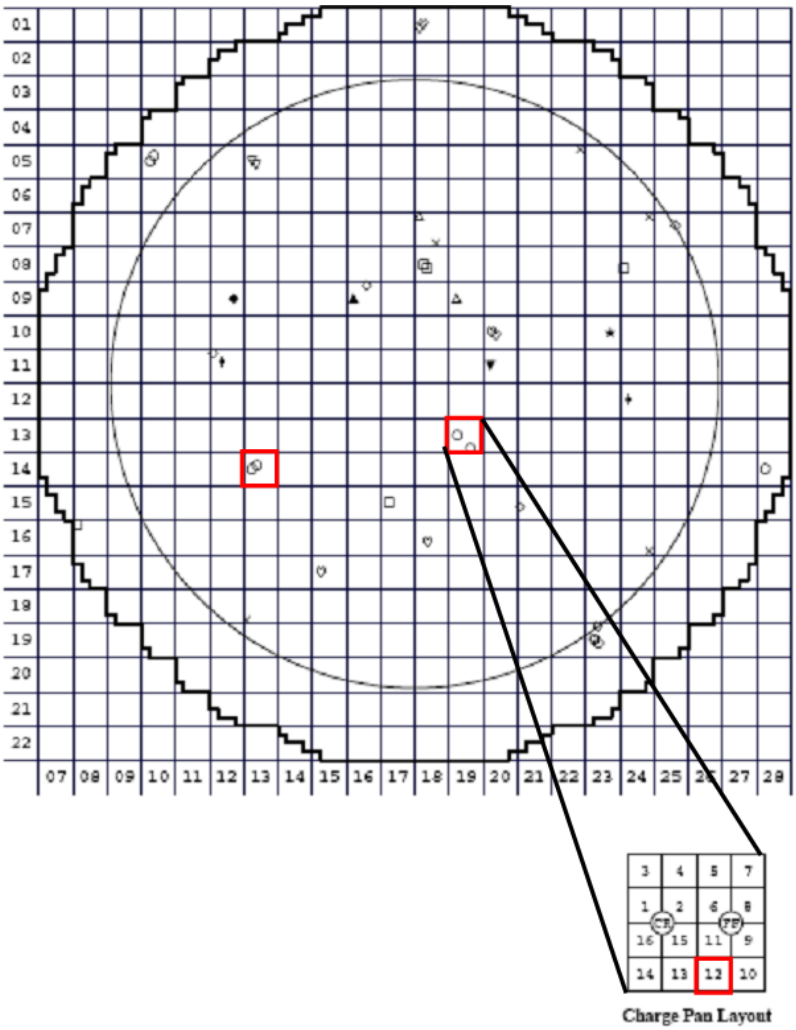

Figure 16 Highlighted in red are the samples taken in 2007 from the Wylfa reactor 1 used in this research

Table 15 Irradiation conditions of Wylfa samples used in this study

Irradiation conditions	1413/02 9U	1319/12 8U

Irradiation temperature (˚C)	352	342
Adjacent fuel dose (MWD/t)	34973	37319
DIDO equivalent dose at channel wall (10^{20} n/cm^2)	34.21	37.11

3.1.4. Wylfa Magnox Isotopic Inventory

Along with the irradiation history of the two trepanned Wylfa Magnox samples provided to the University of Manchester the isotope inventory detailed in Table 17 and shown in Figure 18 was also provided, graphically the vast difference in quantities between each isotope present is observed.

Table 17 Isotopic inventory data provided by National Nuclear Laboratory

Nuclide	Wyfla 1413/02 Specific Activity Bq/g 9th June 2009	Wlfya 1319/12 Specific Activity Bq/g 9th June 2009
^{14}C	22100	22300
^{60}Co	123600	124000
^{137}Cs	2377	2480
^{55}Fe	890000	890000
^{3}H	5465000	5480000

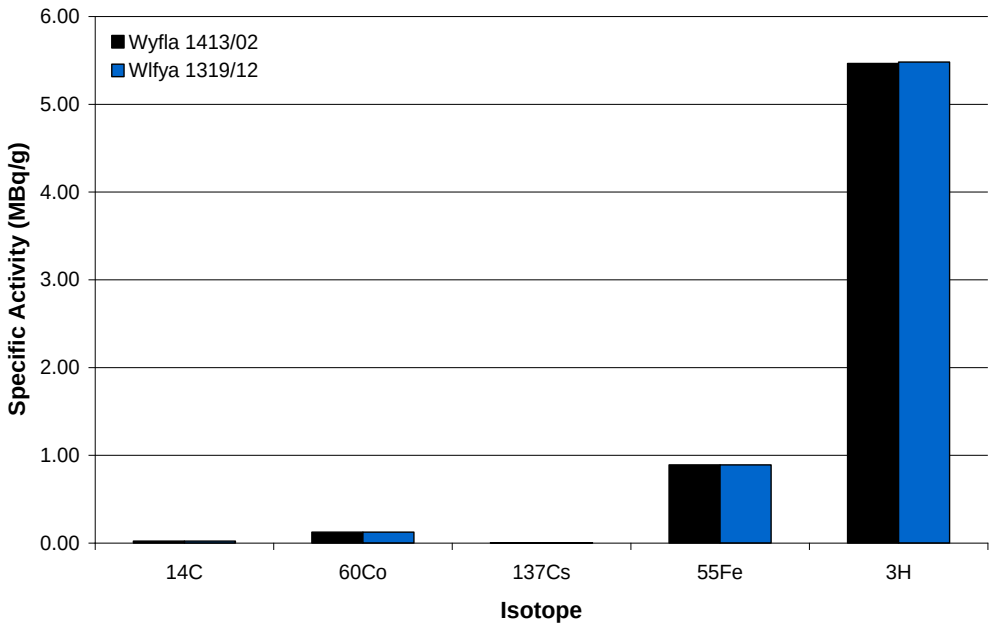

Figure 18 Graph showing the isotopic inventory present in the trepanned samples taken from the Wylfa reactor core in April 2007

3.1.5. I-Graphite Availability

Initially upon staring this program of work approximately 300 grams of BEPO graphite was offered to the University of Manchester for research into decommissioning. This material with its decreased half life was deemed suitable to provide excellent data on proof of concept experiments as well as the chance to used irradiated material with a low inventory to ensure laboratory procedures and best practices were suitable and safe. It was towards the end of this program of study that two trepanned samples from the Wylfa reactor were supplied totalling 7 grams. Wyfla sample 1413/02 9U was crushed into granules and used for leaching and ^{3}H and ^{14}C analysis whereas Wlfya sample 1319/12 8U was kept intact and used for gamma spectroscopy and microstructural analysis.

3.2. Methodology

3.2.1. Controlled Laboratory Setup

This work involved setting up and fully equipping a controlled laboratory and several supervised laboratories at the University of Manchester in order to conduct this research, principally for the purpose of leaching and thermal treatment of graphite waste with microstructural characterisation analysis. Each laboratory required local rules and receipt, storage and handling documentation to support its use and clarify all disposal volumes and route for radioactive material. This documentation detailed how much radioactive material can be stored and disposed of at any one time. Further to this protocol Risk Assessments and COSHH documentation had to be written and approved for each experiment. This detailed protective equipment required; dose to distance calculations, fully isotopic inventory, personal involved and monitoring of the laboratory/equipment after the procedure/experiment is complete. To support this documentation the author prepared record of material in and out of the safe as well as personnel and laboratory monitoring forms. A database is used to keep track of all

active material present and is updated regularly with a yearly review of all the material received and disposed off.

3.3. Leaching Methodology

3.3.1. Liquid Scintillation Counting

Liquid Scintillation Counting (LSC) works on the principle of the conversion of kinetic energy of a nuclear particle traversing the medium into light photons at a maximum efficiency. LSC is the most sensitive and versatile technique for the detection and measurement of radioactivity. It can be used to measure α,β and γ emitters and electron capturing radionuclide. It operates by converting the energy released by nuclear decay into light which is measured by photomultiplier tubes which generates a signal. These electrical signals are then analysed and based on timing and amplitude, determination is possible. The results are given in counts or count rate. The efficiency of a LSC is determined by how well the instrument converts the incident radiation energy into light photons [97].

LSC is a four step process as nuclear particles undergo photophysical and photochemical changes:

1. Absorption of energy by the solvent
2. Formation of the solvent excited state
3. Energy transfer from solvent to solute
4. Fluorescence emission by the solute (radiation transition from the first excited singlet state)

Interference or competition with the orderly progression of these steps, results in what is known as 'quenching' and results in the maximum possible light output of the sample has been reduced [97]. Table 17 provides a brief explanation for LSC terminology used throughout this section.

Table 17 LSC Terminology

Term	Explanation
Cocktail	Scintillation fluid with contains a mixture of three chemicals, namely solvent, emulsifier and fluor. Upon absorbing the energy of radioactive particular decay this cocktail releases light which can be measured.
Solvent	In this instance a solvent is a liquid in which another liquid is dissolved/diluted forming a solution.
Emulsifier	Is an additive that encourages the suspension of one liquid into another.
Fluor	Chemical component of the liquid scintillation cocktail that absorbs UV light emitted by the solvent and emits a flash of blue light.
Swamping	Explains the compatibility of a solution mixed with the cocktail, this covers quenching and luminescence factors which may reduce the LSC counting efficiency.
Efficiency	The ratio of measured counts to the number of decays which occurred over the measurement time, CPM/DPM.
Quenching	Anything that interferes with the conversion of decay energy into blue light flashes that are measured by the instrument. The outcome of which is normally a reduction the counting efficiency.
PMT	Photo-multiplier tube. An electron tube that detects blue light flashes from the fluor and converts them into an electrical pulse.
CPMA	Counts per minute region A. This is the number of light flashes (counts) the LSC has registered per minute. Region A refers to tritium in the dual counting program.
DPMA	Disintegrations per minute region A. Sample activity in units of nuclear decays per minute. Region A refers to tritium in the dual counting program.
SIS	Spectral Index of sample
tSIE	Transformed spectral index of the external standard. This relates how well the instrument is counting the samples compared to the external standard. Values less than 300 mean that quenching and/or luminescence are swamping the sample.

3.3.2. Cocktail Analysis and Suitability

Testing for solubility was carried out prior to analysis. 10mls of the cocktails Prosafe HC and Goldstar were combined with varying quantities of the harshest oxidising conditions with was 2.5M hydrogen peroxide. Each solution was shaken and left to stand for 5 minutes. Transparency determines whether the solution is suitable at this point for LSC counting. Each sample was analysed using the LSC to determine the tSIE values, any tSIE value significantly less than 300 and the luminescence are swamping the sample and an alternative cocktail should be used. Tables 18 and 19 show the results for testing the compatibility of two cocktails namely Prosafe HC and Goldstar; both produced by Merdian. The greater the SIS and tSIE values the more compatable the cocktail is with the solution in which has been mixed with, in this case 2.5M Hydrogen peroxide. The values for CPMA and DPMA are at background levels as this testing was performed on a solution that contained no activity.

Table 18 Prosafe HC analysis results showing the swamping nature of the cocktail used under 2.5M hydrogen peroxide conditions.

Volume addition of 2.5M H_2O_2	Count time (min)	CPMA	DPMA	SIS	tSIE
0ml	1.00	32	34	42.83	449.65
1ml	1.00	33	36	42.14	358.25
2ml	1.00	30	33	45.05	326.30
3ml	1.00	31	34	33.11	301.16
4ml	1.00	49	54	44.89	277.94
5ml	1.00	30	33	33.97	267.94

Table 19 GoldStar analysis results showing the swamping nature of the cocktail used under 2.5M hydrogen peroxide conditions.

Volume addition of 2.5M H_2O_2	Count time (min)	CPMA	DPMA	SIS	tSIE
1ml	1.00	35	38	37.49	386.43
2ml	1.00	32	35	25.93	354.43
3ml	1.00	30	33	29.48	330.36
4ml	1.00	31	34	21.98	312.88
5ml	1.00	41	45	27.30	292.49
10ml	1.00	27	31	24.94	221.51

From the results obtained in Tables 18 and 19 Goldstar was selected as the cocktail suitable for this experiment. With a 5ml of solution added to 10ml Goldstar as each time point. The other conditions under evaluation during this experiment results are detailed in Section 3.3.5 and 3.3.6.

3.3.3. Leaching Parameters Investigated

As detailed in the literature review 2.2.1, there are many possible options available when performing a leaching experiment on radioactive material. The leaching conditions used are often driven by repository environment or ground water systems. Sample history, size and availability also affect the number of experiments and repeats that can be performed. This gives rise to many different approaches to the experimental conditions and length of test. However as discussed in the literature review (2.2) often water conditions are used as a standardised method of comparison with amount leached at 100 days also used. Table 20 shows many of the variations that have been used in previous studies and the methodology employed in this research. This leaching experiment focuses on ^{3}H and ^{14}C removal with minimal damage and weight loss to i-graphite. This research aims to focus on reducing the isotopic inventory of the i-graphite and provide data on the mobility of ^{3}H and ^{14}C within this material. This will contribute to reduction in environmental barriers need for repository conditions and the mobility of the isotopes present has been determined and a reduction in isotopic inventory achieved.

Table 20 Leaching conditions employed in this research

Influencing Parameters	Variations possible	Methodology	In this research
Type of test	Dynamic Semi-dynamic Static	IAEA	Semi-dynamic testing throughout
Temperature	Room Temperature Elevated	Experimental monitoring throughout experiment	Constant 20-25˚C
Providence and sample history	Graphite source and manufacturer Coolant Fluence Weight loss Post closure history Post closure time Removal method and	Known sample history essential IAEA/ANS 16.1	Isotopic inventories and sample history researched Pre-leaching ^{3}H and ^{14}C determination

Influencing Parameters	Variations possible	Methodology	In this research
	storage Avoidance of contamination during PIE Location within reactor		
Inventory	^{3}H and ^{14}C variations and distribution γ isotopes and influences	Pre leaching characterisation γ analysis	Round Robin validation Pre and post leaching ^{3}H and ^{14}C determination
Location of Isotopes	Homogenous distribution Inhomogeneous distribution	Structural and radiochemical analysis	Autoradiography Tomography β& γ analysis
Duration	Short term (< 90 days) Long term (> 90 days)	IAEA	Both tests employed
Testing frequency	Daily Weekly Monthly Yearly Combination	IAEA/ANS 16.1	IAEA methodology employed
Results interpretation	Cumulative release rates Fractional release rates Leach ratio Leach rate	Comparison to existing data	IAEA calculations Comparison to Round robin statistics
Sample type	Solid or powder	Geometry and mass recorded	Both tested for comparison
Porosity	Ratio of open to closed pores Accessibility of internal microstructure	Structural analysis	BET analysis
Sample size	Geometry and mass variations	Geometry and mass recorded	Consistent masses and volumes used whenever possible
Surface area and voume	Isotopic / and chemical solubility Leach rate	IAEA / ANS 16.1	10:1 leachant:sample ratio

Influencing Parameters	Variations possible	Methodology	In this research
ratio	pH		
Leachant	Acidic Alkaline Oxidising Water Brine Ground water	IAEA Buffered solutions used to provide Standardisation	Acidic Alkaline Oxidising Water pH buffers
pH	Changes	Monitoring	pH monitored pre and post leaching
Chemical form	Liquid or gaseous organic or inorganic forms		Pre and post isotopic analysis
External environment	Room temperature changes Reduced conditions or in air environment	Monitoring and recording of all changes	All under air conditions

3.3.4. Leaching Program

This leaching program involved two stages, Stage One focusing on proof of concept and Stage Two utilising other treatment options in addition to leach testing Magnox Wylfa graphite. Table 21 details the number of samples tested, the exposed conditions and length of test for stage one. Table 22 details the number of samples tested, the exposed conditions and the length of test for both BEPO and Magnox graphite for stage two. Testing frequency employed was once weekly until leach rate remained steady then once every two weeks, then monthly as deemed appropriate.

Table 21 Stage One leaching conditions for BEPO channel 16 and 20 samples

Bepo ID	Leachant condition	Number of samples on test	Duration of test
Channels 16 & 20	Water	2 powder 2 solid	85 days
Channels 16 & 20	0.1M Potassium Bromate	4 powder	85 days
Channels 16 & 20	0.2M Potassium Bromate	4 powder	85 days
Channels 16 & 20	0.3M Potassium Bromate	4 powder 2 solid	85 days
Channels 16 & 20	0.4M Potassium Bromate	4 powder	85 days
Channels 16 & 20	0.5M Potassium Bromate	4 powder	85 days
Channels 16 & 20	0.5M Hydrogen Peroxide	4 powder	85 days
Channels 16 & 20	1M Hydrogen Peroxide	4 powder	85 days
Channels 16 & 20	1.5M Hydrogen Peroxide	4 powder 2 solid	85 days
Channels 16 & 20	2M Hydrogen Peroxide	4 powder	85 days

Channels 16 & 20	2.5M Hydrogen Peroxide	4 powder	85 days

Table 22 Stage Two leaching conditions for BEPO and Magnox Wylfa samples

Sample ID	Leachant condition	Number of samples on test	Duration of test
BEPO Channels 1, 16 & 20	Water	4 powder	190 days
Wylfa Magnox		2 solid	
BEPO Channels 1, 16 & 20	pH 1	4 powder	190 days
Wylfa Magnox		2 solid	
BEPO Channels 1, 16 & 20	pH 13	4 powder	190 days
Wylfa Magnox		2 solid	
BEPO Channels 1, 16 & 20	0.5M Hydrogen peroxide	4 powder	190 days
Wylfa Magnox			
BEPO Channels 20	1.5M Hydrogen peroxide	1 powder	190 days
BEPO Channels 1, 16 & 20	0.5M Potassium Bromate	4 powder	190 days
Wylfa Magnox			
BEPO Channels 1, 16 & 20	0.1M Sulphuric acid	2 powder	190 days
BEPO Channels 1, 16 & 20	1M Hydrochloric acid	1 powder	190 days
BEPO Channels 1, 16 & 20	1M Phosphoric acid	4 powder	190 days
Wylfa Magnox		2 solid	

3.3.5. Leaching Phase One conditions

Leaching conditions were testing using liquid scintillation cocktails to ensure chemiluminescence, quenching and counting efficiency would not be affected by the leaching conditions used in stage one. Tables 23 and 24 show the results from this initial testing; SIS and tSIE values are used to determine the suitable of the cocktail used in this experiment as detailed in Section 3.3.2.

Table 23 Background measurement performed on Instrument 406183 (5mls leachant added to 10mls Goldstar)

Leachant condition	Count time (min)	^{3}H (Bq)	^{14}C (Bq)	SIS	tSIE
Water	60.0	0.107	0.270	54.77	291.30
0.1M Potassium Bromate	60.0	0.097	0.390	47.88	294.75
0.2M Potassium Bromate	60.0	0.015	0.519	57.59	292.16
0.3M Potassium Bromate	60.0	0.038	0.612	66.19	290.77
0.4M Potassium Bromate	60.0	0.012	0.789	69.38	290.85
0.5M Potassium Bromate	60.0	0.062	0.888	72.61	292.55
0.5M Hydrogen Peroxide	60.0	0.243	0.308	11.28	305.49
1M Hydrogen Peroxide	60.0	0.126	0.286	25.64	301.64
1.5M Hydrogen Peroxide	60.0	0.476	0.293	8.25	293.67
2M Hydrogen Peroxide	60.0	0.251	0.296	7.95	287.74
2.5M Hydrogen Peroxide	60.0	0.171	0.286	7.86	281.12

Table 24 Background measurement performed on Instrument 421298 (5mls leachant added to 10mls Goldstar)

Leachant condition	Count time (min)	^{3}H (Bq)	^{14}C (Bq)	SIS	tSIE
Water	60.0	0.100	0.253	57.58	297.18
0.1M Potassium Bromate	60.0	0.120	0.369	67.64	302.84
0.2M Potassium Bromate	60.0	0.125	0.474	71.13	302.48
0.3M Potassium Bromate	60.0	0.159	0.560	72.49	300.98
0.4M Potassium Bromate	60.0	0.094	0.781	75.61	304.02
0.5M Potassium Bromate	60.0	0.068	0.811	76.36	303.27
0.5M Hydrogen Peroxide	60.0	4.768	0.080	13.72	310.74
1M Hydrogen Peroxide	60.0	1.374	0.204	26.84	313.35
1.5M Hydrogen Peroxide	60.0	5.742	0.034	12.38	294.56
2M Hydrogen Peroxide	60.0	5.624	0.026	12.05	294.58
2.5M Hydrogen Peroxide	60.0	7.101	0.000	10.52	291.38

3.3.6. Leaching Phase Two conditions

Leaching conditions were testing using liquid scintillation cocktails to ensure chemiluminescence, quenching and counting efficiency would not be affected by the leaching conditions used in stage 1. Tables 25 & 26 show the results from this initial testing; SIS and tSIE values are used to determine the suitable of the cocktail used in this experiment as detailed in Section 3.3.2.

Table 25 Background measurement performed on Instrument 406183 (5mls leachant added to 15mls Goldstar)

Leachant condition	Count time (min)	^{3}H (Bq)	^{14}C (Bq)	SIS	tSIE
Water	60.0	0.128	0.296	60.91	334.23
pH 1	60.0	0.103	0.325	64.06	314.97
pH 13	60.0	0.102	0.280	58.74	315.63
0.5M Hydrogen peroxide	60.0	0.443	0.309	10.98	308.91
1.5M Hydrogen peroxide	60.0	0.577	0.271	8.59	296.54
0.5M Potassium Bromate	60.0	0.244	0.931	72.88	317.13
0.1M Sulphuric acid	60.0	0.208	0.299	56.74	313.49
1M Hydrochloric acid	60.0	0.184	0.291	56.11	286.27
1M Phosphoric acid	60.0	0.147	0.288	60.26	308.51

Table 26 Background measurement performed on Instrument 421298 (5mls leachant added to 15mls Goldstar)

Leachant condition	Count time (min)	^{3}H (Bq)	^{14}C (Bq)	SIS	tSIE
Water	60.0	0.155	0.278	57.72	335.64
pH 1	60.0	0.072	0.315	65.46	317.33
pH 13	60.0	0.083	0.256	60.57	321.31
0.5M Hydrogen peroxide	60.0	0.086	0.299	15.70	309.83
1.5M Hydrogen peroxide	60.0	0.258	0.282	13.63	290.09
0.5M Potassium Bromate	60.0	0.236	0.896	75.72	322.11
0.1M Sulphuric acid	60.0	0.192	0.277	54.11	314.87
1M Hydrochloric acid	60.0	0.119	0.281	55.34	285.19
1M Phosphoric acid	60.0	0.080	0.265	60.30	307.87

The results shown in Sections 3.3.5 and 3.3.6 represent how aggressive each of the leaching/chemical treatment conditions employed in this research is. Using the tSIE values the following raking system can be applied to the leachants used:

Water < Potassium bromate < pH13 < pH1 < Sulphuric Acid < Hydrogen peroxide < Phosphoric Acid < Hydrochloric Acid

More concentrated molarities of the acids where tested however these proved incompatible with all the cocktails available.

3.4. Thermal Methodology

Table 27 provides a brief explanation for thermal analysis terminology used throughout this section.

Table 27 Thermal analysis definitions

Term	Definition
Run	Process of using the furnace to analyse the ^{14}C and ^{3}H within a sample
Recovery check	Analysis of known ^{14}C and ^{3}H standards and calculating the percentage ^{14}C and ^{3}H recovered using the furnace
Quenched standards	1ml of prepared sucrose standard in appropriate cocktail is used as a quenched standard for LSC counting
Unquenched standard	Purchased standards used for LSC efficiency calibration
Carbon Trap	99% 3-methoxypropylamine which traps gaseous carbon species for analysis
Carbon Count	Specially designed LSC cocktail (70-90% 1,2,4-trimethylbenzene) which combines with carbon trap to give good efficiencies and counting in order to determine ^{14}C content.

3.4.1. Furnace Setup

The Furnace is set up by oxidizing the copper catalyst prior to its initial use. The copper catalyst consists of six copper coils placed into furnace, 21 – 22 cm^3 in length using 1 mm diameter copper wire. The furnace is then switched on with the catalyst heating zone at 300˚C for 3 hours with a flow rate of 150 mls/min Oxygen. The combustion tube is turned every 30 minutes to avoid the catalyst damaging the glass as it oxidises. The temperature is then increased to 450˚C for 30 minutes, then 600˚C for 30 minutes with continued turning of the combustion tube. The furnace is then heated to 750˚C for 5-6 hours turning combustion tube every hour. Figure 19 shows a

schematic of the furnace depicting where the catalyst location is in relation to the sample zone and off gas bubblers.

Upon completion of this process the furnace is then ready for a recovery check. A new copper catalyst is to be installed when the recovery check falls below 70% efficiency or if the background collected during a blank is too high. The combustion tube can then be rinsed with 4M HCl to remove any unwanted historic isotopes that may remain inside the tube prior to a new catalyst being oxidised.

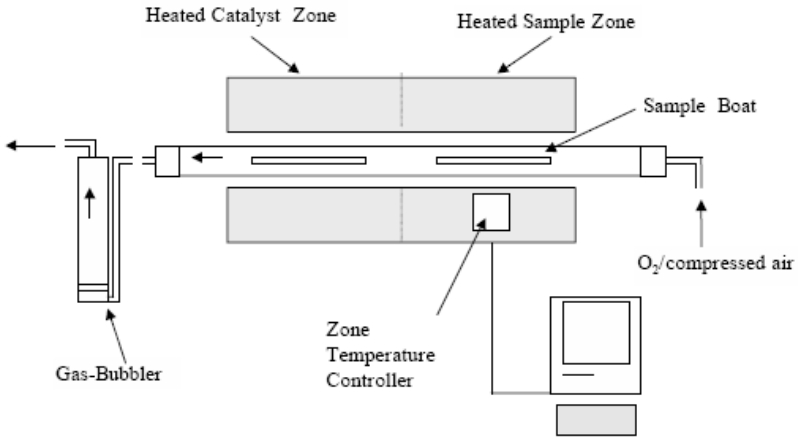

Figure 19 Schematic representation of combustion furnace used during this project

3.4.2. Trapping Agents

The CuO catalyst ensures all hydrogen and carbon species passing over it are converted into HTO and carbon dioxide/carbon monoxide. The first two bubblers at the end of the furnace contain 20 mls of 0.1M Nitric Acid (HNO_3) used for trapping ^3H present as HTO. In the last two bubblers 40 mls of carbon trap is used as a trapping agent for ^{14}C which is present as $^{14}CO_2$.

The tritium collection bubblers are sampled and analysed using 16 mls scintisafe LSC cocktail with 4 mls taken from each bubbler. The carbon trap bubblers are analysed using 14mls carbon count and 8mls taken from each bubbler. The compatibility of these cocktails is specifically designed to work with nitric acid and carbon trap chemicals. Excellent efficiencies are recorded for this mix of trapping reagent and

cocktail. Any unused trapping reagent is kept as stock solution in case reanalysis be required. Upon determining the amount of ^{3}H and ^{14}C present the calculation for how much was present in the sample or in the recovery check is calculated from the known weights of the bubblers pre and post run.

3.4.3. Recovery Checks and Validation

The recovery check procedure involves the preparation of standards that will be used to determine ^{14}C and ^{3}H recovered using the furnace as well as LSC efficiency. ^{14}C and ^{3}H sucrose labelled standards are used and dissolved in 10 grams of deionised water in a 20 ml glass vial. Accurate weights are recorded on a 4 decimal placed balance. The catalyst heating zone for a recovery check is 750˚C. The weight of all bubblers being used in accuracy recorded using a two decimal placed balance. Air is used as the carrier gas and supplied to the furnace at 150 mls/min pressure. A leak test is performed on all glassware connections using ROCOL leak detector spray. A ceramic boat is placed into mouth of furnace with a recorded accurate weight of 1 ml of prepared ^{3}H standard added to boat and 1 ml of ^{14}C prepared standard added to boat. The boat is moved 20cm^{3} into sample heating zone using a ceramic tube as a measure. The run is started and approx 10-15 minutes later a hot air gun is used to remove condensation from end of combustion tube and ensure complete transfer for all liquids into a gaseous state that can be collected by the attached bubblers. After 60 minutes the sample zone temperature reaches 600˚C and the gas is switched to O_2. After a further hour the run is complete and the bubblers are removed and accurately weighed. The furnace is then flushed using a glass boat containing 25 cm^{3} water with an air supply at 80 mls/min. This is collected in 20 mls water in an additional bubbler and LSC analysis performed to ensure no carry over is transferred between runs.

Unquenched standards are run to monitor LSC efficiency over time and quenched standards are prepared using 1 ml prepared sucrose standard in 10 mls LSC cocktail. This determines the LSC standard efficiency for quenched samples. Backgrounds are prepared along side active samples and analysed in LSC to ensure laboratory

procedures are being following and sample contamination is not happening. 60 minute LSC run time is employed for good statistics.

3.4.4. Validation of Inventory Through Round Robin Analysis

Within the CARBOWASTE consortium 5 grams of Magnox graphite was supplied for the purpose of performing a round robin test (RRT) with 11 other laboratories taking part in work package 3. Within the isotopic requirements of this analysis was ^{14}C and ^{3}H. This analysis was performed using the carbolite furnace. The authors results from this work and that of other CARBOWASTE partners is shown is Section 4.4.1. Good correlation was achieved providing confidence in this technique for isotopic analysis of ^{14}C and ^{3}H.

Analysis of ^{3}H and ^{14}C content in irradiated graphite samples are accurately determined using combustion under oxygen conditions. Graphite is an unreactive material at room temperature and utilising temperatures in excess of 600˚C and 100% oxygen gas are required to completely combustion the graphite material being analysed. The carbolite® furnace is specifically designed for of ^{3}H and ^{14}C determination. This methodology is estimated to have a 10% inaccuracy associated with this process due to any gaseous losses which may occur during the analysis. The recovery checks that are performed calculate any losses which may occur during analysis allowing higher levels of accuracy to be achieved. The carbolite® furnace and LSC data of recovery check and system suitability checks are recorded and monitored over all analysis that is carried out is given below:

- ^{3}H recovery checks are typically between 88-94% recovery and quenched LSC standards 99%
- ^{14}C recovery checks are typically between 85-90% recovery and quenched LSC standards 100%
- <1% carryover between bubblers
- All bubblers are analysed to ensure no carryover has occurred
- All measured volumes are weighed on 4 decimal palace balance providing high levels are accuracy

3.4.5. Comparisons to Pre and Post Leached Data

To ensure accurate values for the amount of ^{3}H and ^{14}C present both before and after leaching analysis was carried out on BEPO channel 16 and 20 samples as well as Wylfa Magnox graphite. Powdered samples were taken from both BEPO channel 16 and 20 and analysed utilizing the same methodology employed in the Round robin analysis. BEPO channel 16 and 20 this was repeated three times on 0.5 grams of material, complete destruction of the material was achieved for each analysis and the result given is an average of all three analysis, Section 4.4.2 for BEPO results. For Wylfa Magnox sample 1413/02 only 0.7 grams remained therefore only one analysis could be carried out, however thermal analysis of the post leached samples along with the leached data provided sufficient evidence for concluding that the single analysis was an accurate reflection of the amount of ^{3}H and ^{14}C present, shown in Section 4.4.3 for Wylfa graphite isotopic determination results.

3.5. Microstructural Characterisation

3.5.1. Pore Structure Analysis

This research utilises microstructural techniques such as Computerised X-Ray tomography, Brunauer, Emmett and Teller (BET) surface area analysis [98], Scanning Electron Microscopy, and Confocal Microscopy in order to understand irradiation damage and changes in pore structure. This section of this thesis provides background information on the instruments and technique used during this study, including experiment settings, resolutions, methods of calibration and accuracy.

3.5.2. Tomography

Computerised X-Ray tomography (CT) is a non destructive technique that allows the three dimensional microstructure of graphite to be analysed [99-101]. The CT analysis obtained has been used to determine porosity and density of the BEPO graphite. Figure 20 shows a schematic of the instrumentation. Several factors influence how effective these determinations are. Detection of porosity relies on the resolution of the two dimensional radiographs which is determined by the sample size and CCD camera resolution. Porosity results are also affected by the post-processing of the reconstructed volume, where the greyscale or threshold value may not be obvious and therefore errors in the porosity measurement are introduced. Tomography images were collected using the X-TEK HMX CT instrument using the following settings shown in Table 28.

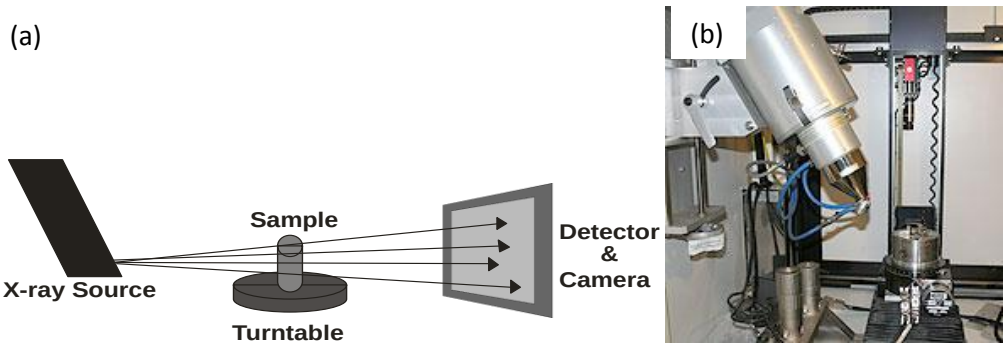

Figure 20 (a) Schematic and (b) Photograph of X-ray tomography scanner; the sample on the turntable inside an aluminium can.

Table 28 X-TEK HMX CT instrument settings.

A calibration was carried out prior to the experiment, to ensure the instrument was working to a satisfactory standard and in order to quantify the attenuation of the incident photons. Table 28 outlines the set up parameters employed throughout this study.

Set up parameters	Setting
Target	Copper
Filter	None
Detector	Beryllium
Voltage	95 kV
Current	105 µA
Rotation	0.3º
Frames/Angle	32 /º
Exposure time	160 s
Voxel size	21.4 µm
Scale factor	250
Offset	0

3.5.3. Brunauer, Emmett and Teller (BET) Surface Area Analysis

Isotopic release is directly related to porosity and surface area. The greater the surface area the more likely isotopic release will occur. This direct relationship makes measurement of porosity and surface area a fundamental requirement in the interpretation of other experimental tests such as leaching, thermal treatment and isotopic distribution. Without knowledge the surface area, leaching release rates can not be calculated.

Gas adsorption and desorption techniques define surface area, pore size and pore size distribution of solid materials. The principle behind this technique is that the amount of gas needed to form a monolayer on the surface of a solid material can be determined from the volume of gas absorbed to the surface at different pressures for a constant temperature. The Brunauer, Emmett and Teller (BET) [98, 102] theory is often used to determine surface area from this technique, however if the absorbed gas is bound persistently in pores with smaller diameters this will affect the rate of desorption and an alternative theory is required to determine the relationship between pore size to pressure change. The BET Equation [98] is given below:

$$\frac{P}{V(P_O - P)} = m\frac{P}{P_O} + b$$

Equation 1

P= Pressure of the absorbed gas

P_O= Saturation vapour pressure

V= Volume of the absorbed gas

m = slope gradient

b= intercept

The Tristar II 3020 utilises physical adsorption to determine surface area and porosity. Specific surface areas from 0.01 m^2/g can be measured using nitrogen gas and 0.001 m^2/g can be achieved using krypton. The Tristar II 3020 has a gas pressure resolution of 0.005 mmHg and a pressure accuracy of 0.5%. The Tristar also includes Density

Functional Theory (DFT) software that allows the determination of microporosity and mesoporosity as a continuous distribution of pore volume to pore size. Figure 21 shows the instrument in use at the University of Manchester. The limitations associated with this technique are that the sample size is small and limited to the vessel geometry therefore must be chosen such that it will fit into the apparatus and must have sufficient surface area in order to give representative results.

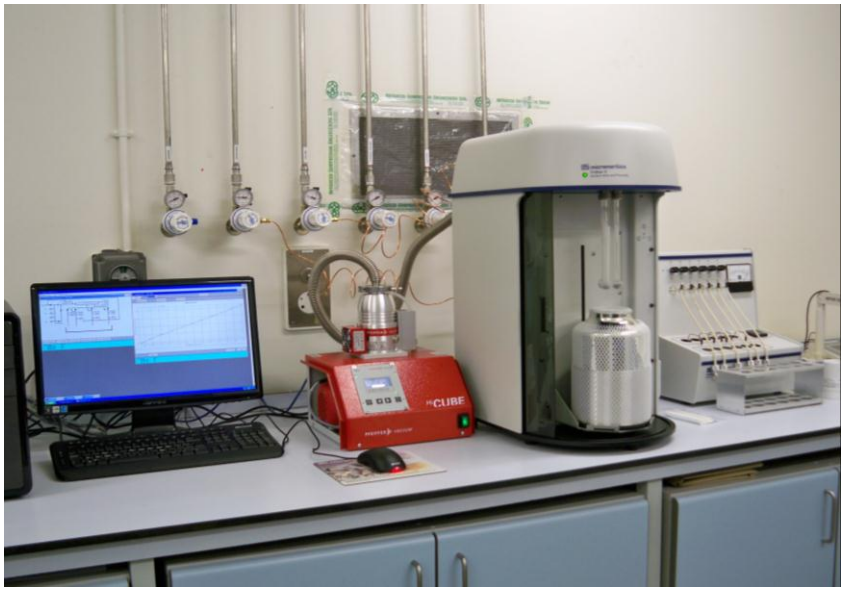

Figure 21 Photograph of the Tristar II 3020

3.5.4. Scanning Electron Microscopy (SEM)

Scanning electron microscopy (SEM) technique produces a detailed magnified image of a sample. A beam of electrons is produced by the electron gun which then follows a vertical path through the microscope. The electron beam is focused through a series of electromagnets which controls the magnification of the sample under vacuum. When the beam hits the sample auger electrons, primary backscattered electrons, secondary electrons and x-rays are emitted. The backscattered electrons, secondary electrons and x-rays are collected by the detector and are processed to produce a rastered image Figure 22 outline the basic schematic of operation for a SEM.

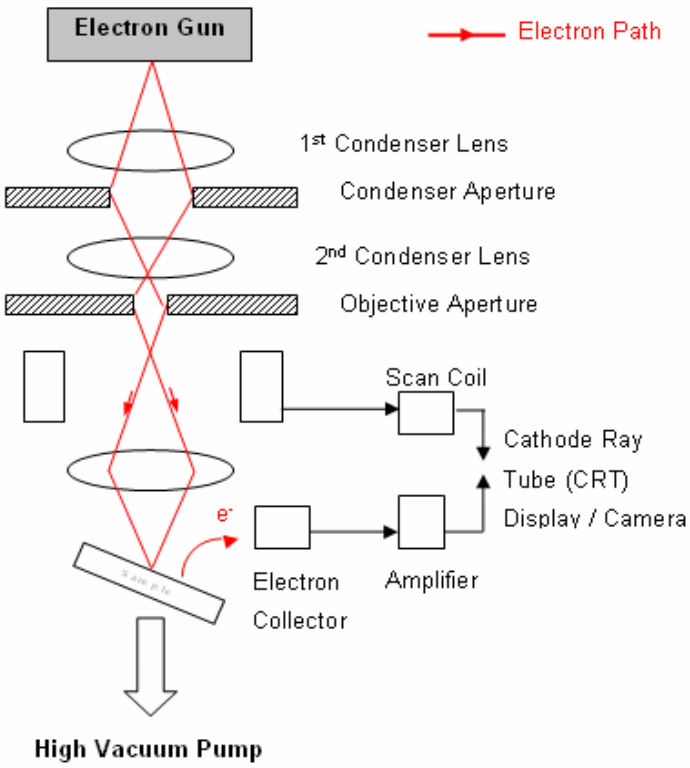

Figure 22 Schematic of an SEM

3.5.5. Confocal Microscopy

Confocal microscopy is an optical imaging microscope that increases optical resolution and contrast of a micrograph by using point illumination and a spatial pinhole to eliminate out-of-focus light in specimens that are thicker than the focal plane. This enables the reconstruction of three-dimensional structures from the obtained images. Confocal microscopy can be used as a replacement for low resolution SEM and is considerably more time efficient. The Olympus LEXT OLS4000 used for this research is a fast scanning confocal microscope with an accuracy of ±2% on measured values and a XY resolution down to 100 nm and a Z resolution to 10 nm. This instrument can be used for three dimensional surface analysis such as texture mapping and roughness analysis. Figure 23 shows a photograph of this instrument at University of Manchester.

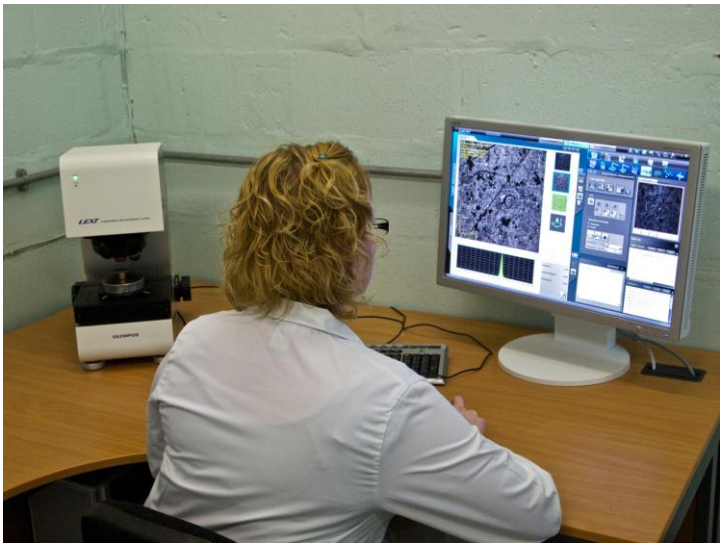

Figure 23 Photograph of the Olympus LEXT OLS4000

3.5.6. Isotopic Distribution by Autoradiography

Autoradiography provides a visual distribution pattern of radiation present in the surface of a sample, depending on isotope energy. Autoradiography can therefore determine β and γ radiation present within a nuclear graphite sample with energy above 0.018MeV. Weak β-emitting particles are stopped by the coating on the phosphorous storage film (which is the recording medium used for this technique). Autoradiography therefore is a qualitative technique used to analyse high energy β and γ isotopes present within a nuclear graphite sample.

The phosphor storage screens are composed of fine crystals of $BaFBr:Eu^{+2}$ in an organic binder. Upon exposure to radiation the Eu^{+2} is excited to the oxidised Eu^{+3} state and the BaFBr is reduced to $BaFBr^{-}$. These ions remain oxidised and reduced after the radioactive sample has been removed from the screen. The phosphor storage screen releases this energy when exposed to light of an appropriate wavelength. A red light with a wavelength of 633nm is absorbed by the $BaFBr^{-}$ complexes which frees electrons reducing Eu^{+3} to Eu^{+2} with an electron in an excited state. As this excited electron falls to the ground state it releases energy in the form of blue light. The optical system collects this emitted light and passes with though the detector (photomultiplier tube). The photomultiplier tube converts and measures the light then produces an electric current proportional to the activity in the sample.

The advantages of this technique using a typhoon 9410 Amersham instrument include, a reduced exposure time compared to traditional autoradiography using X-ray film, increased sensitivity with a linear dynamic range of 1 to 100000 which allows both weak and strong energy isotopes to be analysed simultaneously in a single exposure, and the fact that phosphor storage films are reusable.

Sample size, or preferentially diameter has significant affect on the autoradiography results. High energy radionuclides have sufficient energy to pass through the graphite matrix and excite the autoradiography film being used, lower energy radionuclide's would be hinder by a sufficiently thick piece of graphite. Autoradiography analysis of graphite samples thicker than 1cm have proved difficult to analyse with the high energy radionuclides saturating the film after only a few hours, making comparisons

between graphite samples that have had varying levels of dose or exposure inconclusive. Each of the BEPO channel samples analysed here were 1mm in diameter and cut using a saw without any lubricant, see Section 4.5.4 for results. Several samples were cut at a time and chosen at random to be analysed. The phosphor storage film is wiped clean after each use using a light box and a lint free cloth. The samples were placed on the screen in a glove box and left for 20 hours, this length of time is determined by sufficient exposure time without saturating the film due to the activity present in the graphite and will vary for each type of sample being analysed.

Analysis of the film is then carried out using the Amersham 9410 selecting the red laser with a wavelength of 633nm and a pixel size of 50 microns which is appropriate to the type of film being used. Average intensity, standard deviation, variance, minimum and maximum intensity and area can then be calculated using the software package for any highlighted region. This allows the background to be deducted from the samples being analysed and highlights any discrepancies between results. Figure 24 shows that the phosphor storage screen used is showing consistency in the results produced and the method possible quantitative use.

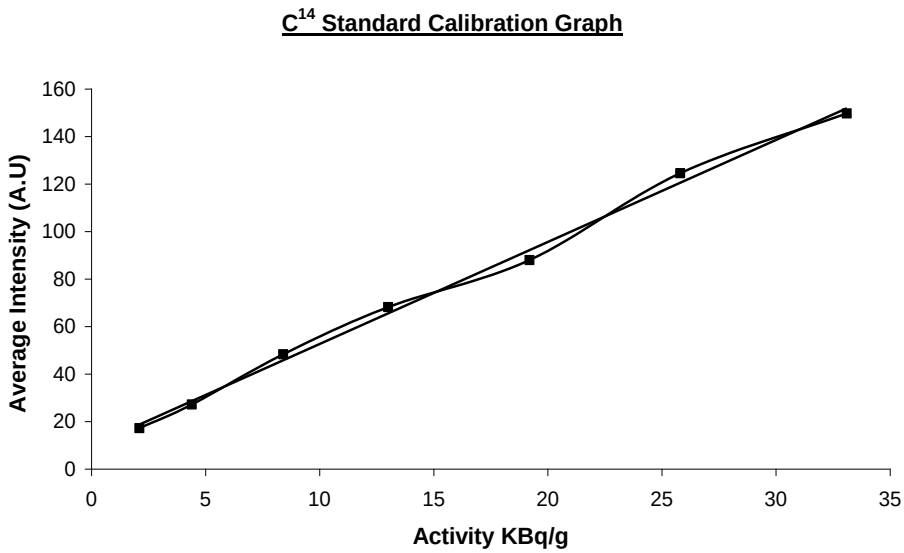

Figure 24 ^{14}C Autoradiography calibration showing the correlation between activity and intensity.

3.5.7. Crystal Structure Determination by RAMAN

Raman spectroscopy is a technique which relies on absorption and re-emission of energy by the material being analysed. Renishaw inVia spectrometer with a fixed laser energy of 2.41 eV (514.5 nm) was used for this research, Figure 25 shows the internal set up within a Raman spectrometer.

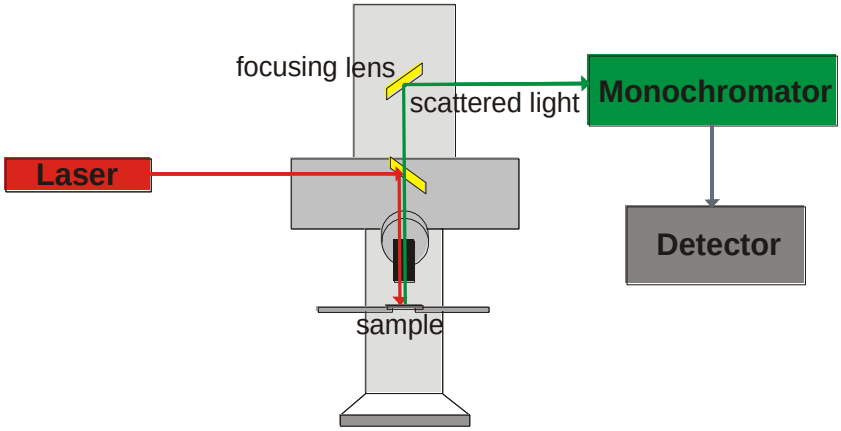

Figure 25 Schematic of a Raman spectrometer apparatus.

Raman spectroscopy is technique used to characterise the rotation, vibration and bending of molecules which when excited by a laser emit photons at specific energy levels or vibrational states [103]. It is commonly used to study and understand the bonding states within carbon materials [104, 105] and in this study is used to characterise and classify the sp^2 and sp^3 ratios of carbon bonds within irradiated graphite. This technique is particularly valuable due to the high spatial resolution (~1 µm) and a penetration depth of ~40 nm achieved in graphite. The presence, position and intensity of the peaks are dependent on excitation wavelength, laser power output and internal stress within the sample [105, 106]. Typical graphite spectrums exhibit bands present which have characteristics related to the π states present within the graphite structure.

The Raman spectrum of each graphite sample depends upon [104]:

- The clustering of the sp^2 phase
- Bond disorder
- The presence of sp^2 rings or chains
- The sp^2/sp^3 ratio

The Raman spectra of all disordered carbons are dominated by the relatively sharp D and G peaks of the sp^2 sites at 1350 cm^{-1} and 1580 cm^{-1} respectively. This is assigned to much greater cross section of the π states within the graphite structure [104]. Raman active vibrations and rotations are identified using quantum mechanics or group theory. Raman active modes are found on molecules that exhibit symmetry such as graphite these modes are schematically represented in Figure 26.

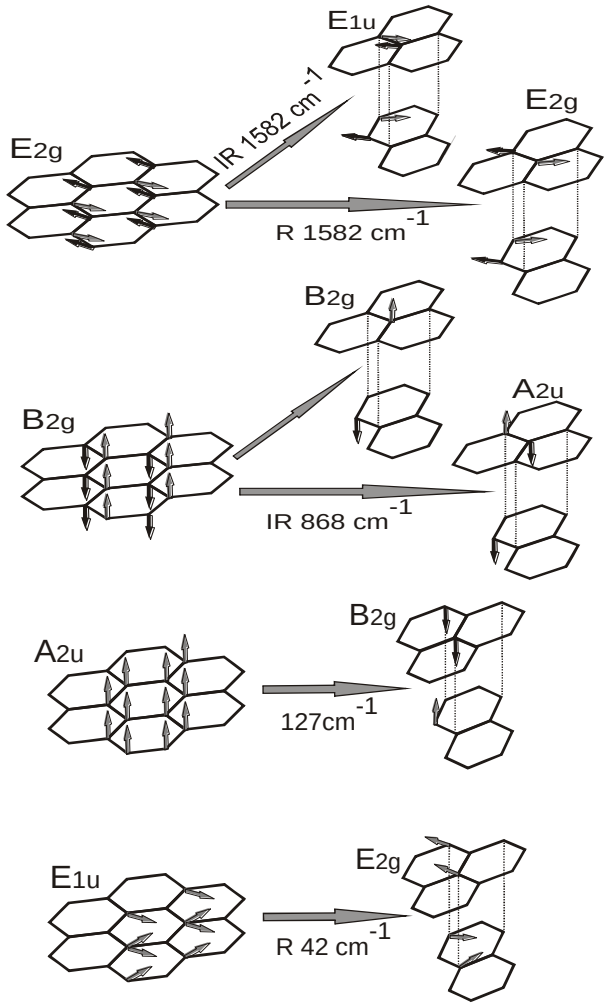

Figure 26 Vibrational modes of graphite showing Raman active and Infrared active breathing modes of the graphite structure [107].

Graphite produced by this technique shows two intense modes which are Raman active, firstly, the G peak positioned around 1582 cm^{-1} assigned to the E_{2g} symmetry of the carbon bonds, as depicted in Figure 27 and where disordered carbon is present this is accompanied with a D peak situated around 1350 cm^{-1} which is assigned to the A_{1g} symmetry.

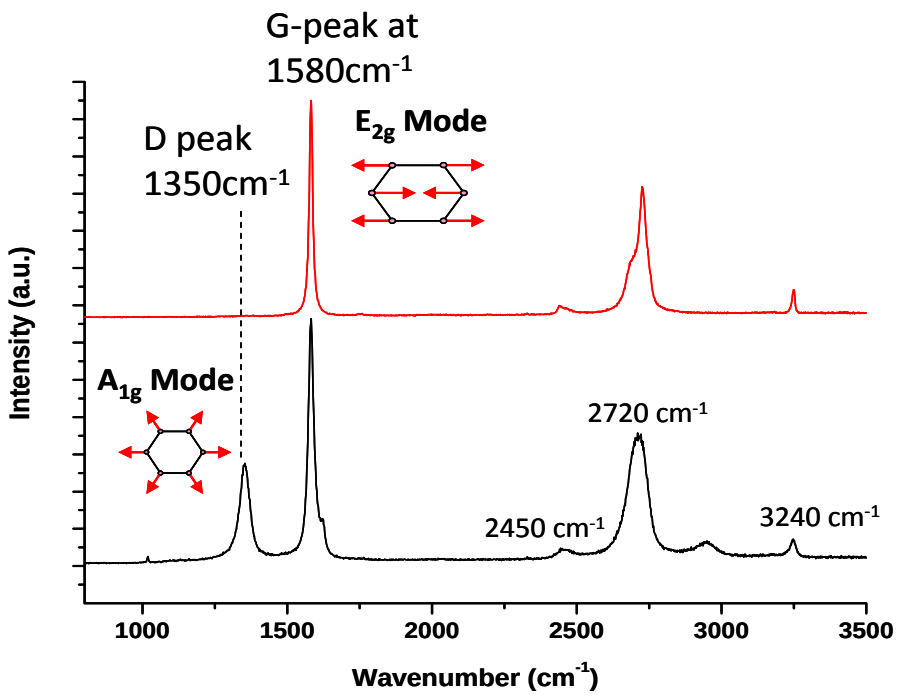

Figure 27 Two intense modes which are Raman Active for graphite

The ratio of the peak intensities for the D and G peaks (ID/IG) is shown to be inversely proportional to the in-plane crystallite size, Equation 2 shows that the ratio between the D band and G band [105, 108] can be used to calculate crystallite size in the a axis (L_a).

$$\frac{I_D}{I_G} = \frac{C(\lambda)}{L_a}$$

Equation 2

I_D = Peak intensities for the D peak

I_G = Peak intensities for the G peak

C (λ) = C—C bond force constant at 514.5nm (4.4nm) [104, 105, 108, 109]

L_a = Crystallite size (Nm) in the a axis

The present of the D peak and the broadening of all the peaks is associated with a disordered structure of the graphite compared to HOPG. Peak broadening is calculated by measuring the full width half maximum (FWHM) of the G peak. Table 29 further explains the common naming system used for the Raman bands present on a Graphite spectrum and their origin.

Table 29 Labelling of Raman Bands for Graphite.

Raman Order	Raman Rules	Band	Wavelength	Reasoning
1st order	Disorder induced	D band	~1350 cm^{-1}	Arises from the breathing motion of the sp^2 rings and possible disorder sp^3 motion [108, 110].
1st order	First order allowed	G band	~1580 cm^{-1}	Caused by in-plane vibrations of the layers.
1st order	Disorder induced	D' band	~1620 cm^{-1}	Amorphous carbon or microcrystalline graphite, alternatively the feature is assigned to hydrogen bound to sp^2 carbon [110].
2nd order	Structural changes along the c-axis	G' band	~2700 cm^{-1}	Graphitic 2D and 3D determination.
2nd order		D'' band	~2950 cm^{-1}	Combination of D and G bands
2nd order			~3234 cm^{-1}	Amorphous carbon or microcrystalline graphite, alternatively the feature is assigned to hydrogen bound to sp^2 carbon [110].
2nd order		2D'	~3250 cm^{-1}	Counterpart in the second

	band	order spectrum of D’ band

3.5.8. Summary of Materials and Methodology

This research focuses on the leachability of ^{3}H and ^{14}C from i-graphite and his section details the microstructural techniques used including Computerised X-Ray tomography, Brunauer, Emmett and Teller (BET) surface area analysis, Scanning Electron Microscopy, Confocal Microscopy, Autoradiography and Raman Spectroscopy. These characterisation techniques have been used to understand irradiation damage and changes in pore structure to the BEPO and Magnox Wylfa graphite tested.

In addition this section provides background information on the all the leaching parameters possible and the variables chosen to investigate further in this research. It also highlights what background data is essential when performing leaching experiments and validation of LSC and thermal analysis. All the instrumentation and technique used during this study experiment settings are detailed with reference to resolution, methods of calibration and accuracy whenever necessary.

Combining leaching, thermal and microstructural analysis in this way provides a full detailed scientific approach to ^{3}H and ^{14}C migration promoted through chemical treatment, which enables strong conclusions to be made from the data produced in this thesis as confidence in the analytical approach has been achieved by calibration and validation methods detailed in this section.

4. Results and Discussions

This section will examine the various methods employed for treatment of irradiated graphite using the methodologies outline in Section 3.3. Chemical treatment phase one will focuses on BEPO graphite for up to 84 days in an oxidising environment, samples were powdered to maximise the surface area available to the leachant and have been contrasted against solid samples. In this phase, hydrogen peroxide and potassium bromate have been contrasted and compared with a baseline (water) in order to determine a steady state leach release rate. Chemcial treatment phase two will expand on the findings from phase one using various acidic environments and will examine the behaviour of BEPO and Wylfa Magnox graphite for longer leaching periods, the results from which are discussed herein. This chapter will also attempt to link any chemical releases from the graphite to that of material changes and will detail a variety of microstructural characterisation techniques employed to determine porosity size, available surface area, porosity distribution and crystal changes with irradiation and leach rate. Finally this section will address the validation of results and will discuss various methods which have been developed in order to give confidence to the research findings.

4.1. Chemical Leach Treatment

Chemical leach treatments within this study focused on removing of ^{3}H and ^{14}C from i-graphite. In phase one a standardised leach methodology was developed and employed throughout this research. For each chemical environment, 0.5 grams of graphite were tested in 50 ml of leachant and each test was performed in duplicate. Each sample pair was accompanied by a standard water baseline. All chemical tests were performed at 20 ± 5°C. Samples were powdered in order to maximise the geometrical surface area and compared against solid samples for both Phase one and two. The testing methodology has been adapted according to IAEA standard for 'Semi-dynamic leach test' [46], in which a 5ml leachant sample is removed every 7 days and

replaced with a fresh 5ml of leachant. Figure 28 shows the glassware and laboratory set-up employed during both stages of chemical treatment.

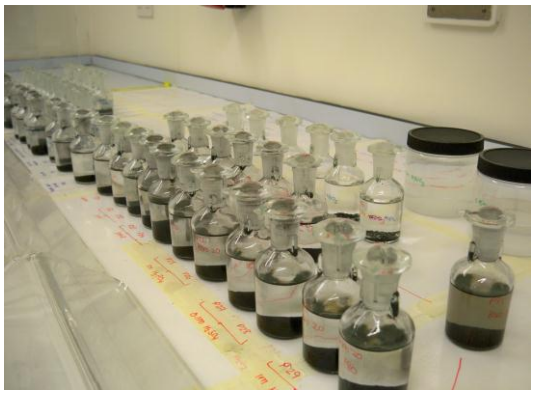

Figure 28 Photograph of Leaching set up.

The isotopic release rates have been calculated for ^{14}C and ^{3}H and are given as cumulative fraction of isotopic released as a function of time and takes into account the sum of isotopic release taken to reach a steady state and beyond which not further significant release is exhibited. The Cumulative Fraction Released equations are shown in equations 3 and 4 and also take into account the dilution factor experienced by the replacement of fresh leachant at testing intervals.

$$\sigma_d = A_n - (0.9A_{n-1})$$

Equation 3

σ_d = Actual activity released at time point with dilution factor/Bq

A_n = Activity at time point/Bq

A_{n-1}= Activity at previous time point/Bq

$$CFR = \sum \frac{\sigma_d + \sigma_{n-1}}{A_0}$$

Equation 4

CFR= Cumulative Fractional Release

σ_{n-1} = Activity released at previous time point /Bq

A_0 = Activity present in sample being analysed and corrected for half life /Bq

4.2. Chemical Treatment Phase One

The phase one leaching test was carried out using a deionised water baseline with H_2O_2, $KBr0_3$ leachants. Samples from BEPO reactor channels 16 and 20 were used throughout the 84 day test. An 8% error is associated with this leaching data which is based on LSC counting error, ±1% weight distribution and electronic pipette standard deviation. All equipment was calibrated before testing was carried out but errors are associated with the equipment are included in the assessments. All calculations include half life correction and weight correction for solid samples due to machining limitations on active material, all solid sample used where 0.5 grams ±1%.

4.2.1. ^{3}H release under Phase One Conditions

The cumulative fraction of ^{3}H released from BEPO Channel 16 under water conditions for 84 days is shown in Figure 29. Preliminary indications are that ^{3}H release began quickly and release of ^{3}H was again extremely low as 3.1% of the total tritium inventory was released from the powdered sample and only 1.8% was released from the solid sample. These release rates illustrate both the mobility of HTO species within the graphite is likely to be bound to the surface groupings which are susceptible to exchange with hydrogen atoms in the water and that the differences observed between solid and powder material may be due to a function of exposed surface area.
Very low levels of ^{3}H were released under water conditions over the course of this experiment and a steady-state leach rate appears to have been achieved for ^{3}H after 60 days. The low reactive nature seen in this experiment leads to the conclusion that any activity removed under water conditions was surface contamination and easily removed regardless of the conditions employed. These samples had >97% of the ^{3}H and remaining at the end of this experiment.

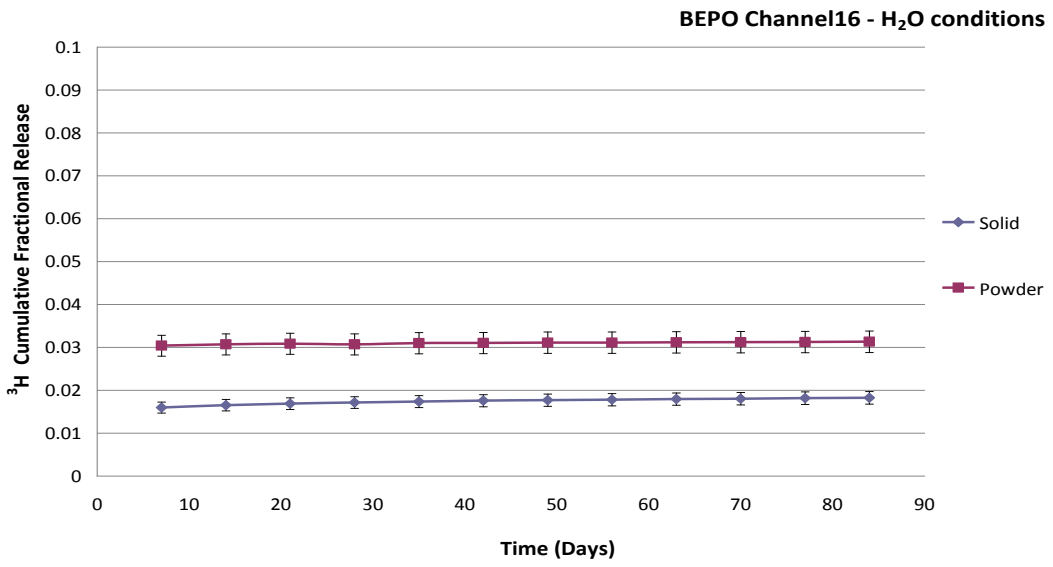

Figure 29 BEPO Channel 16 ^{3}H release under water conditions

Potassium bromate ($KBr0_3$) was used in concentrations ranging from 0.1M – 0.5M. Figure 30 shows the results obtained for ^{3}H release from leaching BEPO channel 16. All these samples were powdered in order to maximise the surface area and leached under varied potassium bromate concentrations. As with water the ^{3}H results show a very slow release, this is only marginally increased with increasing concentrations. 4.2% of the total ^{3}H inventory was released under 0.1M $KBrO_3$ conditions, compared with 5.4% of the total ^{3}H inventory released under 0.4M $KBrO_3$ conditions and 5.6% of the total ^{3}H inventory was released under 0.5M $KBrO_3$ conditions. Compared to leaching by water which resulted in a 3.4% ^{3}H release it could be concluded that the oxidising environment provided by the potassium bromate and notably the brO_3^- ion, has little effect on leach rate and on ^{3}H interaction and promotes the HTO exchange theory which is examined with water.

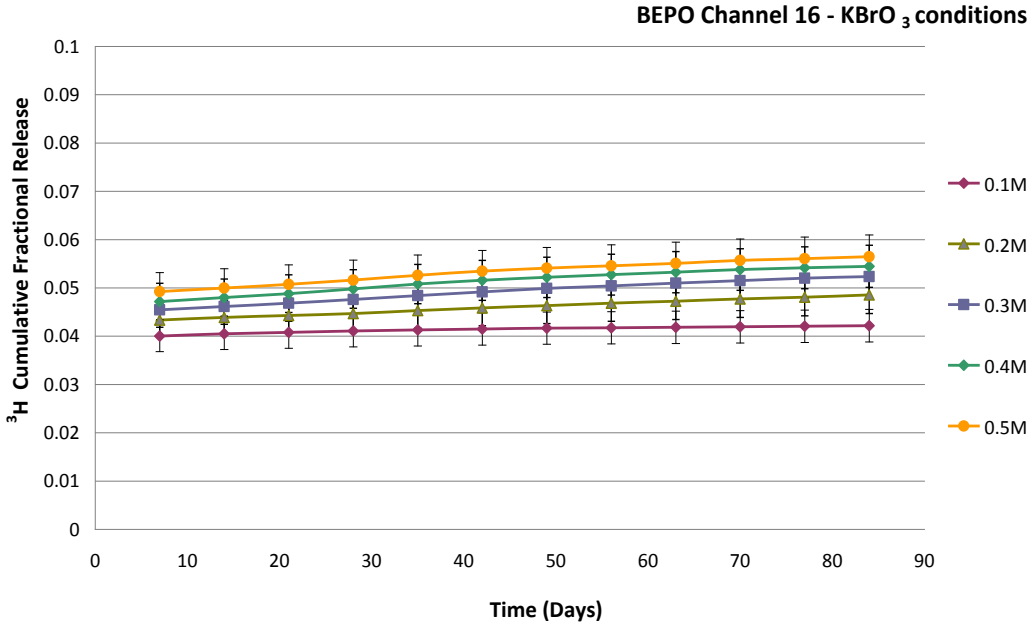

Figure 30 Powdered BEPO Channel 16 ^{3}H release under potassium bromate conditions

Hydrogen peroxide (H_2O_2) was used in concentrations ranging from 0.5M – 2.5M. Figure 31 shows the ^{3}H released under hydrogen peroxide conditions for powdered BEPO Channel 16 samples. In these tests preliminary indications are that ^{3}H release began quickly and 9.7% of the total ^{3}H was released under 0.5M H_2O_2conditions, compared with 16.2% of the total ^{3}H inventory released under 2M H_2O_2 conditions. A maximum of 17.4% of the total ^{3}H inventory was released under 2.5M H_2O_2 conditions. It is clear by the significant increase in the rate of ^{3}H released is observed under hydrogen peroxide conditions that radiolysis and isotopic exchange of the ^{3}H with the hydrogen peroxide is considered to be the mechanism behind this increased release rate. Hydrogen peroxide promotes radiolysis and the exchange of HTO from the graphite to the leachant in comparison to the water condition results where only the 3.1% of the total ^{3}H inventory released

$H_2O_2 \rightarrow OH^{\bullet} + OH^{\bullet}$	Hydroxyl radicals
$H^{\bullet} + OH^{\bullet} \rightarrow H_2O$	Isotopic exchange – Radicals
$H^{+} + OH^{-} \rightarrow H_2O$	Isotopic exchange – Hydroxyl ion

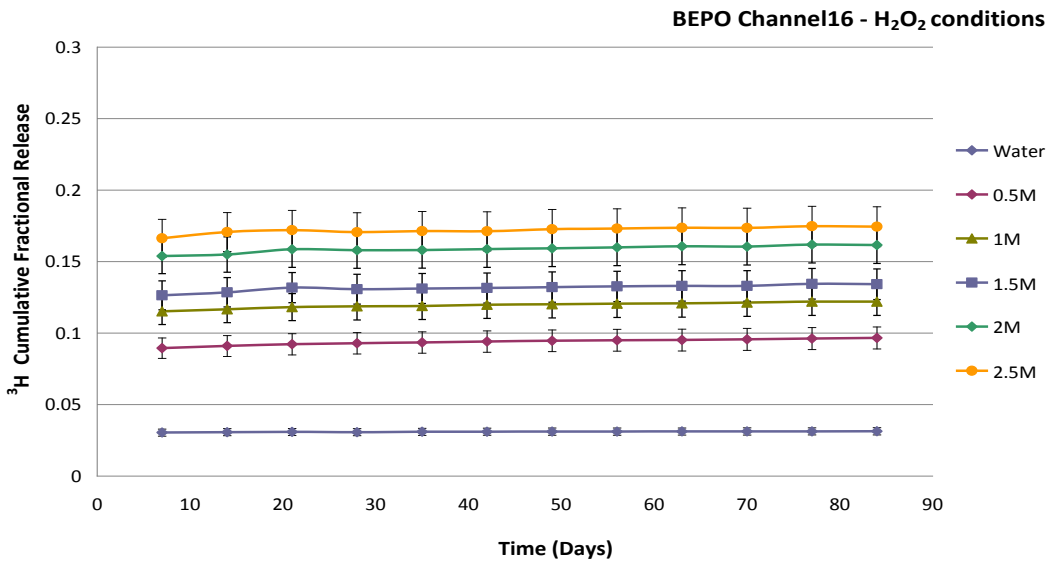

Figure 31 Powder BEPO Channel 16 ^3H release under hydrogen peroxide conditions

4.2.2. ^{14}C release under phase One Conditions

Figure 32 shows BEPO Channel 16 ^{14}C release under water conditions. under this aqueous environment the release rate of ^{14}C is very slow with only 0.87% of the total ^{14}C inventory released from the powdered sample and 0.34% of the total ^{14}C inventory was released from the solid sample, Less ^{14}C mobility is observed under water conditions for BEPO Channel 16 . The speciation responsible for this release indicates dissolved $^{14}CO_2$ as there is approximately 0.04% by volume of CO_2 is present in the atmosphere and water typically contains less than 10 mg/L, however several hundred mg/L of CO_2 can be dissolved into water should the appropriate conditions be met the limited release of ^{14}C under water conditions is most probably derived from dissolved $^{14}CO_2$ species.

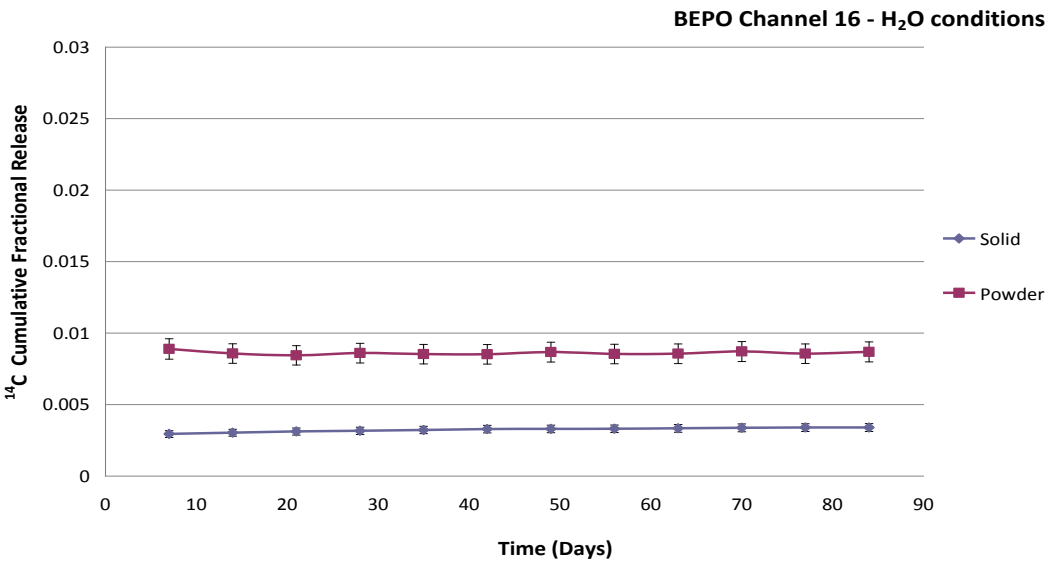

Figure 32 BEPO Channel 16 ^{14}C release under water conditions

Figure 33 shows the results obtained for ^{14}C release from leaching BEPO channel 16 powdered samples under potassium bromate conditions. Under the bromate environment, a maximum of 5.7% of the total ^{14}C inventory was released under 0.5M $KBrO_3$ conditions. This can be compared to release under water conditions where approximately 1% of the total ^{14}C inventory was released. Bromine is well known as an intercalation element capable of separating the graphite layers, the bromate ion BrO_3^- present in potassium bromate has had little effect on the graphite structure which is observed through the limited release of ^{14}C.

Lower release rates for ^{14}C than expected where achieved under potassium bromate conditions, which leads to the conclusion that mobile/weakly bound isotopes are being removed/release, however due to the large size of the bromate ion and the reduced concentration there is little further interaction occurring between the graphite and the potassium bromate solution after 60 days.

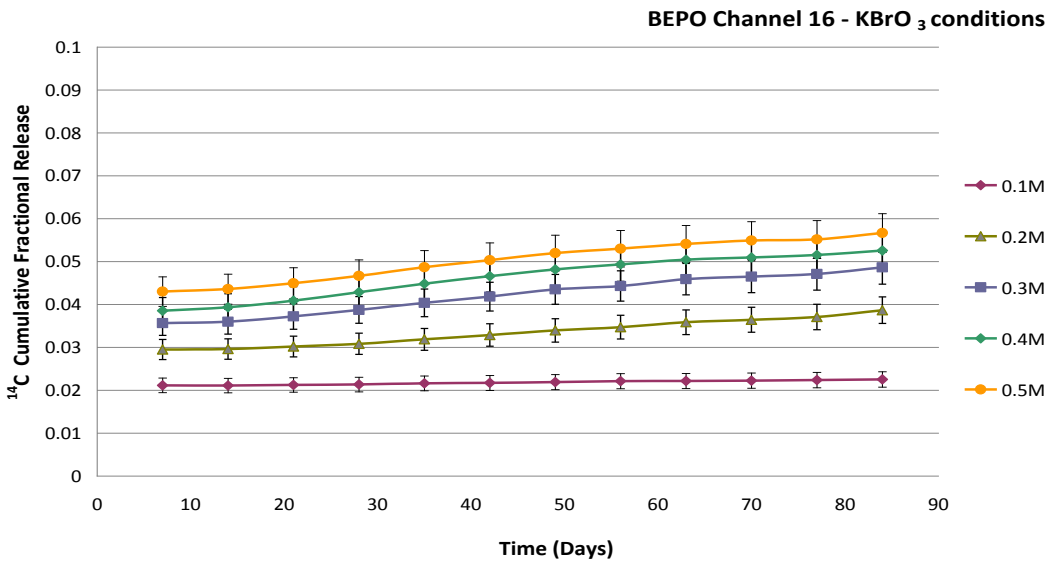

Figure 33 Powder BEPO Channel 16 ^{14}C release under potassium bromate conditions

Figure 34 shows the ^{14}C released under hydrogen peroxide conditions for powder BEPO Channel 16 samples. Compared to the 0.9% of the total ^{14}C inventory for the powdered sample released under water conditions: 11.7% of the total ^{14}C inventory for the powdered sample was released under 0.5M H_2O_2conditions, and a maximum of 15.4% of the total ^{14}C inventory under concentrations greater than 2M H_2O_2 .

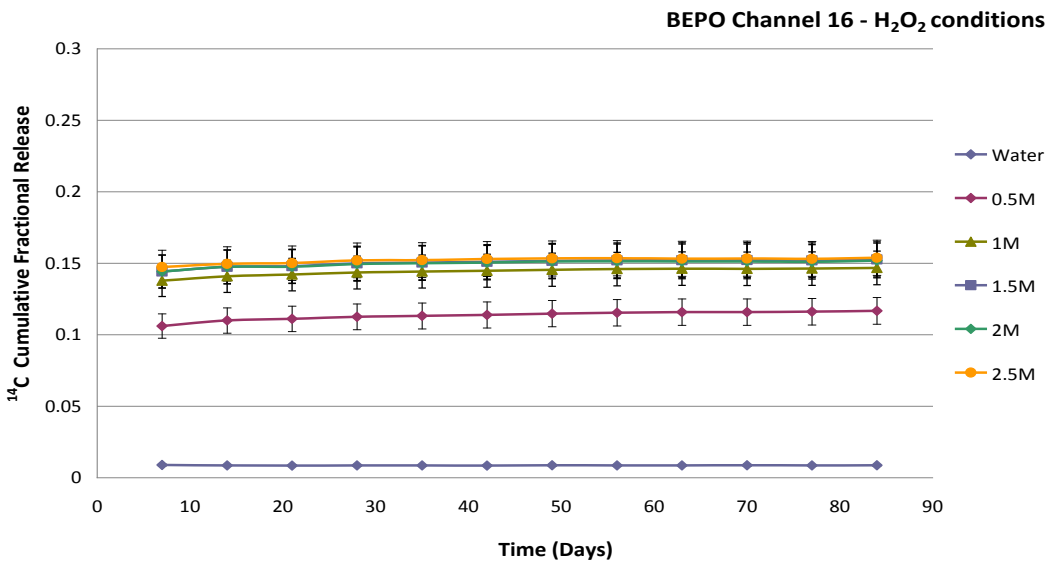

Figure 34 Powder BEPO Channel 16 ^{14}C release under hydrogen peroxide conditions

The mechanism behind the release of ^{14}C by hydrogen peroxide is thought to be chemical oxidation by intercalation of any surface bound ^{14}C .With 15 % of the inventory has been released the bulk of the activity has remained locked within the graphite micro-structure.

Samples taken from BEPO channel 20 were found to release less ^{3}H and ^{14}C under all conditions when compared with samples taken from BEPO channel 16. The inventory and reactor history of these two channels is reported as being similar [96] however isotopic determination via thermal analysis has shown that this distribution of ^{3}H and ^{14}C is not uniformed throughout the bulk of the material supplied. BEPO channel 20 samples under hydrogen peroxide conditions were also found to turn the leachant solution grey in colour. As coloured samples interfere with LSC counting efficiency this will have lead to additional inaccuracy due to the opacity of the liquid which should be accounted for when analysing this data. Therefore BEPO channel 20 data has had a correction factor added and the 84 incremental leach rates have been reported which considers surface area and cumulative release up to 84 days Section 4.3.6 for leach rate data.

4.2.3. Surface Area Effects on ^3H release

This section compares the release rates of ^3H and for solid versus powder BEPO channel 16 samples. All data has been corrected for the weight of each sample used. Figure 35 shows BEPO Channel 16 ^3H release under 0.3M potassium bromate. 2.1% of the total ^3H inventory for the solid sample was released and 5.2% of the total ^3H inventory for the powdered sample was released under 0.3M $KBrO_3$ conditions.

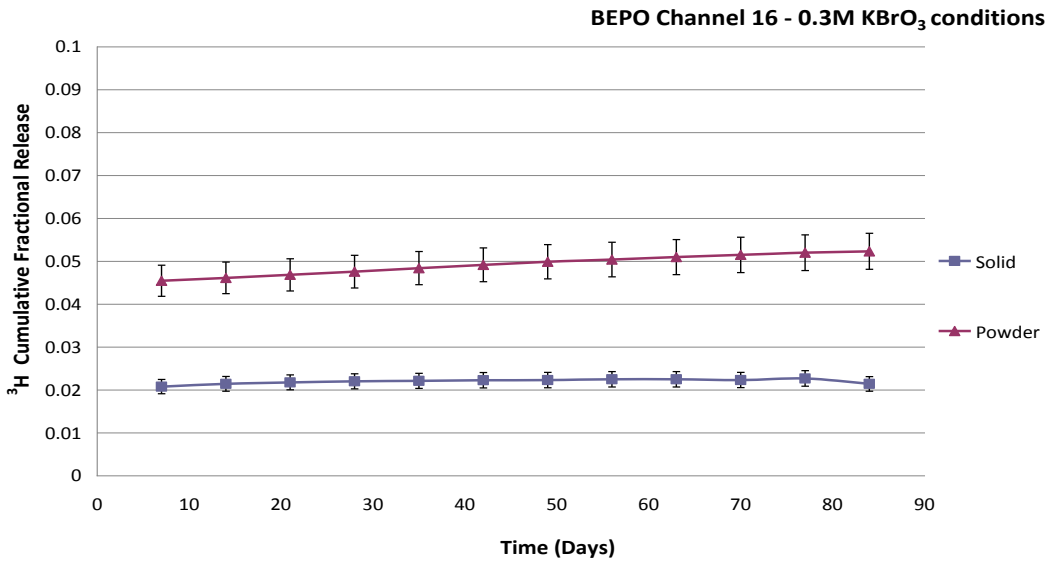

Figure 35 BEPO Channel 16 ^3H release under 0.3M potassium bromate conditions

Figure 36 shows BEPO Channel 16 ^3H release under 1.5M hydrogen peroxide. In these tests 13.4% of the total ^3H inventory for the powdered sample was released under 1.5M H_2O_2 conditions and 4.7% of the total ^3H inventory for the solid sample was released under 1.5M H_2O_2 conditions.

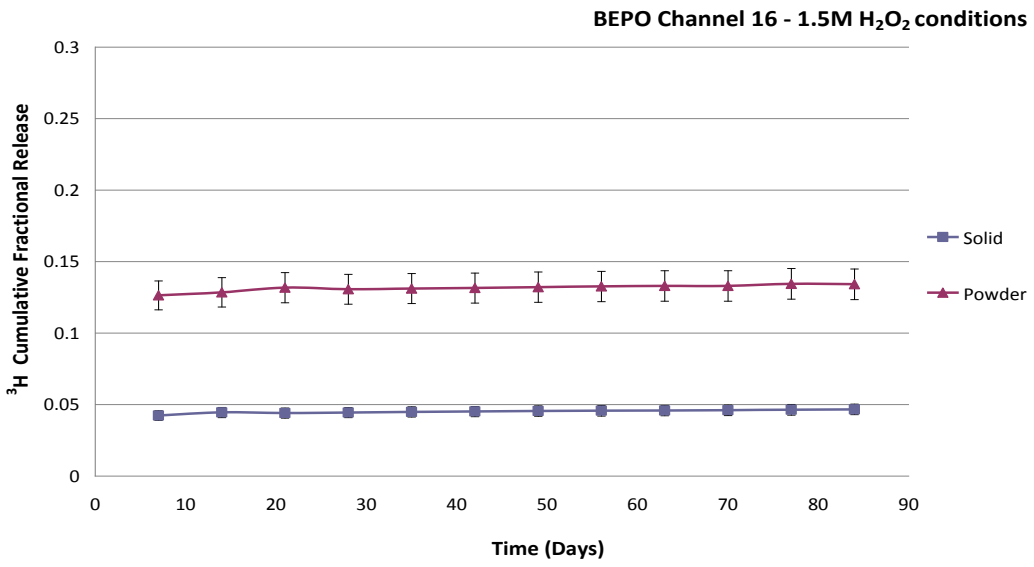

Figure 36 BEPO Channel 16 ^3H release under 1.5M hydrogen peroxide conditions

Comparing powder to solid release rates of tritium surface area has enabled a significant increase in isotopic release of ^3H. Under 0.3M potassium bromate conditions the solid release rate after the initial few time points is minimal with the graph showing a decrease in release towards 84 days. The powder however is increasing still at day 84, this result was one of the driving factors behind extending the phase two leaching experiment to over 100 days to observe when all the mobile or reactive forms of ^3H are released.

4.2.4. Surface Area Effects on ^{14}C release

Figure 37 shows BEPO Channel 16 ^{14}C release under 0.3M potassium bromate solution. In these tests 0.9% of the total ^{14}C inventory for the solid sample was released under 0.3M $KBrO_3$ conditions and 4.9% of the total ^{14}C inventory for the powdered sample was released under 0.3M $KBrO_3$ conditions.

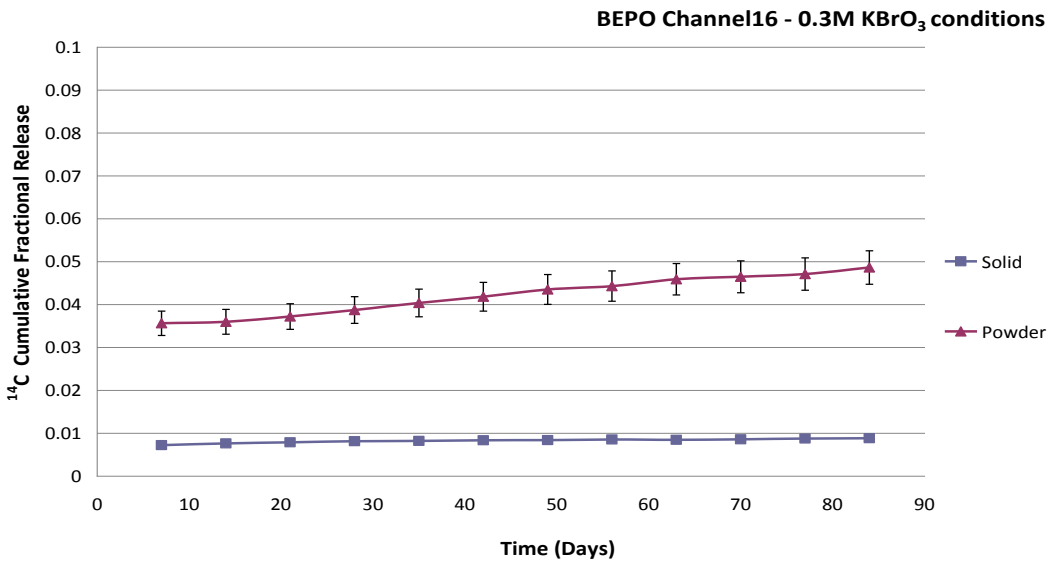

Figure 37 BEPO Channel 16 ^{14}C released under 0.3M potassium bromate conditions

The release of ^{14}C under potassium bromate conditions for solid BEPO Channel 16 material gives a steady state release by day 60. Whereas for the powdered material ^{14}C continues to be released. Continuing this experiment further would have provided data to support just how much ^{14}C can be released under potassium bromate conditions. The materials surface area has promoted this release and allowed 14C to become more mobile**.**

Figure 38 shows BEPO Channel 16 ^{14}C release under 1.5M hydrogen peroxide. In these tests 15.3% of the total ^{14}C inventory for the powdered sample was released under 1.5M H_2O_2 conditions and 3.9% of the total ^{14}C inventory for the solid sample was released under 1.5M H_2O_2 conditions.

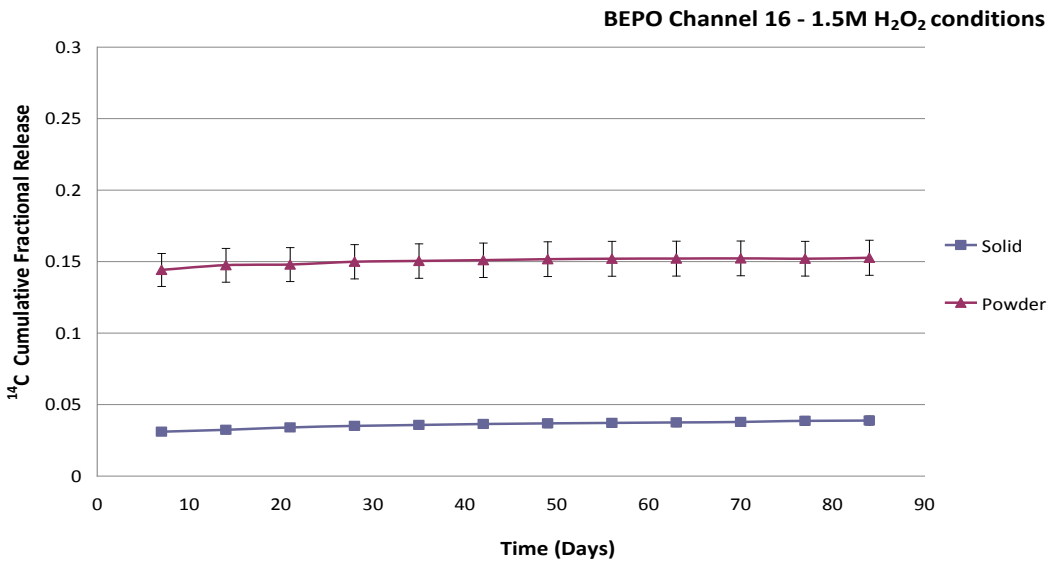

Figure 38 BEPO Channel 16 ^{14}C released under 1.5M hydrogen peroxide conditions

A steady state of ^{14}C release is achieved by day 60 for both solid and powdered material under 1.5M hydrogen peroxide conditions. Surface area has increased the mobility and availability of the ^{14}C. Given the aggressive environment of 1.5M hydrogen peroxide and the powdered structure of the material only 15% of the ^{14}C was leached out provides interesting results regarding the structure and bonding of the ^{14}C which remains. A possible conclusion would be that to remove the remaining ^{14}C from the graphite the material it must be destroyed. Employing more aggressive environments for long periods of time will provide further data to support such a statement.

4.2.5. Leaching Discussion

The leaching results and experimental techniques and conditions taken forward into stage two leaching experiment are summarised below:

- The oxidising environment of Hydrogen peroxide yielded the highest release activities for both of ^{3}H and ^{14}C removal.
- Graphite taken from channels 16 and 20 behaved differently under all leaching conditions, BEPO Channel 20 graphite provided a murky solution which interfered with the LSC counting efficiency. The trend of release rate of ^{3}H and ^{14}C versus leaching environment were consistent with BEPO Channel 16 results therefore a correction factor was applied to be data, the results of which can be seen in Section 4.3.6.
- Levels of ^{3}H and ^{14}C removal under water conditions were at the LOD limits for the LSC.
- The highest values of release where achieved under 2.5M hydrogen peroxide. Hydrogen peroxide reacted with the graphite promoting ^{3}H and ^{14}C releases.
- Hydrogen peroxide and potassium bromate were considered from this experiment as an aggressive oxidising environments leading to the promotion of significant isotopic release. Comparing 0.5M conditions of both solutions hydrogen peroxide is noted to give the greater release rates. Some bubbles were observed within the hydrogen peroxide solutions which may be associated with ^{3}H-labelled gaseous species being released.
- An average overall weight loss of 12% was recorded, with 4% attributed to transfer between containers and filtering the material at the end of the experiment.
- Leach rates calculated for all conditions are summarised in Section 4.3.6 this allows a comparison of amount of activity released with exposed surface area of the material on test.

4.3. Chemical Treatment Phase Two

Phase two leaching test were carried out at room temperature, with a weekly testing frequency up to 190 days. Samples from BEPO reactor channels 1, 16 and 20 and Magnox Wylfa were used. An 8% error is associated with this leaching test; this is based on LSC counting error, ±1% weight distribution and electronic pipette standard deviation. All equipment was calibrated before testing was carried out but some errors are associated with the equipment are accounted for in the 8% error. All calculations include half life and weight corrections taking into account that for the solid samples due to machining limitations on active material not all solid sample used where 0.5 grams ±1%. Some of the solid samples used weighed more and there weight and activity per gram was taken into account.

4.3.1. BEPO Channel 1 Leaching Results - All Conditions

I-graphite from BEPO channel 1 was leached under water, pH1, pH13, 1M phosphoric acid (H_3PO_4), 0.5M Hydrogen peroxide (H_2O_2) and 0.5M Potassium Bromate ($KBrO_3$). Very limited quantities of BEPO Channel 1 graphite was available so these conditions where chosen to provide a comparison to leaching phase one data as well as to provide information on the mobility of the isotopes under an acidic environment. A solution of 1M phosphoric acid (H_3PO_4) was chosen as the acidic environment and was kept remain constant throughout leaching phase two program this was to provide a contrast to the pH1 buffer which contained 0.2M Hydrochloric acid (HCl). Figure 39 shows the cumulative release rates achieved by BEPO Channel 1 graphite for ^3H release. In this test 4.4% of the total ^3H inventory was released under water conditions, 7.8% of the total ^3H inventory was released under pH1, 4.3% of the total ^3H inventory was released under pH13, 9.6% of the total ^3H inventory was released under 1M H_3PO_4, 4.7% of the total ^3H inventory was released under 0.5M $KBrO_3$ conditions and 23.2% of the total ^3H inventory was released under 0.5M H_2O_2 conditions.

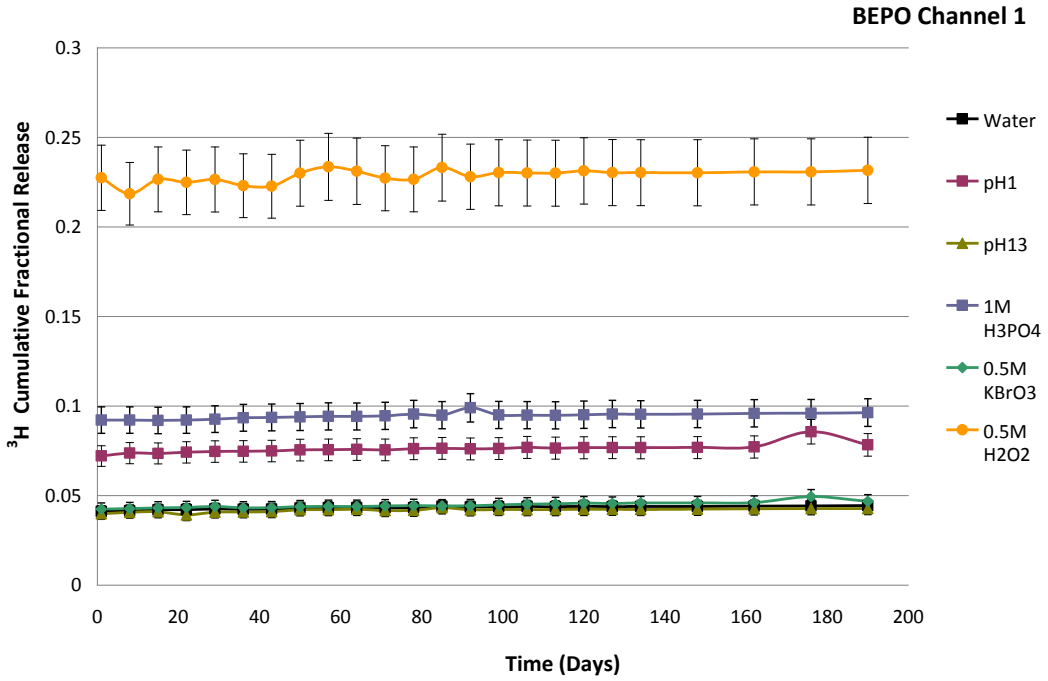

Figure 39 BEPO Channel 1 graphite ^{3}H release

Water and pH13 release rates for ^{3}H are comparable, this was expected for pH13 conditions, the mobility of the tritium is determined by the amount that is mobile. No additional ^{3}H activity compared to water has been released under pH13. 0.5M potassium bromate conditions did not produce an increase in release rate, as was previously observed in phase one. The 1M Phosphoric acid and pH1 solutions gave similar results with concentration of the acid contributing to release rate, the aggressive nature of the acid is known to breakdown the graphite structure [111]. The aim of using weaker acidic solutions was to promote isotopic removal without the complete destruction of the graphite. The strength of the acid used was determined by the LSC cocktail as detailed in Section 3.3.2. The 0.5M Hydrogen peroxide solution resulted in a very high release rate of ^{3}H; this supports a hydrogen ion isotopic exchange mechanism.

Figure 40 shows the cumulative ^{14}C leaching results for BEPO channel 1. Under water conditions 2.9% of the total ^{14}C inventory was released, under pH1 conditions 20.8% of the total ^{14}C inventory was released, under pH13 conditions 4.6% of the total ^{14}C inventory was released, under 1M H_3PO_4 conditions 19.8% of the total ^{14}C inventory was released, under 0.5M $KBrO_3$ conditions 6.5% of the total ^{14}C inventory was released and under 0.5M H_2O_2 conditions 0.31% of the total ^{14}C inventory was released.

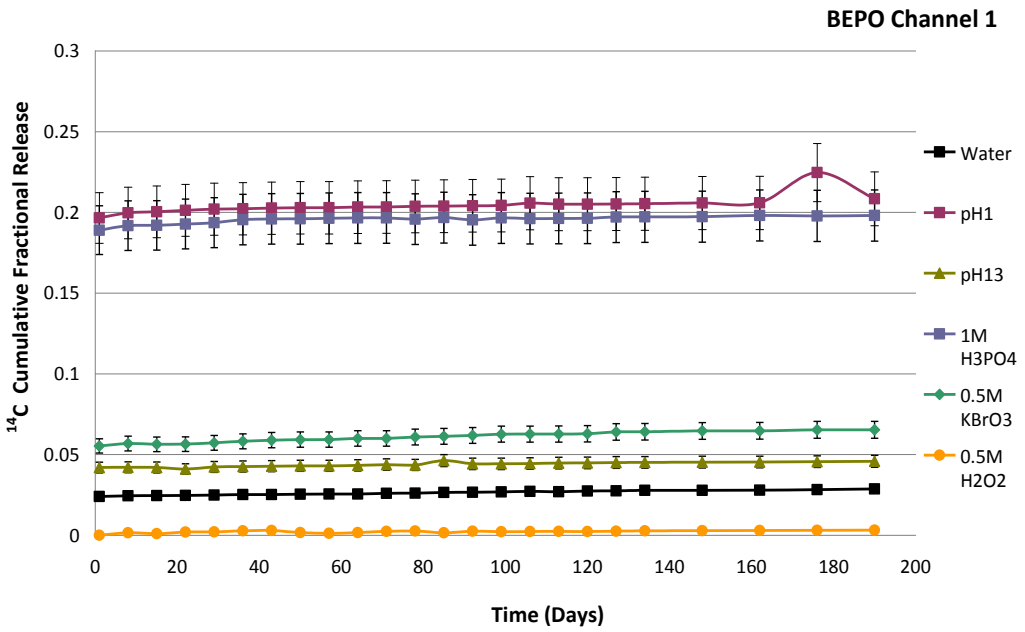

Figure 40 BEPO Channel 1 graphite ^{14}C release

Under phase one lower release of ^{14}C under Hydrogen peroxide conditions where observed, however such an extremely low result as seen in Figure 40 should be viewed with cautious as Figure 56 shows that some of the ^{14}C represent in the sample is not accounted for and therefore the author considers this result to be inaccurate.

The data shows that limited amounts of ^{14}C have been released under pH13 and 0.5M Potassium bromate solution there in an increase in release compared to water which was observed under phase one. Interestingly the acidic environments have removed more ^{14}C from the graphite material than previously observed under any other

conditions. The mechanism behind this acidic attack is thought to be intercalation of the surface material (penetration of interlayer spaces within the graphite structure), which is a significantly different process to the mechanism behind ^{3}H release. This ^{14}C release under acidic conditions is thought to be due to intercalation [111, 112].

4.3.2. pH 1 and pH13 Conditions

This section shows the results for cumulative fractional release for BEPO Channels 1 and 16, including BEPO Channel 16 solid samples under pH1 and pH13 buffered solution. Unfortunately BEPO Channel 1 solid material wasn't available. Figure 41 shows that 7.8% of the total ^{3}H inventory was released from BEPO channel 1 powdered graphite, 11.2% of the total ^{3}H inventory was released from BEPO channel 16 powdered graphite and 3.2% of the total ^{3}H inventory was released from BEPO channel 16 solid graphite released under pH1. Under pH13 4.3% of the total ^{3}H inventory was released from BEPO channel 1 powdered graphite, 3.4% of the total ^{3}H inventory was released from BEPO channel 16 powdered graphite and 0.27% of the total ^{3}H inventory was released from BEPO channel 16 solid graphite.

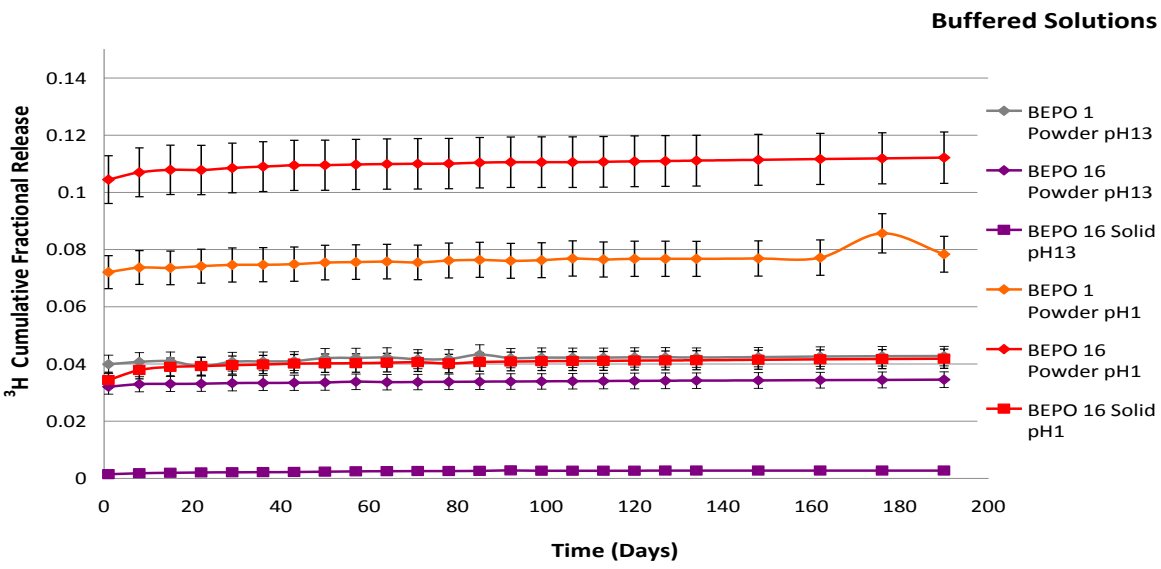

Figure 41 BEPO graphite ^{3}H release under pH1 and pH13 conditions

Figure 42 shows the ^{14}C cumulative release for BEPO Channels 1 and 16, including BEPO Channel 16 solid samples under pH1 and pH13 conditions. 20.8% of the total ^{14}C inventory was released from BEPO channel 1 powdered graphite, 25.4% of the total ^{14}C inventory was released from BEPO channel 16 powdered graphite and 6.1% of the total ^{14}C inventory was released from BEPO channel 16 solid graphite under pH1. Under pH13 solution 4.6% of the total ^{14}C inventory was released from BEPO channel 1 powdered graphite, 3.5% of the total ^{14}C inventory was released from BEPO channel 16 powdered graphite and 0.30% of the total ^{14}C inventory was released from BEPO channel 16 solid graphite.

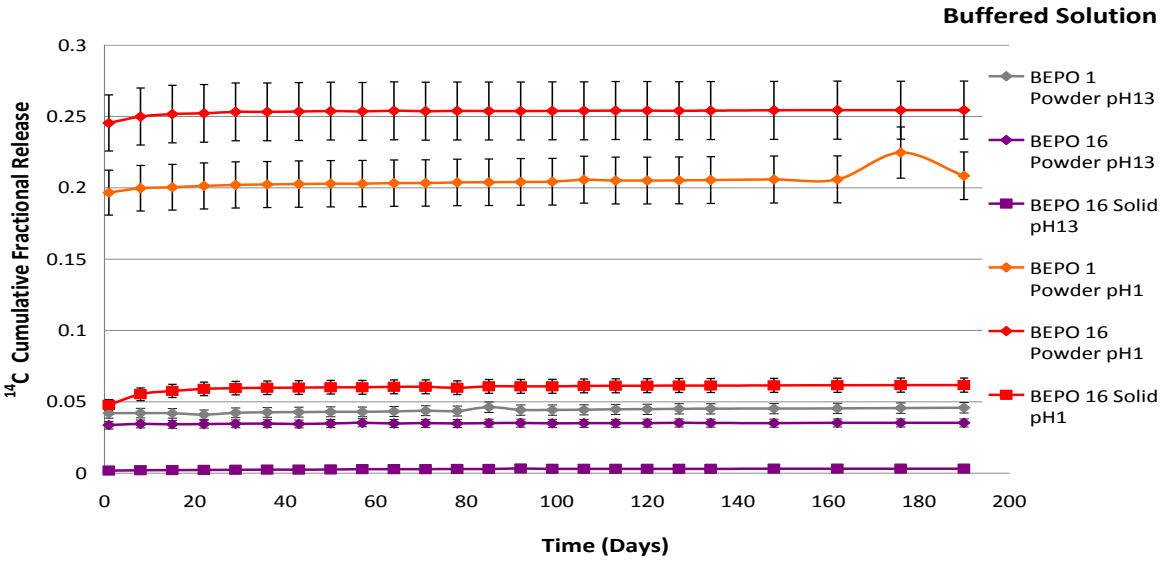

Figure 42 BEPO graphite ^{14}C release under pH1 and pH13 conditions

A significant increase is observed for ^{14}C release under pH1 conditions, the mechanism of intercalation is thought to promote this release. This proposed mechanism behind ^{14}C release is based on the acid intercalation with the graphite [111, 112], this requires the anion of the acid to penetrate the interlayer spaces within the graphite structure allowing the release of loosely bound ^{14}C species.

Acids Conditions

Figure 43 shows BEPO Channel 16 powder graphite ^{3}H release under all acidic conditions. In these tests 10.5% of the total ^{3}H inventory was released under 1M phosphoric acid (H_3PO_4) and 0.1M Sulphuric Acid (H_2SO_4), 11.8% of the total ^{3}H inventory was released under 1M Hydrochloric acid (HCl) and 11.2% of the total ^{3}H inventory was released under pH1.

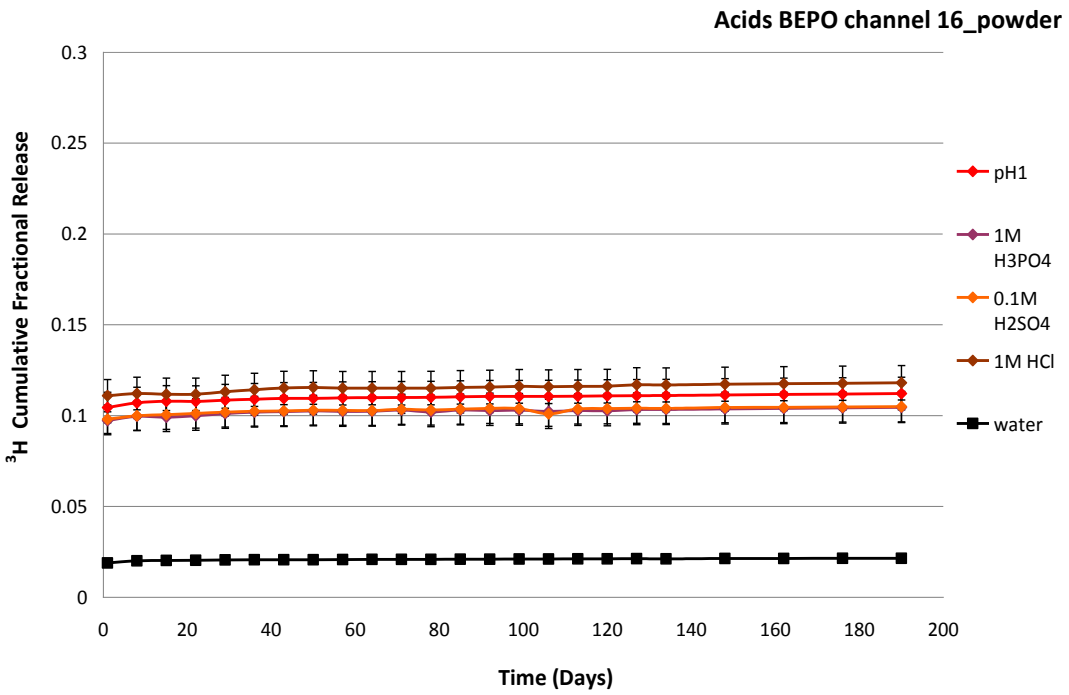

Figure 43 BEPO Channel 16 graphite ^{3}H release under acidic conditions

The data represented in Figure 43 supports the previous results for isotopic exchange being the mechanism behind ^{3}H removal as long as there is hydrogen atoms present in the right environment isotopic exchange with ^{3}H will occur. The other species present such as Cl^{-}, SO_4^{2-} and PO_4^{3-}may promote the availability of ^{3}H through intercalation within the graphite structure but they do not appear to be directly responsible for the release rate. The water data is shown on the graph is used as a comparison tool. The data achieved for BEPO Channel 20 is shown in the leach rate results Section 4.3.6.

Figure 44 shows BEPO Channel 16 powder graphite ^{14}C release under acidic conditions. 23.8% was released under 1M Orthophosphoric acid (H_3PO_4), 24.8% released under 0.1M Sulphuric Acid (H2SO4), 26.5% ^{14}C released under 1M Hydrochloric acid (HCl) and 25.4% released under pH1.

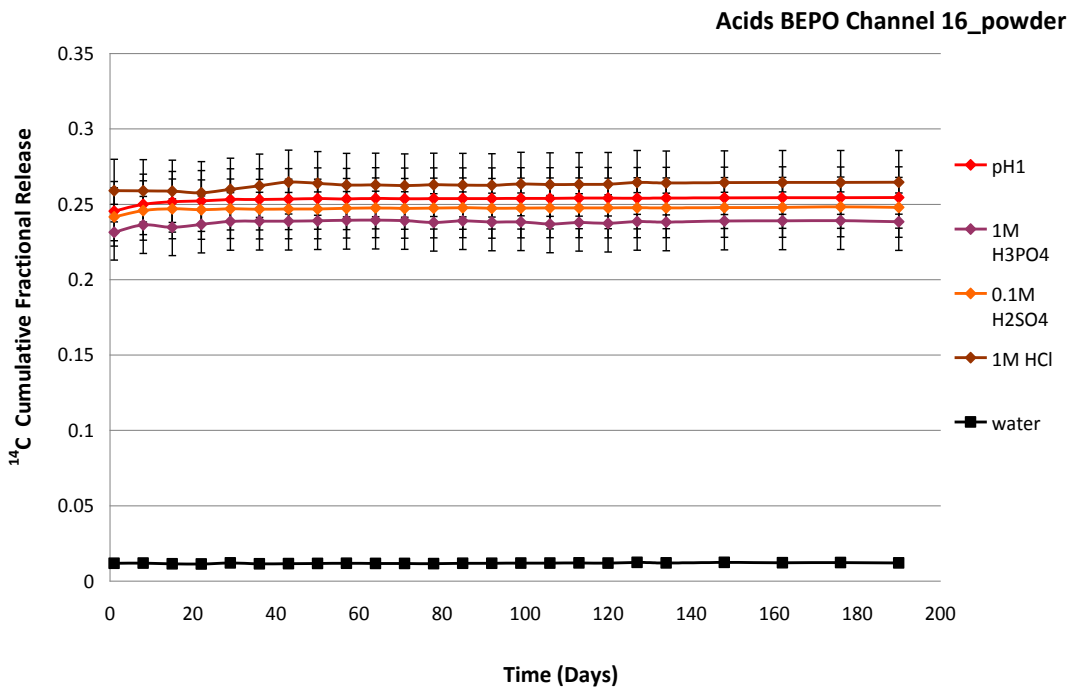

Figure 44 BEPO Channel 16 graphite ^{14}C release under acidic conditions

The data represented in Figure 44 supports the previous results for intercalation being the mechanism behind ^{14}C removal. The species present in the acids such as Cl^-,SO_4^{2-} and PO_4^{3-} are all capable of intercalation [16, 111]. Using stronger concentrations of these acidic would result in the complete breakdown of the graphite structure, an interesting experiment would be to analyse how much ^{14}C is released under such conditions however the dilution required and the incompatibility of the environment with the LSC cocktail hold some limitations for this experiment and the focus of which is slightly different to the research detailed here. The water data is shown on the graph is given for comparison. The data achieved for BEPO Channel 20 is shown in the leach rate results Section 4.3.6.

4.3.3. MAGNOX graphite leaching

The same conditions utilized for BEPO Channel 1 material was tested on Magnox Wylfa graphite. Figure 45 shows the results achieved for ^{3}H release this leaching experiment. In these tests 0.13% was released under water conditions, 9.3% was released under pH1, 0.11% was released under pH13, 19.0% was released under 1M H_3PO_4., 0.09% was released under 0.5M $KBrO_3$ conditions and 0.47% was released under 0.5M H_2O_2 conditions.

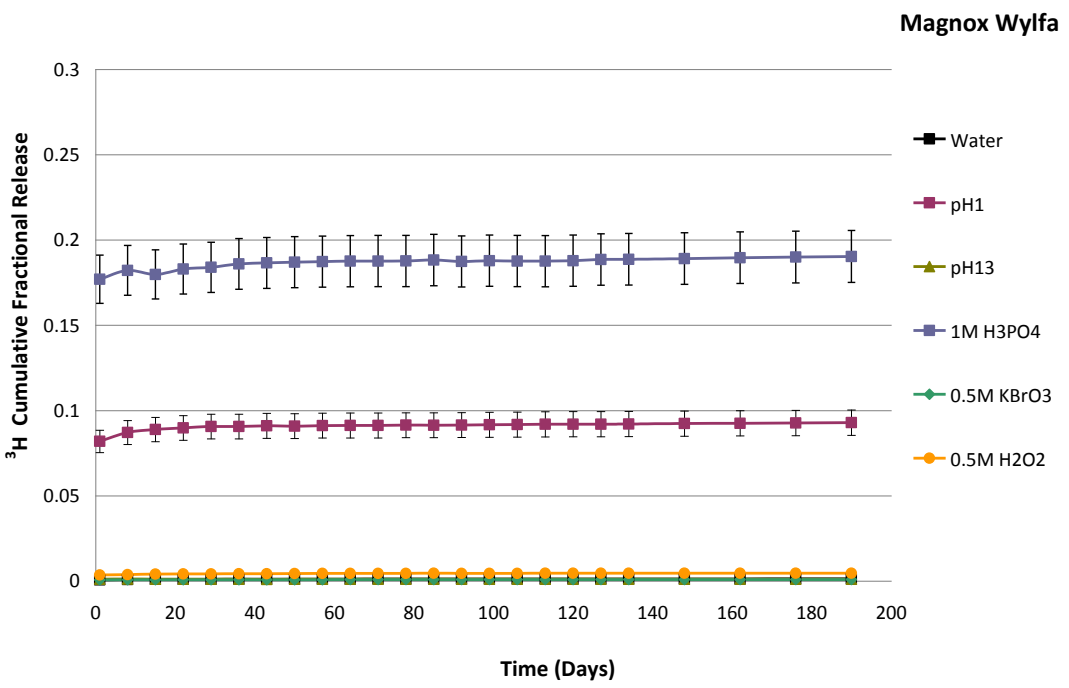

Figure 45 Magnox Wylfa ^{3}H release under all leaching conditions

Limited amounts of ^{3}H were released under water, 0.5M hydrogen peroxide and potassium bromate conditions. The Magnox material was supplied in a granulated form with a smaller surface area than the powdered BEPO graphite. From this data the conclusion can be drawn that as seen previously for tests with solid graphite samples, which are that under these three conditions hydrogen ion isotopic exchange, can only occur if the ^{3}H is easily accessible. Limited release is consistently observed under pH13 as well as ^{3}H release under acidic conditions gives results in the same order of magnitude as previously achieved.

Figure 46 shows the cumulative release rate for ^{14}C from Magnox Wylfa graphite. In these tests 2.5% was released under water conditions, 18.4% was released under pH1, 1.1% was released under pH13, 26.8% was released under 1M H_3PO_4, 1.6% was released under 0.5M $KBrO_3$ and 3.5% was released under 0.5M H_2O_2 solution.

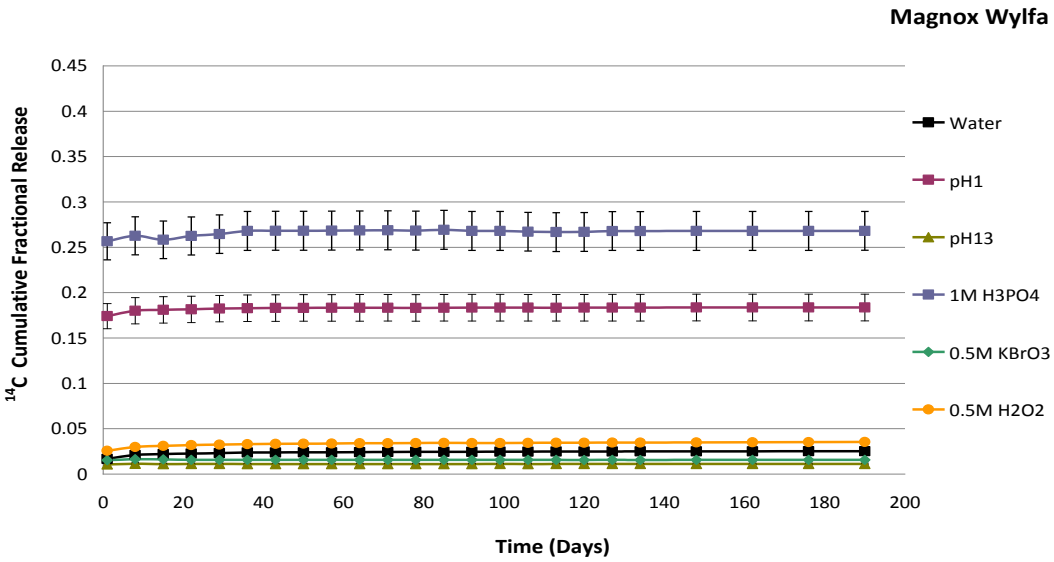

Figure 46 Magnox Wylfa ^{14}C release under all leaching conditions

Figure 46 show that limited release of ^{14}C occurred under water, pH13, 0.5M Hydrogen peroxide and potassium bromate. However, ^{14}C release under acidic conditions are similar to that achieved under BEPO Channel 1 and 16 powdered graphite. The pH1 solution contains 0.2M Hydrochloric acid which maybe the reason why this solution gives a lower release compared to 1M phosphoric acid. The Magnox Wylfa graphite contains significantly more activity per gram compared to the BEPO graphite which maybe why the concentration gives a significantly higher isotopic release for ^{14}C. In addition the surface area reduction may have limited the pH1 intercalation effectiveness. From these results ^{14}C appears to be present within the graphite structure in two forms, leachable and non-leachable ^{14}C species. This could well be related to the two main production pathways of ^{14}C origin as detailed in Table 6.

4.3.4. Leach Rate Calculations

Incremental day leach rate is a very important parameter when comparing leaching data. Calculating a comparable leach rate takes into account surface area, sample geometry and activity present per sample. Equation 5 [5] details how leach rate has been calculated for each of the samples and conditions analysed in this thesis. The 10 day leach rate results are detailed in Tables 30 to 35.

$$R_n = \frac{(a_n / A_n)}{(F/V)t_n}$$ **Equation 5**

R_n= Leach Rate cm.d^{-1}

a_n= Radioactivity released at renewal period

A_o= Radioactivity present in specimen

F= Exposed surface area (cm^2)

V= Volume of specimen (cm^3)

t_n= Duration of leachant renewal period

As previously discussed the BEPO Channel 20 produced a cloudy solution which interfered with the LSC counting, rather than not include this data a correction factor has been derived. The trends observed for BEPO Channel 16 are consistent with the BEPO Channel 20 data, which is why a correction factor has been used. Figures 55 and 56 show the thermal analysis performed on post leached BEPO Channel 20. The discrepancy between thermal analysed post leaching and thermal analysed sample prior to leaching has provided the information necessary for a realistic correction factor for the BEPO Channel 20 data.

4.3.5. Leach Rate Results

Leach rate results are detailed in Tables 30 to 35 for all leaching parameters tested in the research. For phase one leaching the majority of leach rate has reached a steady state by day 84 however it must be noted at 0.3M potassium bromate is still slightly increasing at day 84.

Table 30 Leaching phase one BEPO channel 16 Leach rates

Leachant condition	Type of material		Leach Rate at 84 days		Leach Rate at 84 days
Water	powder	^{3}H	$4.15E^{-6}$	^{14}C	$1.15E^{-6}$
Water	solid	^{3}H	$1.70E^{-4}$	^{14}C	$3.17E^{-5}$
0.1M Potassium Bromate	powder	^{3}H	$5.59E^{-6}$	^{14}C	$2.99E^{-6}$
0.2M Potassium Bromate	powder	^{3}H	$6.44E^{-6}$	^{14}C	$5.13E^{-6}$
0.3M Potassium Bromate	powder	^{3}H	$6.94E^{-6}$	^{14}C	$6.45E^{-6}$
0.3M Potassium Bromate	solid	^{3}H	$2.00E^{-4}$	^{14}C	$8.25E^{-5}$
0.4M Potassium Bromate	powder	^{3}H	$7.22E^{-6}$	^{14}C	$6.97E^{-6}$
0.5M Potassium Bromate	powder	^{3}H	$7.49E^{-6}$	^{14}C	$7.51E^{-6}$
0.5M Hydrogen Peroxide	powder	^{3}H	$1.28E^{-5}$	^{14}C	$1.55E^{-5}$
1M Hydrogen Peroxide	powder	^{3}H	$1.62E^{-5}$	^{14}C	$1.95E^{-5}$
1.5M Hydrogen Peroxide	powder	^{3}H	$1.78E^{-5}$	^{14}C	$2.02E^{-5}$
1.5M Hydrogen Peroxide	solid	^{3}H	$4.35E^{-4}$	^{14}C	$3.63E^{-4}$
2M Hydrogen Peroxide	powder	^{3}H	$2.14E^{-5}$	^{14}C	$2.01E^{-5}$
2.5M Hydrogen Peroxide	powder	^{3}H	$2.31E^{-5}$	^{14}C	$2.04E^{-5}$

Table 31 Leaching phase one BEPO channel 20 Leach rates

Leachant condition	Type of material		Leach Rate at 84 days		Leach Rate at 84 days
Water	powder	^{3}H	$6.57E^{-7}$	^{14}C	$3.88E^{-6}$
Water	solid	^{3}H	$8.79E^{-6}$	^{14}C	$1.16E^{-5}$
0.1M Potassium Bromate	powder	^{3}H	$1.20E^{-5}$	^{14}C	$7.60E^{-6}$
0.2M Potassium Bromate	powder	^{3}H	$1.64E^{-5}$	^{14}C	$1.06E^{-5}$
0.3M Potassium Bromate	powder	^{3}H	$1.53E^{-5}$	^{14}C	$1.26E^{-5}$
0.3M Potassium Bromate	solid	^{3}H	$1.77E^{-5}$	^{14}C	$3.90E^{-4}$
0.4M Potassium Bromate	powder	^{3}H	$1.86E^{-5}$	^{14}C	$1.60E^{-5}$
0.5M Potassium Bromate	powder	^{3}H	$1.79E^{-5}$	^{14}C	$1.59E^{-5}$
0.5M Hydrogen Peroxide	powder	^{3}H	$2.54E^{-5}$	^{14}C	$1.41E^{-5}$
1M Hydrogen Peroxide	powder	^{3}H	$3.57E^{-5}$	^{14}C	$1.80E^{-5}$
1.5M Hydrogen Peroxide	powder	^{3}H	$4.05E^{-5}$	^{14}C	$1.88E^{-5}$
1.5M Hydrogen Peroxide	solid	^{3}H	$8.11E^{-5}$	^{14}C	$4.25E^{-5}$
2M Hydrogen Peroxide	powder	^{3}H	$4.80E^{-5}$	^{14}C	$2.16E^{-5}$
2.5M Hydrogen Peroxide	powder	^{3}H	$5.19E^{-5}$	^{14}C	$2.53E^{-5}$

Table 32 Leaching phase two leach rates for BEPO Channel 1 samples

Leachant condition	Type of material on test		Leach rate at 99 days		Leach rate at 99 days
Water	powder	^{3}H	$1.74E^{-5}$	^{14}C	$1.07E^{-5}$
pH 1	powder	^{3}H	$3.04E^{-5}$	^{14}C	$8.14E^{-5}$
pH 13	powder	^{3}H	$1.68E^{-5}$	^{14}C	$1.76E^{-5}$
0.5M Hydrogen peroxide	powder	^{3}H	$9.18E^{-5}$	^{14}C	$8.88E^{-7}$
0.5M Potassium Bromate	powder	^{3}H	$1.79E^{-5}$	^{14}C	$2.50E^{-5}$
1M Phosphoric acid	Powder	^{3}H	$3.79E^{-5}$	^{14}C	$7.83E^{-5}$

Table 33 Leaching phase two leach rates for BEPO Channel 16 samples

Leachant condition	Type of material on test		Leach rate at 99 days		Leach rate at 99 days
Water	powder	^{3}H	$2.36E^{-6}$	^{14}C	$1.34E^{-6}$
Water	Solid	^{3}H	$4.21E^{-5}$	^{14}C	$5.40E^{-5}$
pH 1	powder	^{3}H	$1.24E^{-5}$	^{14}C	$2.86E^{-5}$
pH 1	Solid	^{3}H	$2.53E^{-4}$	^{14}C	$3.76E^{-4}$
pH 13	powder	^{3}H	$3.81E^{-6}$	^{14}C	$3.93E^{-6}$
pH 13	Solid	^{3}H	$2.07E^{-5}$	^{14}C	$2.33E^{-5}$
0.1M Sulphuric acid	Powder	^{3}H	$1.17E^{-5}$	^{14}C	$2.78E^{-5}$
0.1M Sulphuric acid	solid	^{3}H	$5.10E^{-4}$	^{14}C	$1.11E^{-3}$
1M Hydrochloric acid	Powder	^{3}H	$1.31E^{-5}$	^{14}C	$2.96E^{-5}$
1M Phosphoric acid	Powder	^{3}H	$1.15E^{-5}$	^{14}C	$2.68E^{-5}$
1M Phosphoric acid	solid	^{3}H	$2.37E^{-4}$	^{14}C	$3.21E^{-4}$

Table 34 Leaching phase two leach rates for BEPO Channel 20 samples

Leachant condition	Type of material on test		Leach rate at 99 days		Leach rate at 99 days
Water	powder	^{3}H	$1.67E^{-6}$	^{14}C	$2.02E^{-6}$
Water	Solid	^{3}H	$2.80E^{-7}$	^{14}C	$5.59E^{-6}$
pH 1	powder	^{3}H	$1.02E^{-5}$	^{14}C	$2.73E^{-5}$
pH1	Solid	^{3}H	$2.53E^{-5}$	^{14}C	$6.68E^{-5}$
pH 13	powder	^{3}H	$4.54E^{-6}$	^{14}C	$9.62E^{-6}$
pH 13	Solid	^{3}H	$2.34E^{-5}$	^{14}C	$7.54E^{-6}$
0.1M Sulphuric acid	Powder	^{3}H	$1.06E^{-5}$	^{14}C	$2.87E^{-5}$
1M Phosphoric acid	Powder	^{3}H	$1.02E^{-5}$	^{14}C	$2.77E^{-5}$
1M Phosphoric acid	solid	^{3}H	$3.07E^{-5}$	^{14}C	$8.67E^{-5}$

Table 35 Leaching phase two leach rates for Wylfa Magnox samples

Leachant condition	Type of material on test		Leach rate at 99 days		Leach rate at 99 days
Water	powder	^{3}H	$2.47E^{-7}$	^{14}C	$4.94E^{-6}$
pH 1	powder	^{3}H	$1.84E^{-5}$	^{14}C	$3.69E^{-5}$
pH 13	powder	^{3}H	$2.32E^{-7}$	^{14}C	$2.23E^{-6}$
0.5M Hydrogen peroxide	powder	^{3}H	$9.18E^{-7}$	^{14}C	$6.88E^{-6}$
0.5M Potassium Bromate	powder	^{3}H	$1.79E^{-7}$	^{14}C	$3.12E^{-6}$
1M Phosphoric acid	powder	^{3}H	$3.78E^{-5}$	^{14}C	$5.39E^{-5}$

4.3.6. Leach Rate Comparison of BEPO to Wylfa Graphite

Both phase one and phase two leach rate calculations have been reported in this section. This allows the comparison of amount of ^{3}H and ^{14}C released under powder and solid samples to be compared as it takes into account surface area.

The Magnox material tested has significantly difference irradiation history to that of the BEPO material. Magnox graphite has been subject to radiolytic oxidation as well have received a higher fluence than BEPO graphite. This may have contributed to the lower leach rates observed here as surface bound activity of Wylfa graphite may have already been removed due to these two processes, particularly the former. BEPO material was irradiated in an air environment with a lower fluence at a temperature around 40˚C [40]. The isotopic inventory present in BEPO material may therefore have had less processes promoting migration of interstitials and as a result more mobile surface bound species are present giving rise to increased leach rates.

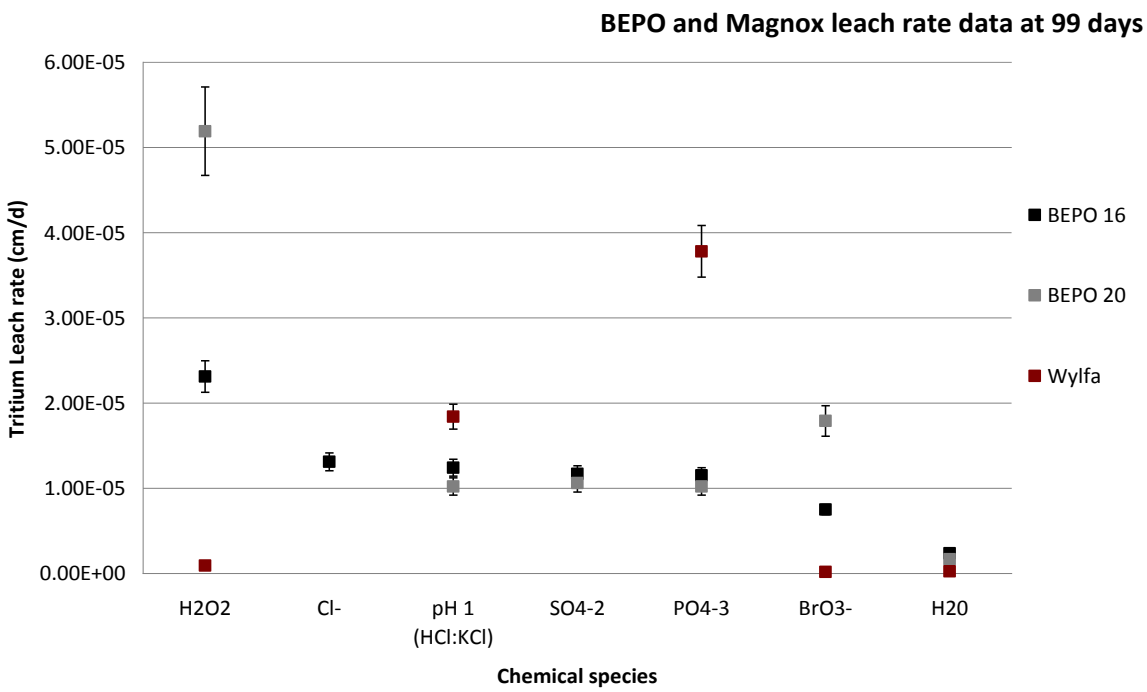

Figure 47 **^{3}H Leach rate comparison under all leaching conditions**

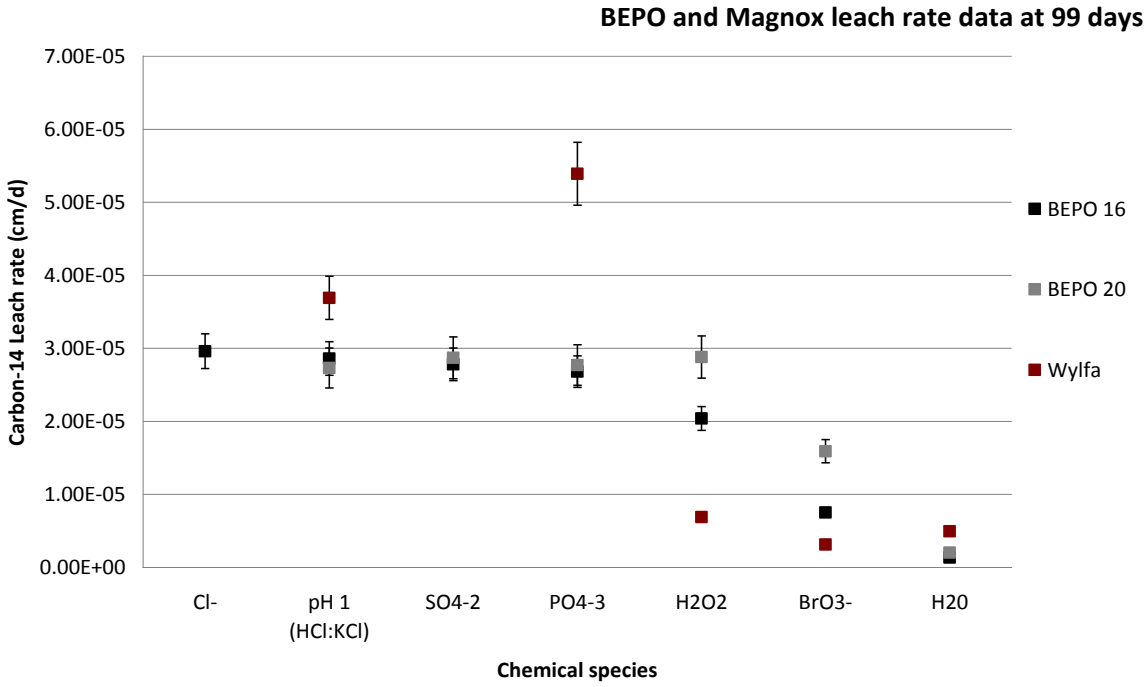

Figure 48 **^{14}C Leach rate comparison under all leaching conditions**

Figures 47 and 48 show the leach rate data for BEPO graphite against speciation and Table 36 details the pH and pKa of the chemicals used during chemical treatment.

Table 36 **Comparison of chemical species used in leaching experiment**

Species	Reaction mechanism	pH	pKa
H_2O_2	$OH^+ + OH^-$	5	11.62
$KBrO_3$	$K^+ + BrO3^-$	5.6	8.8
H_3PO_4	$3H^+ + PO4^{3-}$	1	2.16
H_2SO_4	$2H^+ + SO4^{2-}$	1	1.99
HCl	$H^+ + Cl^-$	1	4
H_2O	$H^+ + OH^-$	6.8	7

4.3.7. Discussion of Chemical Leaching Results

The chemical leaching results and experimental techniques used to determine the release rates and mobility of ^{14}C and ^{3}H from i-graphite material are summarised below:

- The acidic environment yielded the highest release activities for both of ^{3}H and ^{14}C removal.
- The separate mechanisms for ^{3}H and ^{14}C have been proposed though several difference conditions this difference in ^{3}H and ^{14}C interaction have been exploited.
- ^{14}C seems to be present in two separate forms i.e. leachable and non-leachable, the presence of two forms of ^{14}C provides insight in the mechanism of formation and the behaviour under continued irradiation.
- Hydrogen ion isotopic exchange is thought to be the mechanism behind ^{3}H release.
- Intercalation with penetration of interlayer spaces within the graphite structure is thought to be the mechanism behind ^{14}C removal.
- Throughout all leaching experiment no change in pH was observed.
- The weightloss of the samples after chemical leaching averaged 12% making the intercalation mechanism a preferred conclusion as a significant weightloss of the sample was not observed in material that had high acidic percentages of ^{14}C leached out.
- Steady state of release was achieved under all conditions by day 90, after this point very limited amounts of both ^{3}H and ^{14}C were released.

The chemical treatment process removing mobile and accessible ^{3}H and ^{14}C prior to decommissioning or repository storage shows that a significant portion of ^{3}H and ^{14}C remains within the graphite structure. Even in harsh oxidising or acidic environments haven't removed over 30% of the ^{3}H and ^{14}C inventory present. In terms of using this methodology as a pre treatment method the industrial and financial feasibility of these processes would need to be evaluated.

4.4. Thermal Treatment

4.4.1. Round Robin Test (RRT) Validation

As part of the EU CARBOWASTE program University of Manchester took part in a "Round Robin" test. Each sample used in the test was split into two and analysed individually and an average of the LSC results taken. The spread of the LSC data determined the standard deviation and percentage error for each analysis. The University of Manchester was numbered as "Laboratory 6" as presented on the Figures 49 and 50 by L6-1 and L6-2 for the two sets of analysis performed. Figure 49 shows the tritium results for the Round Robin partners to date with the bold line represents the known value of ^{3}H present as determined by the CIEMAT organisation. The grey dotted line represents the boundaries of this analysis, therefore any result within this region is considered sufficiently accurate. Both calculated results for ^{3}H determination are within this region and therefore the methodology employed by Manchester for ^{3}H analysis is considered suitable for ^{3}H determination in i-graphite.

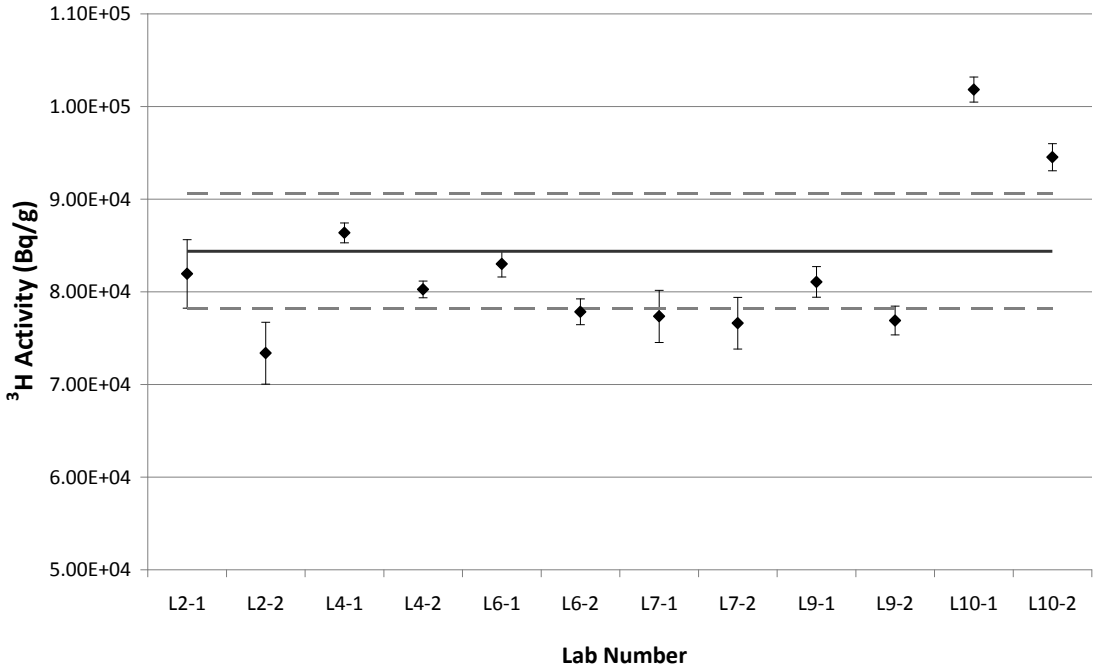

Figure 49 ^{3}H results from the RRT analysis for each laboratory

Figure 50 shows the results calculated for the RRT partners for ^{14}C. The bold line represents the known value of ^{14}C present as determined by the CIEMAT organisation. The grey dotted line represent the boundaries of this analysis, therefore any result within this region is considered correct. Both results for ^{14}C determination are very close to the known value determined by CIEMAT. Therefore the methodology employed by Manchester for ^{14}C analysis is considered suitable for ^{14}C determination in i-graphite.

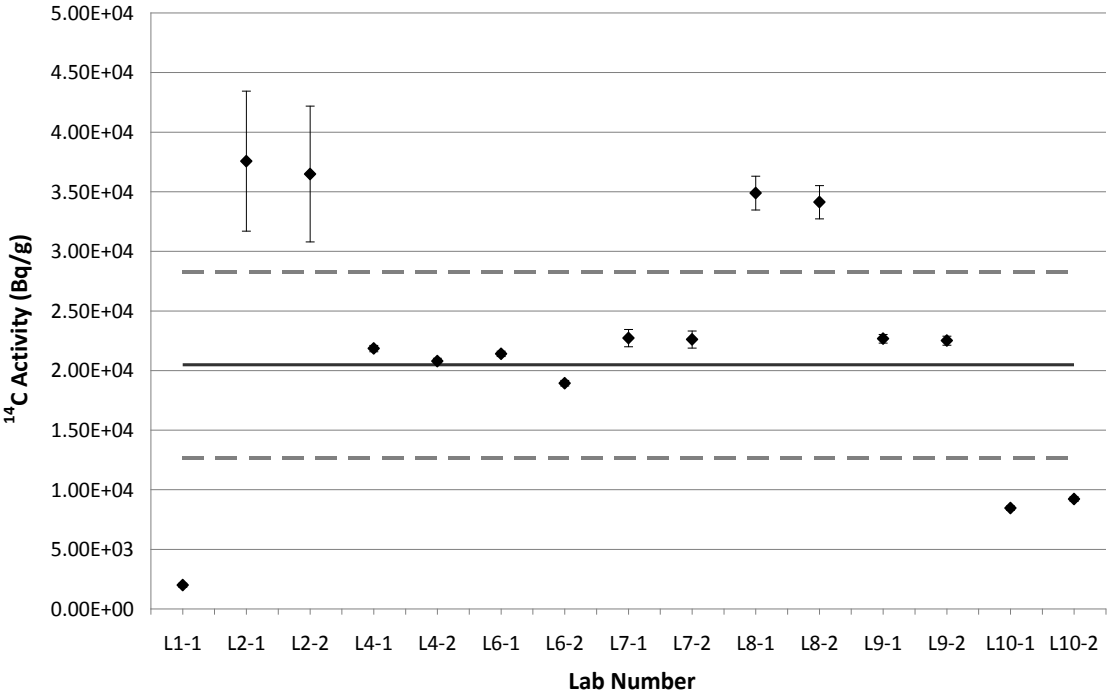

Figure 50 ^{14}C results from the RRT analysis for each laboratory

4.4.2. Determination of ^{3}H and ^{14}C Isotopes in BEPO Graphite

Given the success achieved with the RRT the isotopic inventory for the samples analysed in this research was determined by thermal analysis. This section gives the results achieved as well as the data provided from the companies that provided this material. Table 37 details the isotopic inventory information that was provided with the BEPO graphite supplied to University of Manchester for this research.

Table 37 Isotopic inventory data provided by NIREX on the BEPO graphite 7th December 2007

Nuclide	BEPO Channel 1 Specific Activity Bq/g	BEPO Channel 16 Specific Activity Bq/g	BEPO Channel 20 Specific Activity Bq/g
^{14}C	220	41430	41500
^{3}H	649	122046	122143
^{60}Co	12	2244	2242.9
^{152}Eu	4	768	771
^{154}Eu	2	370	370

The data in Table 38 is the isotopic inventory provided by NIREX which has been corrected for half life to the date in which analysis was performed at University of Manchester. These results are shown in Table 39.

Table 38 Isotopic inventory data provided by NIREX on the BEPO graphite with half life correction to 2nd June 2011

Nuclide	BEPO Channel 1 Specific Activity Bq/g	BEPO Channel 16 Specific Activity Bq/g	BEPO Channel 20 Specific Activity Bq/g
^{14}C	220	41412	41483

^{3}H	533	100317	100397

Analysis was carried on BEPO Channel 1, 16 and 20 samples using the methodology explained in Section 3.4. Table 39 shows the results achieved which enables a comparison to be made of the supplied inventory to the data determined at the University of Manchester. All leaching calculations are based on thermally analysed inventories. The results obtained using thermal analyses have a 10% uncertainty.

Table 39 Isotopic inventory data determined by thermal analysis

Nuclide	BEPO Channel 1 Specific Activity Bq/g 15th June 2011	BEPO Channel 16 Specific Activity Bq/g 1st April 2011	BEPO Channel 20 Specific Activity Bq/g 2nd June 2011
^{14}C	402	16459	19842
^{60}Co	<LOD	<LOD	<LOD
^{3}H	1668	66638	72248

A significant difference between the data provided and the ^{3}H and ^{14}C measured using thermal analysis is observed. Overall between all BEPO samples there is an average variation of 50%. BEPO Channel 1 graphite contained more ^{3}H and ^{14}C than originally expected and BEPO Channels 16 and 20 containing significantly less than expected. An inhomogeneous spread of activity was noticed by the author throughout the material, the analysis here is an average of three samples analysed independently of each other. A significant variation was noticed between results particularly for BEPO Channel 20, which indicates that the isotopic data provided by NIREX may well have been extremities of the material inhomogeneity of the material tested. In addition storage and machining of the material may have been a possible reason for the variation.

4.4.3. Determination of ^{3}H and ^{14}C Isotopes in Magnox Wylfa Graphite

Table 40 details the isotopic inventory information that was provided with the Magnox Wylfa graphite supplied to the University of Manchester for this research and half life correction to the date in which analysis was carried out.

Table 40 Isotopic inventory data provided by NNL on the two Wylfa samples supplied for this research.

	Wyfla 1413/02		Wlfya 1319/12	
Nuclide	**Specific Activity Bq/g 9th June 2009**	**Specific Activity Bq/g Half life corrected to 24th June 2011**	**Specific Activity Bq/g 9th June 2009**	**Specific Activity Bq/g Half life corrected to 24th June 2011**
^{14}C	22100	22095	22300	22295
^{60}Co	123600	94506	124000	94812
^{137}Cs	2377	2268	2480	2366
^{55}Fe	890000	530058	890000	530058
^{3}H	5465000	4872569	5480000	4885943

Thermal analysis was carried out Magnox Wylfa graphite using the methodology outlined in Section 3.4. Table 41 shows the isotopic inventory determined at the University of Manchester this included gamma spectroscopy analysis to determine ^{60}Co and ^{137}Cs. A comparison of the University of Manchester determined inventory to the data that was supplied shows a significant variation in the data supplied. All leaching calculations are based on inventories measured by the author. The results obtained using thermal analyses have a 10% uncertainty and the results obtained using gamma spectroscopy has a 5% uncertainty.

Table 41 Isotopic inventory for Wylfa samples determined

Nuclide	Wyfla 1413/02 Specific Activity Bq/g 24th June 2011	Wlfya 1319/12 Specific Activity Bq/g 24th June 2011
^{3}H	199066	
^{60}Co		23700
^{137}Cs		1140
^{14}C	73208	

4.4.4. Post Leaching Thermal Analysis

Upon the completion of the leaching experiment the samples were filtered weighted and then thermally analysed for the amount of ^{3}H and ^{14}C that remained. An inhomogeneous distribution of activity was observed between the samples however in most cases the combined thermal analyses with the amount leached out are within the expected quantity of activity present.

Figures 51 and 52 show the data for BEPO Channel 1the Grey is activity determined via thermal analysis, Blue is activity leached out and the red line in total activity thought to be present in the sample. The data bars are set to 10% error.

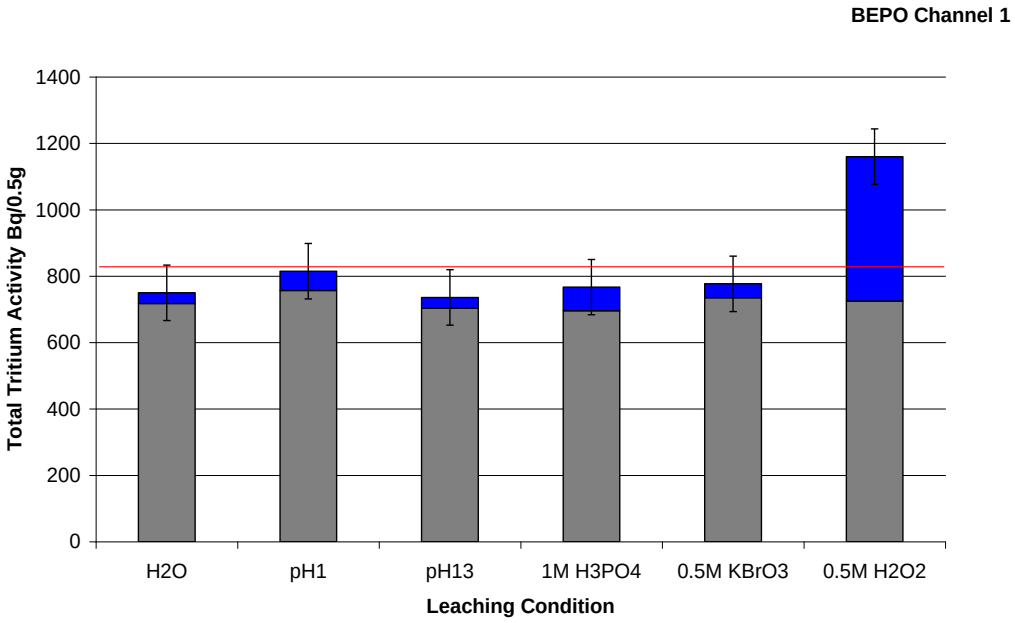

Figure 51 ^{3}H results for BEPO Channel 1 thermal and leaching data combined

Throughout all the conditions for BEPO Channel 1 there is good correlation between combined thermal analysis with leaching data apart from under 0.5M hydrogen peroxide.

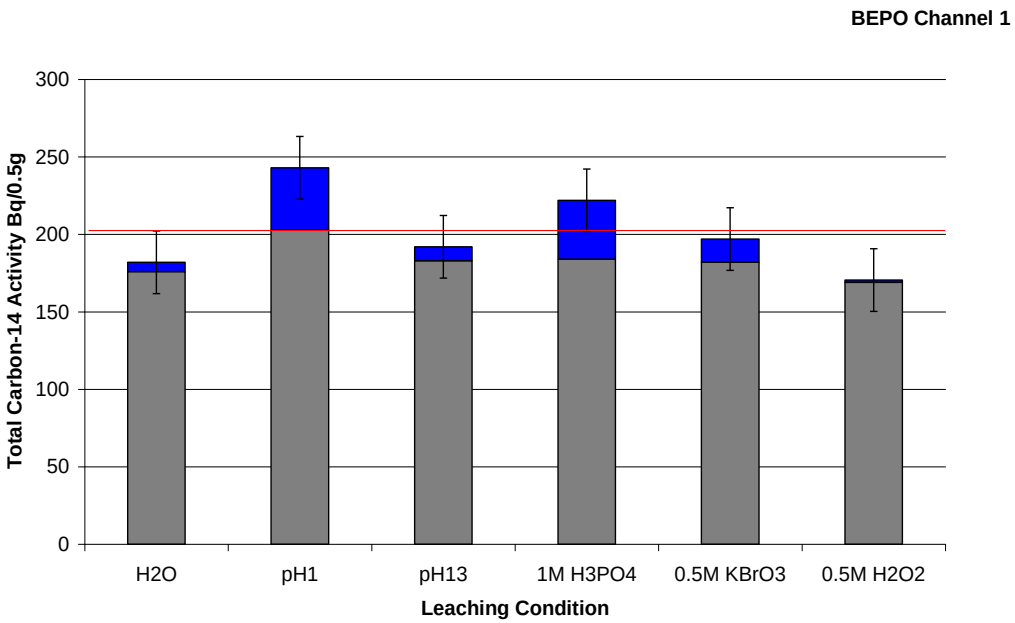

Figure 52 **^{14}C results for BEPO Channel 1 thermal and leaching data combined**

Figure 53 and 54 show the combined thermal analysis and leaching data for Wylfa Magnox graphite analysed in phase two, again the grey activity was determined via thermal analysis, Blue is activity was leached out and the red line signifies the total activity thought to be present in the sample determined by an unleached sample undergoing thermal analysis. The data bars are set to 10% error.

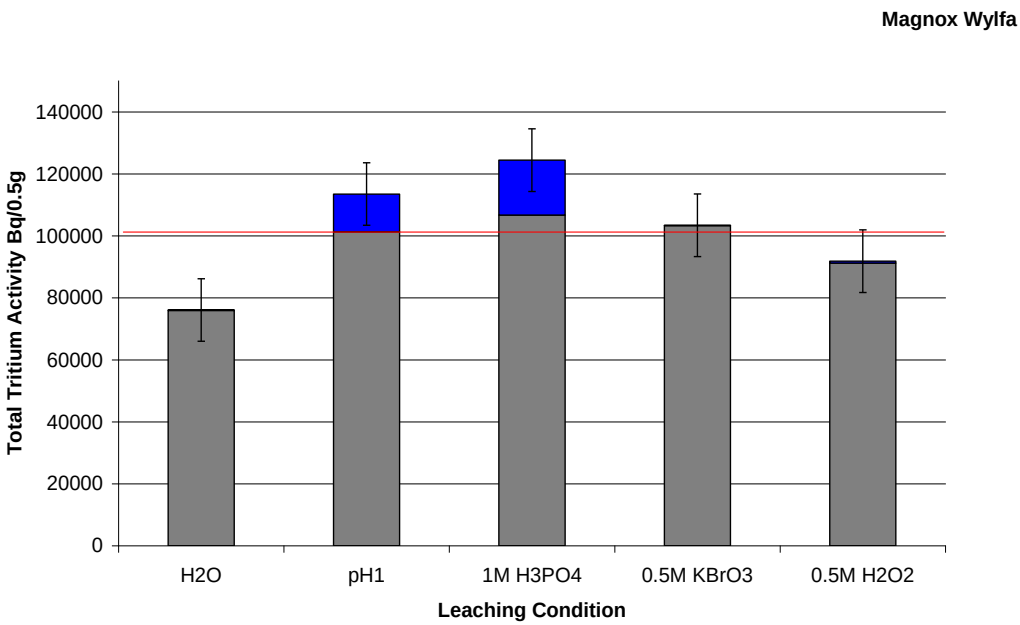

Figure 53 ^{3}H results for Wylfa Magnox thermal and leaching data combined

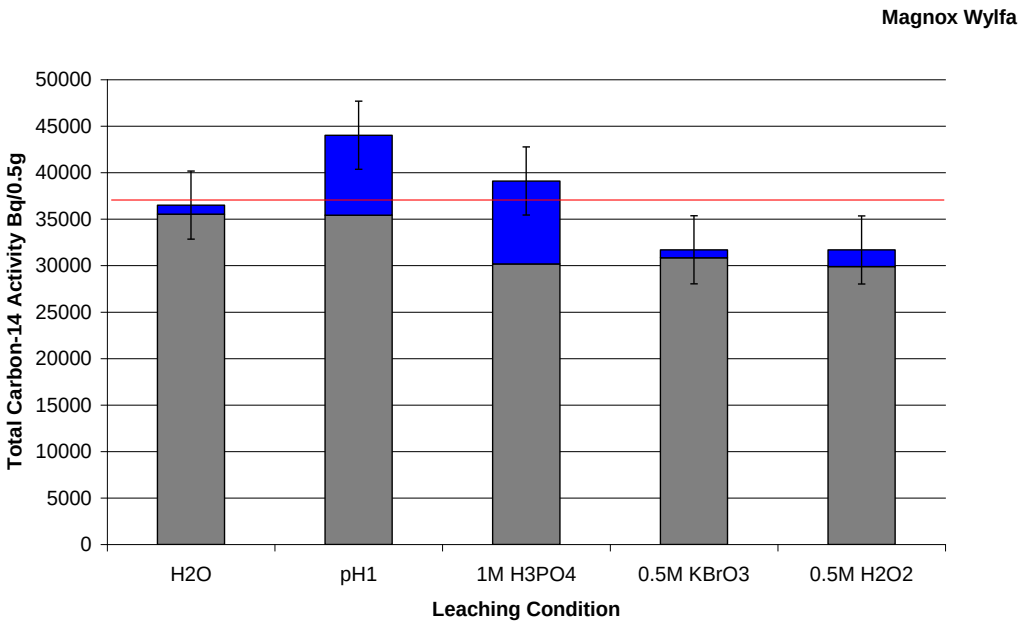

Figure 54 ^{14}C results for Wylfa Magnox thermal and leaching data combined

As previously discussed the BEPO Channel 20 produced a cloudy solution which interfered with the LSC counting, rather than not include this data a correction factor has been derived. The trends observed for BEPO Channel 16 are consistent with the BEPO Channel 20 data, which is why a correction factor has been used. Figures 55 and 56 show the thermal analysis performed on post leached BEPO Channel 20 with a red line indicating the isotopic inventory present before leaching. This discrepancy has provided the information necessary for a realistic correction factor for the BEPO Channel 20 data.

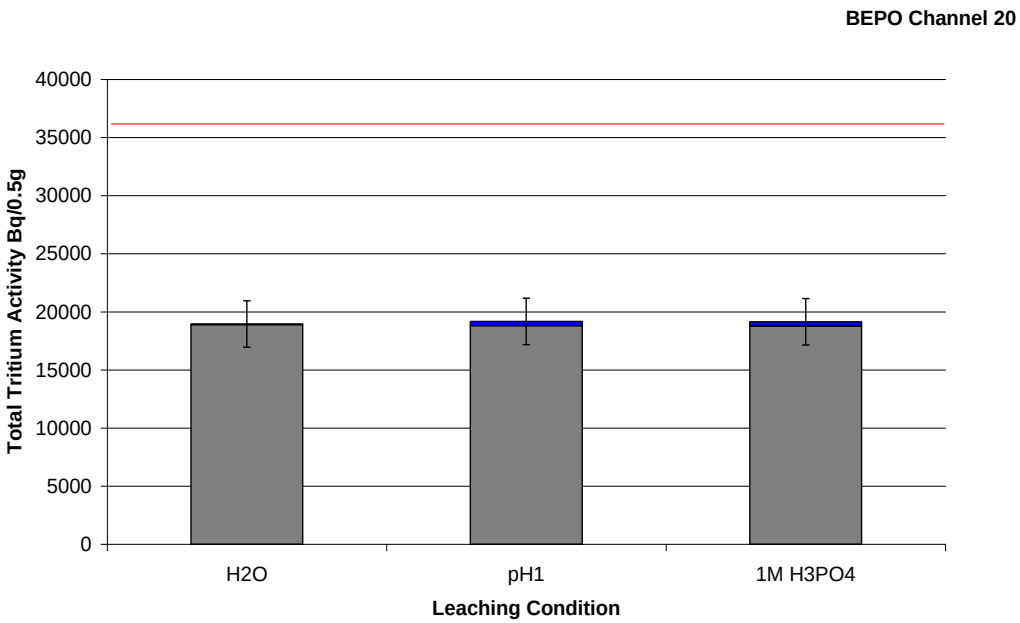

Figure 55 **^{3}H results for BEPO Channel 20 thermal and leaching data combined**

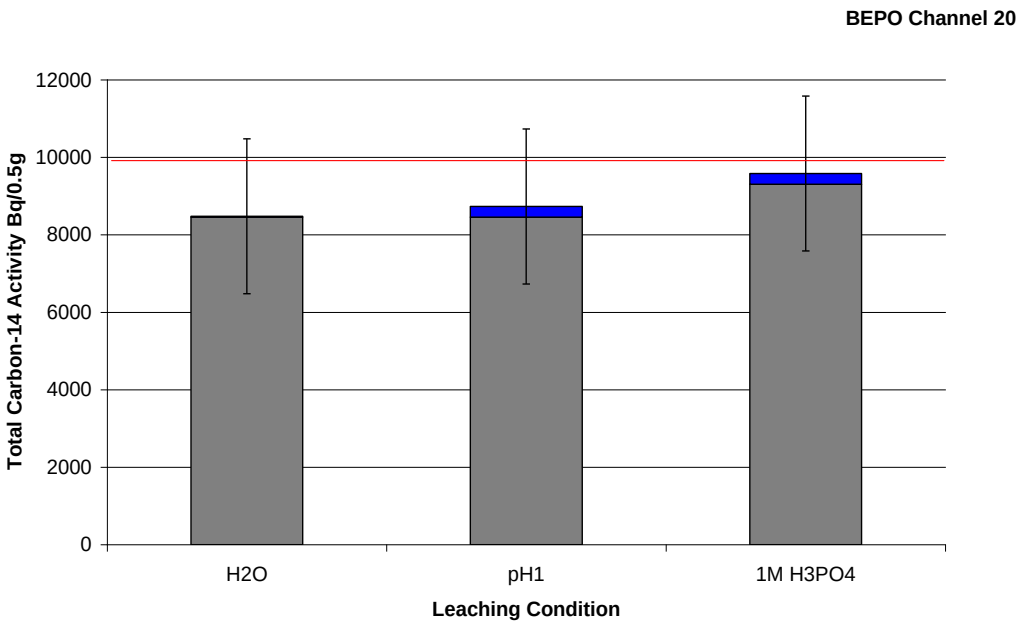

Figure 56 **^{14}C results for BEPO Channel 20 thermal and leaching data combined**

4.4.5. Summary of thermal treatment

Thermal treatment has proved to be a huge success in accuracy determination of ^{3}H and ^{14}C represent in i-graphite. This technique has limitation interms of laboratories resources and inparticualr the time in takes per analysis in both furnace, personnel and LSC resources. However in supporting the leaching analysis performed during this research and identication of activity present it has proven to play a significant and valuable role in this research.

4.5. Microstructural characterisation

4.5.1. Pore structure determination

Several techniques have been used to evaluate the structure of the material used in the leaching and thermal analysis. Confocal microscopy has been used to visually compare the surface, Raman Spectroscopy has used to determine structural changes with irradiation, Autoradiography has been used to examine the spread of activity throughout the material, Tomography has been used to determine internal porosity and high attenuation spots and surface area analysis has been performed to determine the surface area of both solid and powdered material used in the leaching experiments.

4.5.2. Change in structure with irradiation – Confocal Microscopy

The confocal microscope is used to produce images of a materials structure. The confocal microscope combines laser profile images to produce height images which can be reconstruction to produce a three dimensional profile of the sample surface. The confocal microscope can provide depth profiling and roughness values for a surface. Having a surface prepared and analysed and then irradiating this material and comparing it would provide interesting data on changes to the surface. In this case BEPO Channel 1 material has been used as a 'virgin' material to compare BEPO Channel 16. Figure 57 shows a profile image of BEPO Channel 1 which represents the capabilities of this instrument. Figures 58 to 59 compare images of BEPO Channel 1 and 16.

Figure 57 shows a three dimensional depth profile of porosity within the graphite structure with a pore depth of approx 60 microns for the BEPO Channel 1 sample

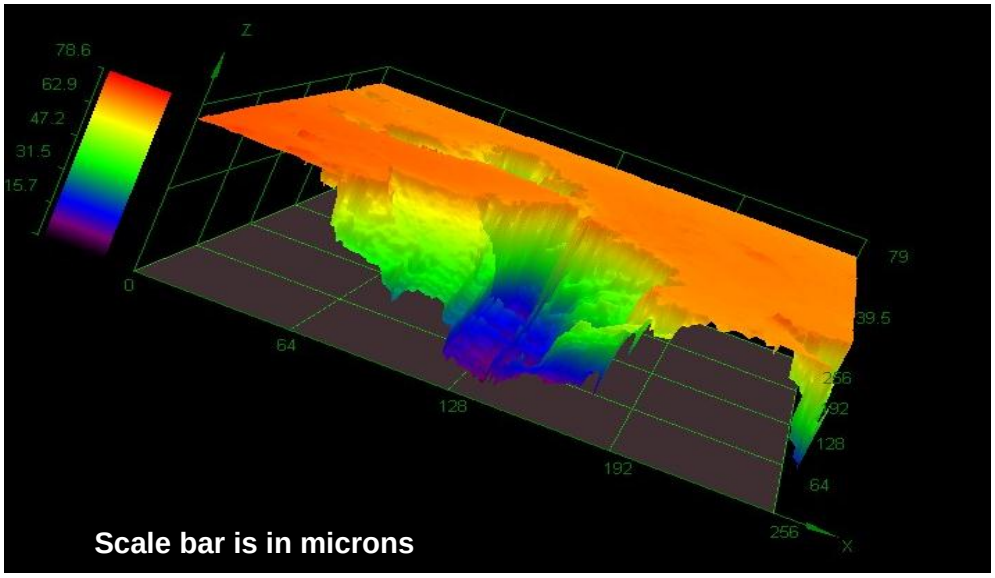

Figure 57 A three dimensional depth profile of BEPO Channel 1 sample.

Figures 58 and 59 show laser images comparing porosity changes with increase irradiation for BEPO Channel 1 and BEPO Channel 16. BEPO Channel 16 has received a higher fluence during the reactor lifetime; these images show the damage done to the structure in comparison to BEPO Channel 1.

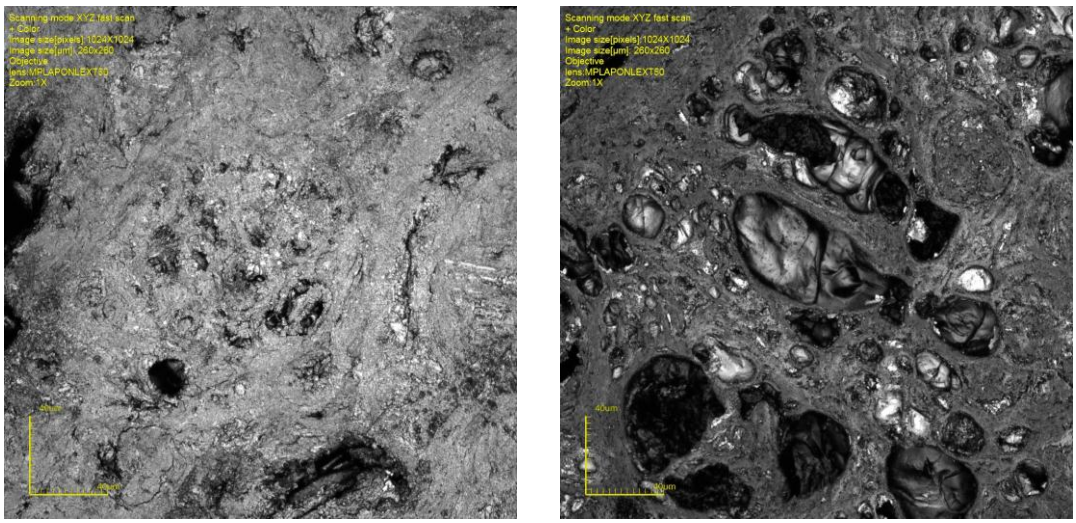

Figure 58 Laser images for BEPO Channel 1 and BEPO Channel 16. The scale bar is 40 microns.

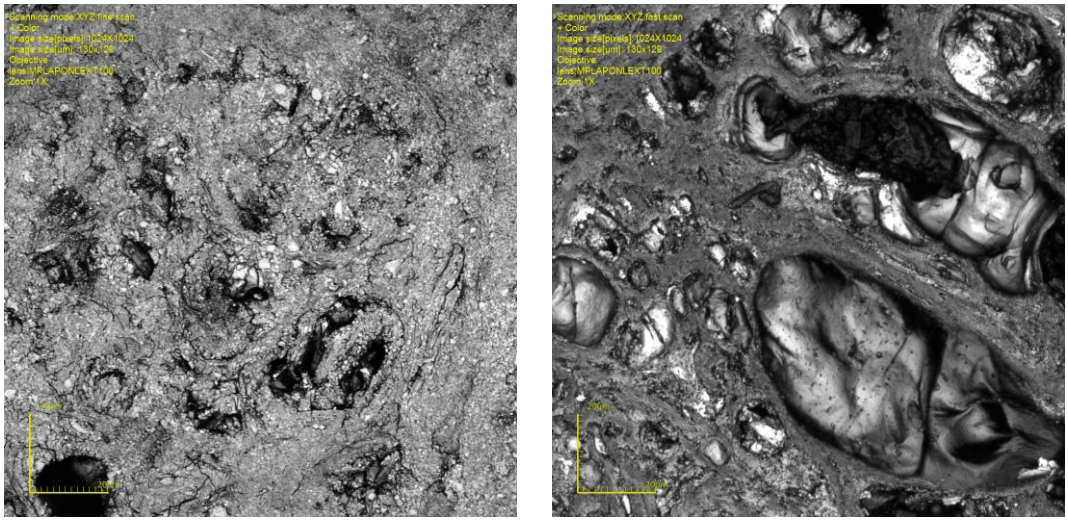

Figure 59 Laser images for BEPO Channel 1 and BEPO Channel 16. The scale bar is 20 microns.

SEM-EDX analysis of this porosity observed in these figures concluded that the only element present is that of carbon.

4.5.3. Tomography

It was observed in the two dimensional slices produced when analysing the tomography that there were high attenuation “spots”, Figure 60. These spots were of a material with a much higher density and therefore elemental number than that of graphite. The majority of these high attenuation spots were noted to be next to or contained within areas of porosity. These spots have been noticed in virgin material before and have been analysed SEM-EDX in order to determine their composition. The results identified that these regions of interest contained both Iron and Nickel. SEM-EDX analysis is planned as future work for this material analysed here once all other tests have been performed as polishing this sample to the correct height will result in significant waste therefore ensure no further testing is required beforehand is a priority.

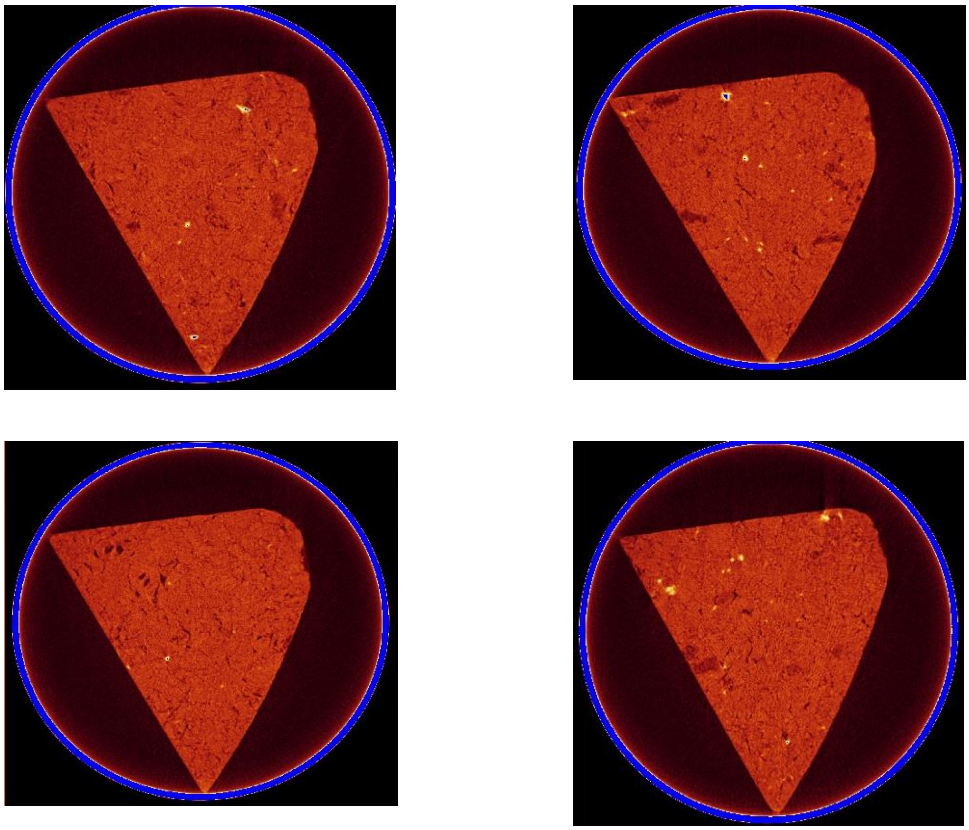

Figure 60 2D tomography Radiographs of BEPO sample 16 graphite contained within a Harwall can.

Three-dimensional volume reconstructions of BEPO sample 16 have been processed using Amira© software are shown in Figure 61. The porosity distribution was calculated and is equivalent to 17.2% porosity. The blue regions display the internal porosity and the red is the high attenuation spots. It can be noted that these high attenuations spots are contained within the porosity and are non-uniformly distributed.

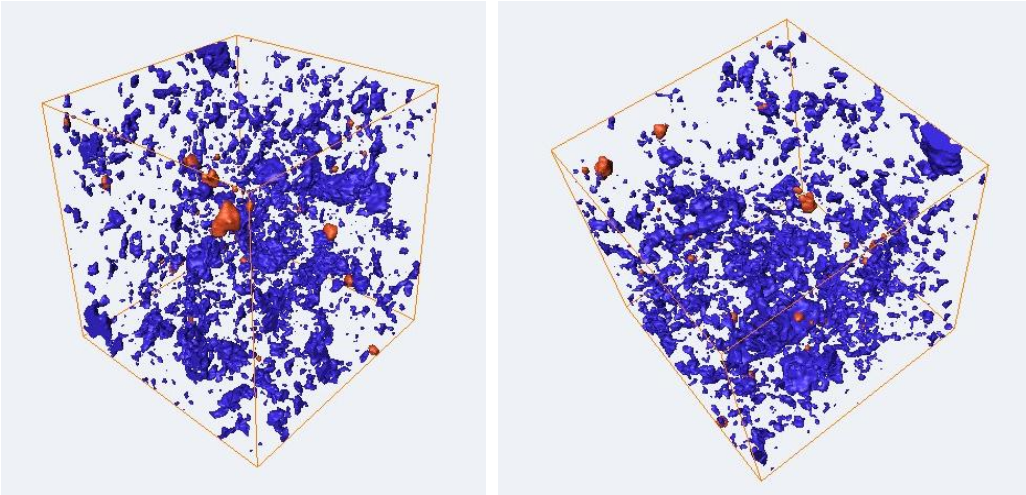

Figure 61. 3D volume reconstructions of BEPO Graphite using Amira© software

4.5.4. Isotopic distribution by autoradiography

Autoradiography was carried out on all BEPO samples in order to gain a qualitative assessment of the distribution of radioisotopes within the irradiated BEPO material. Figure 62 shows the average intensity of the samples with increasing sample number after an exposure time of 20 hours. Sample 1 exhibits the least intensity of the BEPO graphite, which corresponds to the least active samples there is a non uniform distribution of radioisotopes which can be noted by the presence of high intensity regions contained within sample 16 this is also a high distribution of activity with both sample 20 and 21 this film is fully saturated and again shows a non uniform disruption of β and γ activity within the sample.

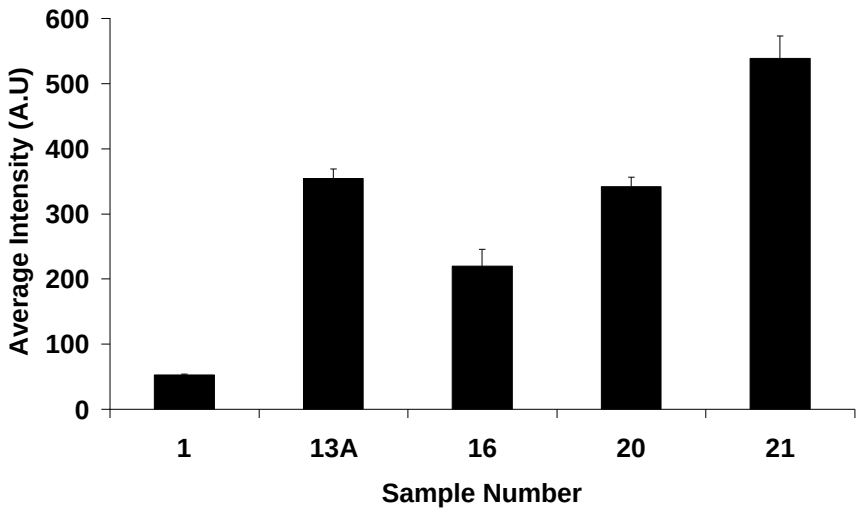

Figure 62 Graph showing the average intensity for BEPO samples calculated from Autoradiography greyscales

Autoradiography was successfully used to characterise the distribution of radioisotopes in BEPO graphite. Utilising thin 1mm thick samples of graphite allows for a reduction in gamma swapping effects and has enabled the investigation of anomalies within the radioisotopic distribution, Figure 63.

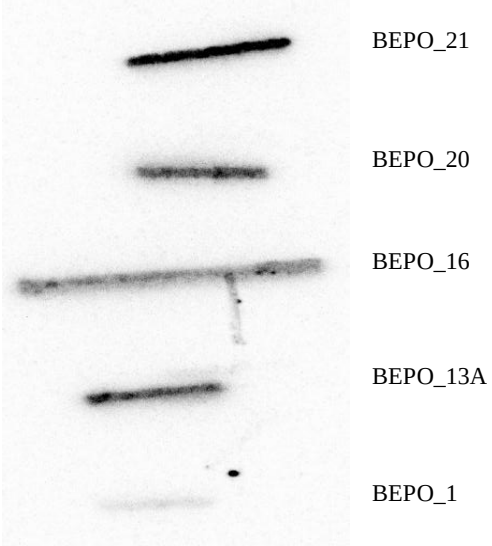

Figure 63 Autoradiograph photograph of increasing greyscale intensities for exposed BEPO samples

The autoradiographs show there is a non-uniform distribution of radioactivity within the samples, this has also been highlighted using X-ray tomography, where high attenuation spots are seen and are attributed to a material with a molecular weight greater than that of graphite. In addition X-ray tomography has been used to analysis the shapes and distribution of porosity in irradiated BEPO.

4.5.5. Crystal structure changes with irradiation damage

Figure 64 compares the Raman spectrums for several types of virgin material with the i-graphite used in this research. From this spectral data in-plane crystallite size can be calculated using Equation 2. It should be noted that the in-plane crystallite size *La* cannot be calculated for HOPG as there is no *D* bands present in the spectrum due to HOPG highly order orientation. The A_{1g} *D* breathing mode is forbidden in perfect graphite (HOPG) and only becomes active in the presence of disorder [104]. The spectra for PGA can be seen in Figure 64, an In-plane crystallite size *La* ratio = 0.275 calculated from peak heights and La = 12.5 nm (Equation 2). PGA spectrum shows the *D* and *D'* induced disorder bands arising from disorder in the microstructure.

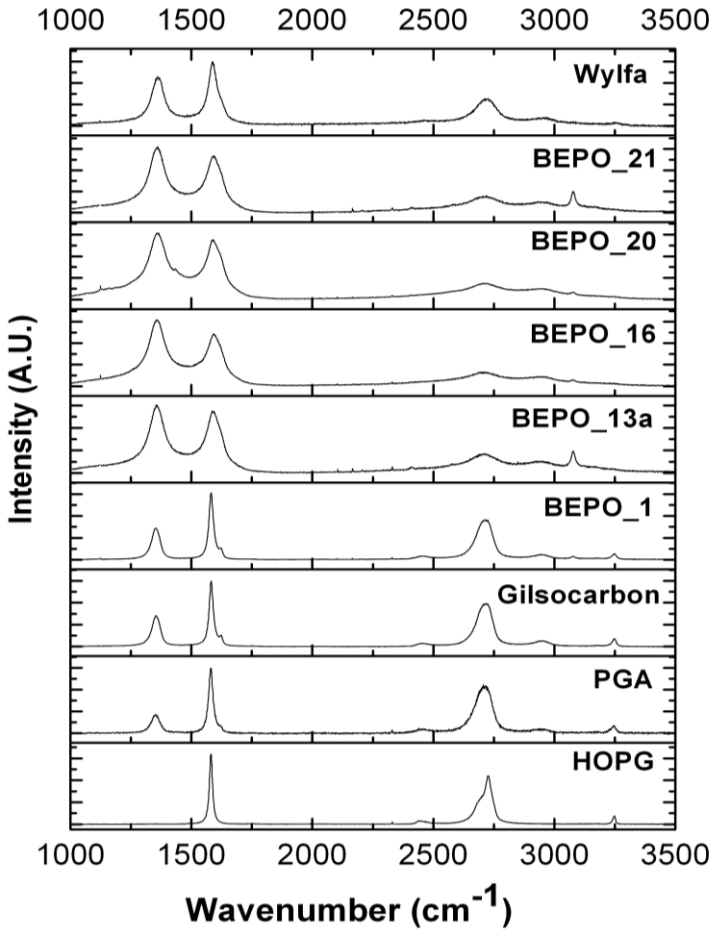

Figure 64 Raman Spectra of HOPG, PGA, Gilsocarbon, Magnox Wylfa and all BEPO samples

Comparing each of the Raman spectrums the scattering intensities vary with polarisation geometries. Polarisation depends on the orientation of the crystal axes with respect to the plane of input light. Scattering intensity is proportional to the square of the induced dipole moment; therefore strong intensities are related to the distribution of the electron cloud in the C-C bonds. Irradiated crystalline dimensional changes cause shrinkage in the a-direction which has been observed here in BEPO samples 13a - 21 having the lowest La values as observed in Figure 64. These results also highlight the variations between each type of nuclear graphite quality as a result of the different manufacturing processes.

Figure 65 allows a visual comparison of the spectrums for each grade of graphite material researched in this thesis. Structurally there is a trend observed with an increase in disorder as the D peak increases in height and width compared to the highly ordered HOPG spectrum. Broadening of the G peak and a reduction in the D'' peak are also indicative of increased disordered and a microstructure different to HOPG. Calculating the ratio of the intensity of the D peak divided by the G peak against the crystallite size calculated using Equation 2 gives the graph in Figure 65.

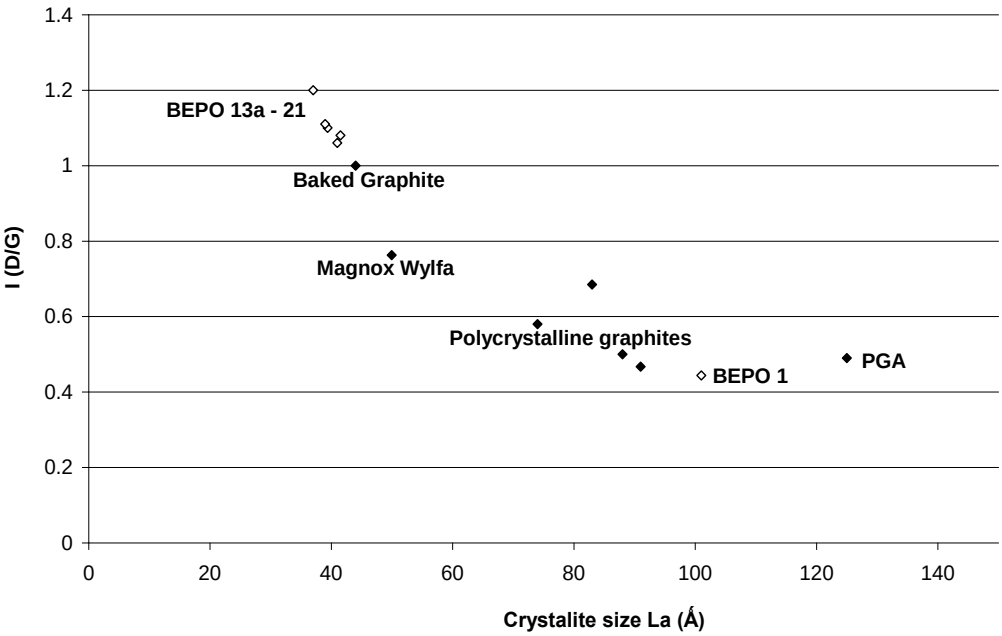

Figure 65 ID/IG ratios versus the crystallite size for polycrystalline graphite, irradiated PGA Magnox Wylfa and irradiated BEPO graphite

Figure 65 show the virgin nuclear graphite structure prior to irradiation damage and the structure after irradiation. BEPO channels 13a, 16, 20 and 21 have produced a Raman spectrum indicative of irradiated graphite. Disordered D band peak being broader and higher than the G band peak. This is also reflected in the 2nd order Raman bands attributed to an increase in disorder within the microstructure.

A trend is observed that post irradiation the crystallite size is reduced and the ID/G peak intensity increases. This data concludes that irradiation damage has increased structural disorder and broken down the graphite crystalline layers to that of a similar structure to baked graphite material.

Taking this analysis completed here and comparing it to knight and white [113] Figure 66 compares the full width half maximum (peak broadening) against ID/IG ratio which exposes the microstructural differences between virgin, coke, baked and irradiated BEPO graphite and Magnox Wylfa.

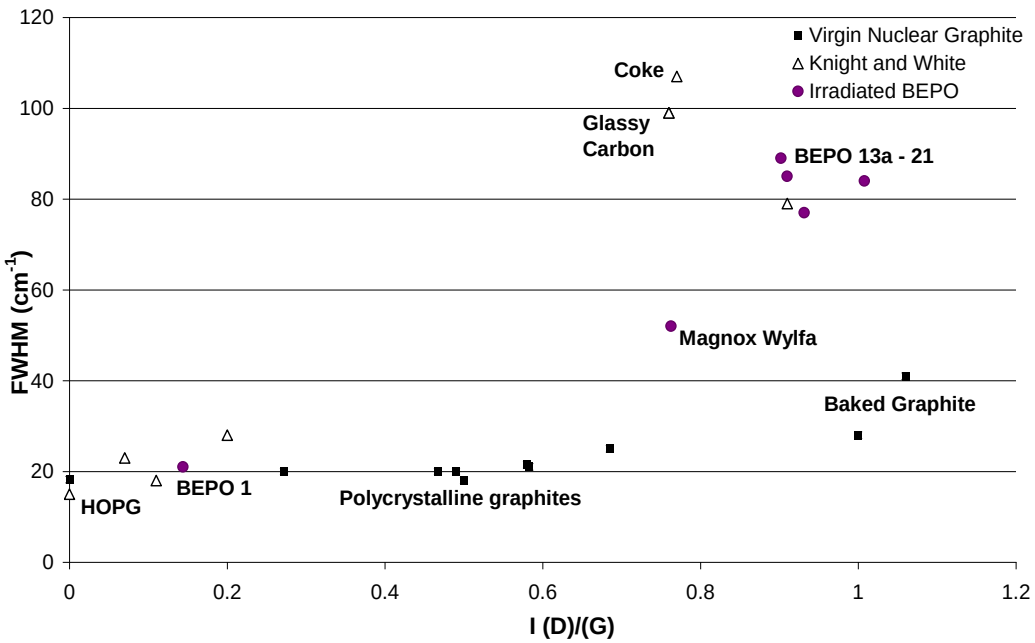

Figure 66 Graph shows full width half maximum of the G peak (FWHM) against ID/IG ratio for virgin and irradiated graphite

A clear difference is observed between highly ordered polycrystalline graphite, virgin and irradiated graphite Raman Spectrums and their results. The data represented here agrees with several literature sources [104, 105, 108-110, 114] Thus Raman is an effective tool in analysing damage caused to the microstructure by neutron irradiation. Trends are observed with virgin material structure and irradiated graphite material.

4.5.6. Surface Area Results

Surface Area determination was carried out using the Tristar II on virgin PGA samples and BEPO samples and Magnox graphite prior to leaching. This analysis was done under nitrogen gas with samples degassed for a minimum of 6 hours prior to analysis.

Table 42 Surface area of vrgin and irradiated graphite

Material	Surface Area (m^2/g)
Virgin PGA powder	60.0191
Virgin PGA solid	1.0243
BEPO Channel 1 powder	15.524
BEPO Channel 16 powder	55.006
BEPO Channel 16 solid	0.781
BEPO Channel 20 powder	62.727
BEPO Channel 20 solid	1.104
Irradiated Magnox Samples	33.490

Nightingale analysed AGXP grade graphite using BET methodology with Nitrogen gas and got a value of 1.2 m^2/g [48]. Nightingale also reported that nuclear grade graphite should have a surface area ranging from 0.25 – 1.2 m^2/g [48]. The solid BEPO graphite and virigin PGA graphite gave results within this region with the powder samples having significantly more surface area.

4.5.7. Overall Summary of Results

Extensive research has been completed on leaching of BEPO and Wylfa graphite focusing on ^{3}H and ^{14}C release. Alongside this work characterisation work has been carried out on the microstructure, isotopic content and distribution of activity within the material. The main points taken from this research into my final conclusions include;

- Validation of thermal treatment for determining ^{3}H and ^{14}C activity
- The mobility of ^{3}H and ^{14}C under various chemical treatment options
- The overall reduction of ^{3}H and ^{14}C under various chemical treatment conditions
- Microstructural characterisation using Raman Spectroscopy and Confocal Microscope
- Distribution of activity using Autoradiography
- Surface area determination of virgin graphite compared to irradiated graphite

5. Conclusions and Future work

The program of work set out in this research was very ambitious which involved major hurdles such as setting up laboratories to carry out active research and obtaining radioactive material for analysis. Some of the techniques used in this research have never been applied to i-graphite before therefore techniques had to be developed before applying them to irradiated graphite. In addition the data obtained from these techniques had to be analysed and understood in terms of the aims and objectives of this work.

Setting up a laboratory and working to high standards and safe practices was a sometimes daunting task as regulations, local rules, receipt handling and storage documentation, risk assessments, protocols and COSHH had to be implemented to a high standard. The laboratories set up at the University of Manchester have now provided a suitable environment for several other students to carry out their research and some students have taken several interesting findings of the authors research to further to create PhD projects.

The main objectives of the research described in this thesis were:

- Set up an active laboratory for research
- Isotopic determination of ^{3}H and ^{14}C
- Location and migration of ^{3}H and ^{14}C
- Mobility / removal of ^{3}H and ^{14}C
- Mechanism / species and rate determining steps of ^{3}H and ^{14}C release

It has been demonstrated that thermal analysis is an excellent technique for ^{3}H and ^{14}C determination; this has been validated through the Round Robin comparisons with other CARBOWASTE partner's results. Leaching has provided insight into ^{3}H and ^{14}C locations, mobility and removal mechanisms. This data has been used to suggest a

possible mechanism behind ^{3}H and ^{14}C release rates and the differences in how ^{3}H and ^{14}C behave.

5.1. Major Findings

The following trends with the irradiated graphite have been found:

- Each type of i-graphite behaved differently under chemical treatment conditions with BEPO Channel 20 providing an example of i-graphite which behaved in an unexpected way. Thus supporting evidence for further testing and evaluation of such chemical treatments prior to use would be required as not all types of i-graphite may be suitable for chemical treatment. Different grades of i-graphite have different irradiation histories and it is recommended that chemical treatment should be investigated on a broader range of i-graphite.
- Phase two leaching showed that acidic environment yielded higher activity releases for both of ^{3}H and ^{14}C removal.
- Separate mechanisms for ^{3}H and ^{14}C are proposed. There appears to be two separate ^{14}C isotopic forms i.e. leachable and non-leachable as under harsh environments and powdered i-graphite never more than 30% of ^{14}C is removed. This theory on leachable and non-leachable forms of ^{14}C provides insight in the mechanism of formation and the behaviour under continued irradiation.
- Radiolysis and hydrogen ion isotope exchange are considered to be the mechanism for ^{3}H release, as ^{3}H release is favoured under solutions which have a suitable environment for these processes to have occured.
- Steady state of release was achieved under all conditions by day 90, after this time very limited amounts of both ^{3}H and ^{14}C were released. All ^{3}H mobile / reactive species have undergone hydrogen ion isotopic exchange prior to day 90 and for ^{14}C the non-leachable forms of ^{14}C which remain in the i-graphite structure at day 90 may require complete destruction of the material for their release.

- Low temperature, low irradiated and air cooled BEPO graphite exhibited very different behaviour in relation to the removal of ^{14}C and ^{3}H under chemical treatment compare to commercial carbon dioxide cooled Magnox reactor graphite. Possible explanation as to why this has occurred could be the higher temperature and gas compositions in the Magnox reactor has resulted in more isotopic release during the reactor lifetime when compared to a cooler experimental reactor.
- Thermal analysis of ^{3}H and ^{14}C along with autoradiography and x-ray tomography demonstrated that the distribution of isotopes within the graphite structure was uneven. These results also supported experimental determination of the isotopic inventory as thermal analysis was carried out on several samples and the average used, in the case of BEPO Channel 20 the standard deviation between these results was high.
- The success and accuracy (within 10% of the CIEMAT value) achieved with the Round Robin Test isotopic inventory experiment gave confidence in the determination of ^{3}H and ^{14}C by thermal analysis. Thermal analysis using a carbolite® furnace is considered a suitable technique for ^{3}H and ^{14}C analysis of i-graphite.
- Raman analysis showed that irradiation damage changed the crystalline structure of the i-graphite compared to virgin graphite. The resulting disordered i-graphite crystalline structure appears to that similar to that of baked graphite. This is considered to be due disorder in the crystallite basal planes.

5.2. Comparison of Chemical Leaching Results

As detailed in the literature review, Section 2.2, leach rate experiments on irradiated graphite initially exhibit rather erratic results but then tend to stabilise to a steady state between 70–140 days [12, 46, 81]. The leaching data achieved in this research also was found to follow this trend with an average steady state release rate achieved at about day 90.

In the literature review the leach rate from several other authors was discussed with Takeshiat [82] and Takahash [61] experiments reporting a leach rate ratio of 10^{-5} for ^{14}C under $H_2SO_4/KMnO_4$ conditions, Gray and Morgan [80,81] reporting a leach rate ratio in the order of 10^{-6} to 10^{-3} and finally White [12] calculated leaching rates in the order of 10^{-5} cm / day. The leach rate results detailed in section 4.3.6 are all within the general region of previous work referred to above, i.e. 10^{-3} to 10^{-6}.

Trying to use leach rate data to support conclusions relating to sample irradiation history was not possible due to the limited quantity of Wylfa Magnox graphite available for testing and the restrictions of only granulated Wylfa material been available. This granulated material had a surface area of 33 m^2/g which is half way between the surface area of powder and solid used in the case of the BEPO i-graphite.
These results do however illustrate some of the similarities between leaching studies that regardless of sample history, geometry, porosity, leaching methodology and sampling frequency all these authors including this work achieved leach rates within this region signifying that utilising this type of methodology will only remove limited amounts of ^{3}H and ^{14}C.There are however some notable exceptions to obtaining a leach rate ratio in the order of 10^{-6} to 10^{-3} such as AMEC [83] and SERCO [84] released reports, the authors of these reports highlight these differences as errors possibly based on supplied information such as isotopic inventory which wasn't was determined by the authors themselves.

5.3. Suggestions for Future Research and Technical Developments

As a direct result of this work on my recommendation other projects have been set up at the University of Manchester:

Initially a project teaming x-ray tomography and thermal treatment under reduced oxygen environment was funded within the CARBOWASTE program. This project aims to investigate if preferential release of ^{14}C occurs from the open porosity within a solid i-graphite. To achieve this sample identification and positing is achieved by laser marking and mapping of the porosity and internal structural changes is achieved by x-ray tomography.

Secondly also based within the CARBOWASTE program an EngD a project has been set up which in part focuses on the modeling the pathways of isotope production. This involves using the thermal analysis data determined for the BEPO and Wylfa irradiated graphite's. The experimental determined inventory is to be to compare to results obtained using theoretical reactor physics models.

The chemical treatment results here have provided an insight into ^{3}H and ^{14}C leaching behaviour and mobility. Further research under these conditions at elevated temperatures such as 50˚C and short term 24 hour experiments with testing every hour could be used to provide further data to support the feasibility of using chemical treatment technique prior to long term storage.

New chemical treatment conditions which could be evaluated include:

- sequestering / chelating agents and surfactants
- repository conditions
- ground / borehole water

The aim of any further chemical treatment work would be to further develop understanding of isotope migration. Further analysis and method development including ^{36}Cl, ^{137}Cs and ^{63}Ni analysis and would be an advantage on Magnox reactor

irradiated graphite which may contain these isotopes. Finally mapping surface area and pore size distribution to virgin and irradiated material to evaluate any trends with irradiation damage would be interesting and a good addition to the research started here.

5.3.1. Publications

2011

L. McDermott, A. N. Jones, B J. Marsden. "^{3}H and ^{14}C Release in UK Nuclear Graphite by Chemical Treatment". Modelling and Measuring Reactor Core Graphite Properties and Performance, Birmingham. 31 October – 3 November 2011

A. N. Jones, L. McDermott, B. J. Marsden. "The Characterisation of Irradiation Damage in Reactor Graphite using High Resolution Transmission Microscopy and Raman Spectroscopy". MRS, Argentina, 3-7 October 2011

G. Black, Dr. A. N. Jones, L. McDermott, Prof. B. J. Marsden. "Modelling the Production of Tritium, Carbon-14 and Cobalt-60 in Irradiated Graphite from a UK Magnox Reactor". MRS, Argentina, 3-7 October 2011

2009

A.N. Jones, L. McDermott, B.J. Marsden, T.J. Marrow, and A.J. Wickham. "Characterisation of Irradiated Graphite Waste in Reactor Decommissioning". Carbon 2009, Biarritz, France, 14 - 19 June, 2009

2008

McDermott L, Jones A N, Marsden B J, Marrow T J. "Characterisation of Irradiated Nuclear Graphite Waste". Securing the Safe Performance of Graphite Reactor Cores, Nottingham. November 2008

6. References

1. NDA, *Radioactive Wastes in the UK: A Summary of the 2001 Inventory*. 2002.
2. von Lensa, W., *CARBOWASTE: New EURATOM Project on 'Treatment and Disposal of Irradiated Graphite and other Carbonaceous Waste'*, in *Proceedings of the 4th International Topical Meeting on High-Temperature Reactor Technology*, HTR2008, Editor. 2008: Washington D.C., USA.
3. von Lensa, W., et al., *Treatment and Disposal of irradiated Graphite and other Carbonaceous Waste.* ATW - International Journal for Nuclear Power., 2011. **56**: p. 263.
4. Kelly, B.T., *Graphite - The Most Fascinating Nuclear Material.* Carbon, 1982. **20**(1): p. 3-11.
5. IAEA. *Technical Committee Meeting* in *Nuclear Graphite Waste Management*. 1999. Manchester: IAEA Austria.
6. NDA, *Final Waste Issues Group Report*. 2007.
7. NDA, *Radioactive Wastes in the UK: A Summary of the 2010 Inventory*. 2010.
8. Bradtec Decon Technologies, L., *Graphite Decommissioning Options for Graphite Treatment, Recycling, or Disposal, including a discussion of Safety-Related Issues*, E.P.R.I. (EPRI). Editor. 2006.
9. HOLT, G. *The decommissioning of commercial Magnox gas cooled reactor power stations in the United Kingdom*. in *Technologies for Gas Cooled Reactor Decommissioning, Fuel Storage and Waste Disposal*. 1998: IAEA-TECDOC Vienna.
10. Marsden, B.J. and A.J. Wickham. *Graphite disposal options - A comparison of the approaches proposed by UK and Russian reactor operators*. in *Nuclear Decommissioning 1998*. 1998. London: Professional Engineering Publishing.
11. Quade, U. *Packaging requirements for graphite and carbon from the decommissioning of the AVR in consideration of the German final disposal regulations*. in *Technologies for Gas Cooled Reactor Decommissioning, Fuel Storage and Waste Disposal*. 1998. Vienna
12. White, I.F., et al., *Assessment of Graphite management modesfor graphite form reactor decommissioning*, in *CEC*, E. Commission, Editor. 1984.
13. Wickham, A.J., *UK Nuclear Graphite Decommissioning*, B.J. Marsden, A.N. Jones, and L. McDermott, Editors. 2008: Manchester.
14. Mould, R.F., *Chernobyl Record: The Definitive History of the Chernobyl Catastrophe*. 2000: Institute of Physics Publishing. 320.
15. Hou, X., L.F. Ostergaard, and S.P. Nielsen, *Determination of 36Cl in Nuclear Waste from Reactor Decommissioning.* Anal. Chem., 2007. **79**(8): p. 3126-3134.
16. Ammar, M.R., et al., *Characterization of graphite implanted with chlorine ions using combined Raman microspectrometry and transmission electron microscopy on thin sections prepared by focused ion beam.* Carbon, 2009. **48**(4): p. 1244-1251.
17. Preston, S.D. and B.J. Marsden, *Changes in the coefficient of thermal expansion in stressed Gilsocarbon graphite.* Carbon, 2006. **44**(7): p. 1250-1257.
18. Zou, Z., et al., *Numerical simulation of strength test on graphite moderator bricks using a continuum damage mechanics model.* Engineering Fracture Mechanics, 2006. **73**(3): p. 318.
19. Mitchell, B.C., et al., *The mechanical testing of nuclear graphite.* Journal of Nuclear Materials, 2003. **322**(2-3): p. 126.

20. Kelly, B.T., *The physics of graphite*. 1981, London: Applied Science Publishers.
21. Lilley, J., *Nuclear Physics: Principles & Applications*, ed. Wiley. 2009, Chichester, UK.
22. Bush, R.P., I.F. White, and G.M. Smith, *Carbon-14 Waste Management*. 1982.
23. Inc., U.C.C., *The Industrial graphite Engineering Handbook*. Copyright © 2001, Parma. 130.
24. Kretchman, H.F., *The Story of Gilsonite*. 1957, Salt Lake City: American Gilsonite Company.
25. Pocock, R.F., *Nuclear Power*, ed. U.B. LtD. 1977, Old Woking: The Gresham Press. 263.
26. Prince, N., C.R. Simons, and J.D. Hart. *Moderator Structure Design In the UK - A historical Survey*. in *Graphite Structures for Nuclear reactors*. 1972. London.
27. UKAEA, *GLEEP reactor*.
28. Cooper, B.E., S.S. Hill, and M. Tomlinson, *Collected BEPO Graphite Oxidation Monitoring Data (November 1957 to December 1959)*, U. Harwell, Editor. 1961, National Archives (unclassified) p. 124.
29. Thewlis, J., *British Experimental Pile (BEPO) - Graphite Supplies*, A.E.R.E. Harwell, Editor. 1945, National Archives (unclassified).
30. Marsden, B.J. and M.A. Davies, *The design of the British Production Pile Graphite Moderator Cores*, AEA, Editor. 1992, AEA Technology.
31. Handy, B.J., *Experimental study of C-14 and H-3 release from irradiated WAGR and BEPO graphite samples in alkaline solutions*. 2009, Amec NNC.
32. Shaw, E.N., *Europe's Nuclear Power Experiment - History of the OECD Dragon Project*, ed. P. Press. 1983, Oxford: Pergamon Press. 337.
33. Brindley, C.E., *History of Graphite Used in Chapel cross reactors for initial loading to present*. 1981, B.N.F.L.
34. Davis, W., *Management of Low Level Radioactive Waste*. Vol. 1. 1979: Pergamon Press. 151.
35. Marsden, B.J., *Production, Retention and Location of Carbon 14 in Irradiated Graphite*, A.T. plc, Editor. 2001.
36. Hou, X., *Rapid analysis of 14C and 3H in graphite and concrete for decommissioning of nuclear reactor.* Applied Radiation and Isotopes, 2005. **62**(6): p. 871-882.
37. Hou, X., L.F. Ostergaard, and S.P. Nielsen, *Determination of 63Ni and 55Fe in nuclear waste samples using radiochemical separation and liquid scintillation counting.* Analytica Chimica Acta, 2005. **535**(1-2): p. 297-307.
38. Costes, J.R., C. de Tassigny, and H. Vidal, *Conditioning of graphite bricks from dismantled gas-cooled reactors for disposal.* Waste Management, 1990. **10**(4): p. 297-302.
39. Shukolyukov, Y.A., et al., *Xenon and krypton isotopic anomalies in a natural nuclear reactor and at the epicenter of a nuclear explosion.* Atomic Energy, 1987. **63**(6): p. 903-911.
40. Wise, M., *Management of UKAEA Graphite Liabilies*, P.P.a.E. Division, Editor, United Kingdom Atomic Energy Authority.
41. Colin, B. and K. Langley, *Nuclear Decommissioning, Waste Management, and Environmental Site Remediation*. 2003: Amsterdam : Butterworth-Heinemann.
42. NDA, *Final Waste Issues Group Report*. June 2007.
43. NDA, *Radioactive Wastes in the UK: A Summary of the 2010 Inventory*. 2010, NDA.
44. NDA, *2010 Inventory - waste quantities by site*. 2010, NDA.
45. NDA, *Radioactive Wastes in the UK:A Summary of the 2010 Inventory*. 2010. p. 12.

46. Wickham, A.J. and B.J. Marsden, *Characterisation, Treatment and Conditioning of Radioactive Graphite from Decommissioning of Nuclear Reactors.* IAEA TECDOC-1521,, 2006.
47. Bradford, M.R. and A.G. Steer, *A structurally-based model of irradiated graphite properties.* Journal of Nuclear Materials, 2008. **381**: p. 137-144.
48. Nightingale, R.E., *Nuclear Graphite*. 1962: Academic Press.
49. Simmons, J.H.W., *Radiation Damage in Graphite*, ed. Pergamon. Vol. Chapter 2. 1965, Oxford
50. Thrower, P.A., *55. Vacancy and interstitial loops in graphite produced by high temperature irradiation and annealing.* Carbon, 1968. **6**(2): p. 211-211.
51. Thrower, P.A., *The Study of Defects in Graphite by Transmission Electron Microscopy*, in *Chemistry and Physics of Carbon* P.L. Walker, Editor. 1969, DEKKER: New York.
52. Thrower, P.A. and W.N. Reynolds, *Microstructural Changes in Neutron-Irradiated Graphite.* Journal of Nuclear Materials, 1963. **8**(2): p. 221-226.
53. Best, J.V., W.J. Stephen, and A.J. Wickham, *Radiolytic graphite oxidation.* Progress in Nuclear Energy, 1985. **16**(2): p. 127-178.
54. Johnson, P.A.V., A. Blanchard, and B.T. Kelly, *151. Theory of the effect of radiolytic oxidation in carbon dioxide on the transport of gases through graphite.* Carbon, 1982. **20**(2): p. 141-178.
55. Johnson, P.A.V., et al., *152. Analysis of the effect of radiolytic oxidation in carbon dioxide on the transport of gases through graphite.* Carbon, 1982. **20**(2): p. 141-142.
56. Standring, J. and B.W. Ashton, *The effect of radiolytic oxidation by carbon dioxide on the porosity of graphite.* Carbon, 1965. **3**(2): p. 157-158.
57. Kelly, B.T., *The radiolytic corrosion of advanced gas-cooled reactor graphite.* Progress in Nuclear Energy, 1985. **16**(1): p. 73-96.
58. Telling, R.H., et al., *Wigner defects bridge the graphite gap.* Nature Materials, 2003. **2**(5): p. 333-337.
59. Wörner, J., W. Botzem, and S.D. Preston. *Heat Treatment of Graphite and Resulting Tritium Emissions*. in *Nuclear Graphite Waste Management*. 1999. Manchester, United Kingdom International Atomic Energy Agency, Vienna (Austria).
60. Wickham, A.J., *Caring for the Graphite Cores*, in *The Review of Safety at Magnox Nuclear Installations*. 1989, I.Mech E: London. p. 79-87.
61. Takahashi, R., et al. *Investigation of morphology and impurity of nuclear-grade graphite, and leaching mechanism of carbon-14*. in *IAEA Technical Committee Meeting on Nuclear Graphite Waste Management* 1999. Manchester, United Kingdom.
62. Korsmeyer, R.B., *Fission Product Transport Through Graphite Matrices*. 1961, Union Carbide Nuclear Company Report.
63. Libby, W.F., *Atmospheric Helium Three and Radiocarbon from Cosmic Radiation.* Physical Review, 1946. **69**(11-12): p. 671.
64. Defra, *Radioactive wastes in the UK: A Summary of the 2005 Inventory*. 2005, Nirex.
65. CoRWM, *Managing our radioactive waste safely*, C.o.R.W. Management, Editor. 2006, .
66. Nirex, *Options for Monitoring During the Phased Development of a Repository for Radioactive Waste*. 2002. p. 176.
67. NDA, *NDA Strategy 2006*. 2006. p. 164.
68. NDA, *NDA Strategy and UK Nuclear LLW Strategy: Strategic Environmental Assessment Response to Consultation on the Scoping Report*. 2008, Entec UK Limited. p. 69.

69. Bradbury, D., et al. *Pyrolysis / Steam Reforming and its Potential Use in Graphite Disposal*. in *Proc. 3rd EPRI International Decommissioning and Radioactive Waste Workshop*. 2004. Lyon, France.
70. UKAEA, *Reactors UK*. 4th ed. 1969: UKAEA. 116.
71. Podruzhina, T., *Graphite as radioactive waste corrosion behaviour under final repository conditions and thermal treatment.*, in *FZJ Report* 2004: Jülich.
72. Fachinger, J., *14C and 3H Thermal Treatment from Merlin Graphite*, in *CARBOWASTE: 2nd Annual steering committee meeting*, A.N. Jones, Editor. 2009: Marcoule, France.
73. Mason, J.B. and D. Bradbury, *Pyrolysis and its potential use in nuclear graphite disposal*, in *AEA Technical Committee Meeting on "Nuclear Graphite Waste Management"*, I.A.E. Agency, Editor. 1999, IAEA: Manchester, United Kingdom. p. 77-84
74. Antunes, E.F., et al., *Comparative study of first- and second-order Raman spectra of MWCNT at visible and infrared laser excitation.* Carbon, 2006. **44**(11): p. 2202-2211.
75. http://www.corwm.org/pdf/FullReport.pdf, C.o.R.W.M., *Managing our radioactive waste safely*. 2006, CoRWM
76. Izumi, J., et al., *14CO and 12CO Separation on Na-X Using Pressure Swing Adsorption at Low Temperatures.* Adsorption, 2005. **11**(0): p. 817-821.
77. Arnold, J.R. and W.F. Libby, *Radiocarbon from Pile Graphite; Chemical Methods for Its Concentrations*, in U.S.A.E.C. (AEC), Editor. 1946, Argonne National Labs.
78. Hespe, E.D., *Leaching testing of immobilised reactive waste solids.* Atomic Energy Reviews, 1971. **9**: p. 195-207.
79. Gray, W.J., *A study of the oxidation of graphite in liquid water for radioactive waste storage applications.* Radioactive Waste management, 1982. **2**(3): p. 137.
80. Gray, W.J. and W.C. Morgan, *Leaching of 14C and 36Cl from Hanford Reactor Graphite*, P.N. Labs, Editor. 1988.
81. Gray, W.J. and W.C. Morgan, *Leaching of 14C and 36Cl from irradiated french graphite*, P.N. Labs, Editor. 1989.
82. Takeshita, K., et al., *Recovery of C14 from Graphite Moderator of Gas-Cooled Reactor (GCR).* Nuclear Science and Technology, 2002. **39**: p. 1207-1212.
83. Handy, B.J., *Experimental Study of C-14 and tritium release from irradiated graphite spigot samples in alkaline solutions*, Nirex, Editor. 2006, AMEC NNC: Didcot. p. 1-11.
84. Baston, G.M.N. and T.A. Marshall, *Longer term release of carbon-14 from irradiated graphite*. 2009, Serco.
85. Marshall, T.A. and G.M.N. Baston, *Longer-term release of C-14 from irradiated graphite*. 2011, Serco.
86. Sambell, R.A.J., C. Smitton, and A. Elsden, *A contribution towards a standard leach test for immobilized low and medium level waste.* Nuclear and Chemical Waste Management, 1982. **3**(2): p. 125-129.
87. Hespe, E.D., *Leach testing of immobilised radioactive waste solids: a proposal for a standard method.* Atomic Energy Review, 1971. **9**: p. 195-207.
88. International Standards Organization (ISO), *Long-term leach testing of radioactive waste solidification products.* ISO/TC 85/SC 5/WG 38, 1979.
89. American Nuclear Society, *Measurement of the Leachability of Solidified Low-Level Radioactive Wastes by a Short-Term Test Procedure*. 2008.
90. www.ukaea.org.uk/.
91. Nair, A.S., *A model for the global dispersion of 14C released to the atmosphere as CO2.* Journal of the Society for Radiological Protection, 1983. **3**: p. 16-22.

92. FZJ, *CARBOWASTE Treatment and Disposal of Irradiated Graphite and Other Carbonaceous Waste Grant agreement no.: 211333*. 2008.
93. von Lensa, W. *CABOWASTE*. 2008 2009 [cited 2011 26/07/2011]; Available from: http://www.carbowaste.eu/.
94. UKAEA, *Harwell project profiles: British Experimental Pile O*.
95. Wickham, A.J., *BEPO Graphite: Compilation of Data Relevant to Test of GIRM Methodology*. 2002, Department of Trade and Industry. p. 59.
96. Wickham, A.J., *Deposition of Graphite Samples from BEPO as Supplied to NIREX*. 2007.
97. Peng, C.T., *Sample Preparation in Liquid Scintillation Counting*. Review 17 ed: Amersham. 112.
98. Brunauer, S., P.H. Emmett, and E. Teller, *Adsorption of Gases in Multimolecular Layers.* 1938. **60**: p. 309-319.
99. Berre, C., et al., *Numerical modelling of the effects of porosity changes on the mechanical properties of nuclear graphite.* Journal of Nuclear Materials, 2006. **352**(1-3): p. 1-5.
100. Babout, L., et al., *The effect of thermal oxidation on polycrystalline graphite studied by X-ray tomography.* Carbon, 2005. **43**(4): p. 765-774.
101. Babout, L., et al., *Three-dimensional characterization and thermal property modelling of thermally oxidized nuclear graphite.* Acta Materialia, 2008. **56**(16): p. 4242-4254.
102. Seri-Levy, A. and D. Avnir', *The Brunauer-Emmett-Teller Equation and the Effects of Lateral Interactions. A Simulation Study.* Langmuir, 1993. **9**(2623): p. 2523-2529.
103. Nemanich, R.J. and S.A. Solin, *Observation of an anomolously sharp feature in the 2nd order Raman spectrum of graphite.* Solid State Communications, 1977. **23**(7): p. 417-420.
104. Ferrari, A.C. and J. Robertson, *Interpretation of Raman spectra of disordered and amorphous carbon.* Journal of Physics Review B, 2000. **61**: p. 14095-14107.
105. Ferrari, A.C., *Raman spectroscopy of graphene and graphite: Disorder, electron-phonon coupling, doping and nonadiabatic effects.* Solid State Communications, 2007. **143**(1-2): p. 47-57.
106. Solin, S.A. and R.J. Nemanich, *First and Second order Raman scattering from finite-size crystals of graphite.* Physics Review, 1979. **B20**: p. 392.
107. Reich, S. and C. Thomsen, *Raman spectroscopy of graphite.* Phil. Trans. R. Soc, 2004(362): p. 2271-2288.
108. Tuinstra, F. and J.K. Koeing, *Raman Spectrum of Graphite.* The Journal of Chemical Physics, 1970. **53**(3): p. 1126-1130.
109. Lee, Y.-J., *The second order Raman spectroscopy in carbon crystallinity.* Journal of Nuclear Materials, 2004. **325**(2-3): p. 174-179.
110. Knight, D.S. and W.B. White, *Charaterization of Diamond Films by Raman Spectroscopy.* Journal of Materials Research, 1989. **4**(2): p. 385-393.
111. Enoki, T., M. Suzuki, and M. Endo, *Graphite Intercalation Compounds and Applications*. 2003: Oxford University Press. 440.
112. *Chemistry and Physics of Carbon*. A Series of Advances, ed. J. Philip L. Walker. Vol. 5. 1969. 389.
113. Knight, D.S. and W.B. White, *Characterization of diamond films by Raman spectroscopy.* journal of Materials Research, 1989. **4**(2): p. 385 - 392.
114. Cancado, L.G., et al., *Measuring the degree of stacking order in graphite by Raman spectroscopy.* 2007.